Université catholique de Louvain

Faculté de médecine

Institut d'éducation physique et de réadaptation

Unité de réadaptation et médecine physique

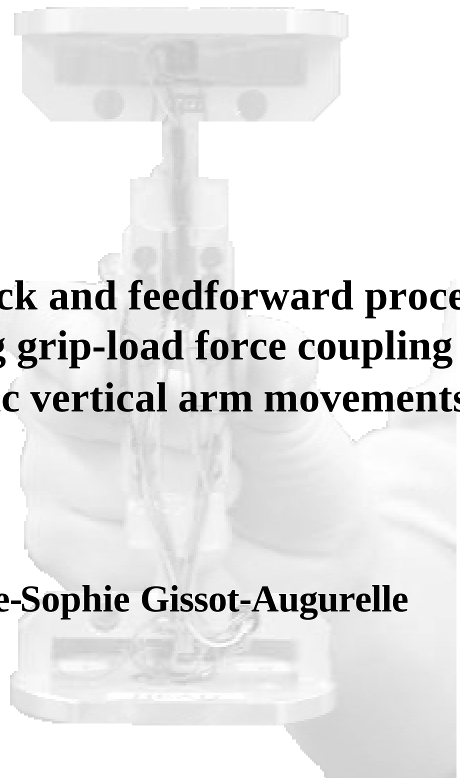

Feedback and feedforward processes underlying grip-load force coupling during cyclic vertical arm movements.

Anne-Sophie Gissot-Augurelle

Thèse présentée en vue de l'obtention du grade de Docteur en Kinésithérapie et Réadaptation
Orientation: Neurosciences

Promoteur: Prof. J-L. Thonnard

Avril 2003

Université catholique de Louvain
Faculté de médecine
Institut d'éducation physique et de réadaptation
Unité de réadaptation et médecine physique

Feedback and feedforward processes underlying grip-load force coupling during cyclic vertical arm movements.

Anne-Sophie Gissot-Augurelle

Thèse présentée en vue de l'obtention du grade de Docteur en Kinésithérapie et Réadaptation
Orientation: Neurosciences

Promoteur: Prof. J-L. Thonnard

Avril 2003

Remerciements

Cette thèse est l'aboutissement de quatre années de recherche menée au sein de l'unité de médecine physique et de réadaptation à l'Université catholique de Louvain. Je tiens à remercier le Professeur Jean-Louis Thonnard, mon promoteur, de m'avoir ouvert la porte au doctorat et de m'avoir aidée dans toutes les étapes de ce travail.

Ce travail a pu être réalisé grâce au support financier des services fédéraux des affaires scientifiques, techniques et culturelles (SSTC). Que cette institution trouve ici les signes de ma reconnaissance. Je tiens tout particulièrement à remercier Madame M.C. Limbourg et Monsieur Y. Bernard pour leur soutien et leur confiance. Cette thèse n'aurait pas été possible sans la collaboration de l'Agence Spatiale Européenne qui m'a permis de participer aux campagnes de vols paraboliques. Le Dr Benny Elmann-Larsen a soutenu et dynamisé mon projet. Qu'il trouve ici le témoignage de ma sincère gratitude. De par son professionnalisme, le Dr Vladimir Pletser m'a permis d'effectuer mes expériences dans les meilleures conditions. Je l'en remercie très sincèrement.

Les Professeurs Marc Crommelinck, Philippe Lefèvre, Allan Smith et Allan Wing ainsi que le Dr Thierry Lejeune ont accepté de faire partie du jury de cette thèse. Leurs critiques constructives et leurs conseils m'ont guidée dans la finalisation de ce travail. Je les en remercie sincèrement. Je tiens aussi à exprimer ma gratitude au Professeur Etienne Olivier qui a toujours soutenu le projet en y portant son regard critique. Le Professeur Joe Mc Intyre a aussi beaucoup contribué à la discussion des résultats de la deuxième campagne de vols paraboliques. Je l'en remercie.

Ce travail n'aurait pu être réalisé sans une importante aide technique. R. Lemaire est l'ingénieur qui a conçu le premier manipulandum. Massimo Penta est l'ingénieur à l'origine du premier set up d'acquisition des données et des premiers balbutiements du programme d'analyse. Sa clairvoyance et nos longues discussions théoriques m'ont permis d'avancer pas à pas dans l'analyse des résultats. Olivier White est l'ingénieur qui après de longues heures devant son écran et de nombreuses modifications a mis au point un programme d'analyse complet et performant. Il est aussi le concepteur du deuxième manipulandum et de tout le set up d'acquisition des données de la deuxième campagne de vols paraboliques. L'aide de notre technicien, Christian Lebègue a été précieuse. Les Professeurs Norman Heglund et Patrick Willems ont apporté leur expertise dans la réalisation de ce projet. Qu'ils trouvent ici le témoignage de ma reconnaissance et de mon amitié!

Je voudrais aussi remercier tous mes autres collègues de l'unité de réadaptation pour leur soutien et leur aide.

Finalement, je tiens à remercier ma famille et tout spécialement Grégoire de m'avoir apporté toute leur affection et encouragée même dans les moments les plus difficiles.

Contents

Abstract

During transport of hand-held objects, the grip force is modulated in parallel with the load force changes. The control scheme underlying this grip-load force coupling involves subtle interplay between feedforward and feedback mechanisms. Based on internal models of the motor system and object properties, the load force can be predicted and the GF motor command can be specified in a feedforward manner. Moreover, during the course of arm movement, the CNS is informed by sensory feedback about mechanical events such as the lift-off of the object, slippage or excessive grip force. This information is used to correct the motor commands and to update the internal model of the motor apparatus and object.

In this thesis, three experiments were conducted to examine the relative contributions of sensory-driven and anticipatory control of GF adjustments during cyclic vertical movement with a hand-held load. The main point was to assess whether internal models underlying the grip-load force coupling are robust when the environmental context was changed or when the sensory feedback was suppressed.

Two experiments in parabolic flight were conducted to study the effects of a change in gravity on the dynamics of prehension. The main perturbation was that the novice subjects applied unnecessarily high safety margins during their first trial at 0 and 1.8 g in order to secure the grasp insofar as the gravitational component of the load force was unpredictable. By contrast, the temporal coupling between GF and LF was maintained regardless of the gravity conditions because the inertial component of the load could be still predicted from the arm motor command (efference copy).

In the second study performed during parabolic flight, we have observed that the subjects were able to exert the same grip force for equivalent load generated either by a change of mass, gravity or acceleration despite the fact that it requires different arm motor commands.

These two experiments brought further evidence that the predictive mechanisms largely contribute to the GF adjustment. Static forces such gravity are taken into account in the motor plan allowing adequate motor command and precise prediction of the incoming load force change. The GF output would depend on the precision of this prediction that can be evaluated only after the movement onset through sensory information about the actual state of the system.

The third experiment performed in this thesis studied the role of cutaneous afferents in object manipulation by anesthetizing the thumb and index finger. In addition to their phasic slip-detection function, the cutaneous afferents are required for setting the background level of the grip force. Actually, in absence of tactile feedback, the temporal coupling between the grip and load forces is maintained but the mean magnitude of GF progressively decreases leading to object slipping. It is hypothesized that accumulating error occurred in the LF prediction leading to inadequate level of GF. Cutaneous afferents are thus required to correct and maintain the internal model of the arm-hand object system.

Key words: Grip-load force coupling, Internal model, Microgravity, Sensory feedback.

Chapter 0: Introduction

The fabrication of tools and their use for solving more and more complex problems, as well as the gestures associated with language as bodily expressions has appeared as a big revolution in the time scale of evolution from hominids to Homo sapiens sapiens (Wiesendanger 1999). From a support for balance and locomotion, the hand has evolved to a free and dexterous tool for sensing and acting on objects in the environment. The human hand has become a very complex organ that involves a large network of neural structures devoted to control about thirty muscles and to process the afferent information provided by about 17000 mechanoreceptors. As some hand muscles span multiple joints and others act on more than one digit, fine independent finger movements that are regarded by most of our manual activities, are actually very difficult. Hand control is the result of a cooperation of many cortical and subcortical hand “representations” (Lemon 1999).

Tool manipulation includes the ability to analyze the qualities of the perceived object, then based upon its intrinsic physical properties and the desired task, to reach for it, grasp it with an adequate grip configuration, lift and transport it from one point to another with adequate grip force to prevent either slip or muscle fatigue and finally place it back down. In this way, the brain must solve several computational issues. First the arm and hand movement has to be planned, i.e. the optimal trajectory has to be selected from the many alternatives which are consistent with the task (Jordan and Wolpert 1999). Then the forces required to generate this desired motion have to be determined by taking into account the mechanical interactions between limbs segments. Sensory feedback can be used to correct the errors of this motor command on the basis of the moment-to-moment discrepancy between the intended and the actual paths. However, because of the sensorimotor transmission delay within the CNS, inaccuracies can arise for fast movements. It is thus suggested that an internal model of the dynamics of the arm would calculate the motor commands necessary to realize the planned trajectory in a feedforward manner, i.e. prior to the onset of movement. In this way, the role of the feedback loop becomes marginal and useful only at the very end of the trajectory (Desmurget and Grafton 2000).

Once the object is reached, it must be grasped and lifted for further manipulation. The grip force required to restrain the object will depend on skin-object friction and on the tangential load force resulting from the weight (Johansson and Westling 1984) and the inertial forces (Flanagan and Wing 1993, 1995). Past experience in handling tools, visual and haptic information about the object properties and an efference copy of the arm motor command would allow a forward model of the dynamics of the body and environment to predict the forthcoming load force and the necessary minimal grip force to squeeze the object without slip. In this way, the grip force can be modulated in parallel with the load force fluctuation so that the grip-load force ratio remains always greater by a small safety margin than the minimum required to prevent slip. If the preprogrammed grip force is insufficient, microslip occurs at the fingertips that stimulates the mechanoreceptors in the skin. The resultant afferent signal triggers a reflex increase in grip force with a delay sufficiently short to reestablish the grasp before the object drops (Johansson and Westling 1984, 1987, 1988; Johansson et al 1992).

However, the relative contributions of feedforward and feedback processes to precision grip are not clearly established in the large variety of studies about the motor control of manipulative action. In this thesis, we examine the pattern of grip force modulation during cyclic vertical arm movements with a hand-held object. The main point is to assess if the internal models underlying the anticipatory process of the grip-load force coupling are adaptable when the environmental context is changed or when the sensory feedback is suppressed.

The major features of sensorimotor coordination of hand function in man are defined and reviewed in Chapter 1 including, among others, the works of Johansson and colleagues. The recent theoretical concepts about the computational motor control are then described in the Chapter 2 based on the general schema of motor control proposed by Wolpert (1997). The motor planning, the internal inverse models as controller, the internal forward models as predictors, the state estimation by an observer and the motor learning are successively envisaged. That provides a theoretical background in order to build a control schema of grip-load force coupling. The robustness of this control is then tested through three experimental chapters (3-5) that are presented as stand-alone papers consisting of an abstract, an introduction, a method, a result and a discussion section.

The study in Chapter 3 examines the effects of a change in gravity on the motor control of prehension. Two subject groups were tested. In the first, the subjects had previous experience of hyper-and microgravity and in the second the subjects were novices. The results showed that the grip-load force relationship observed at 1 g was conserved in altered gravity field from the first parabola for all the subjects. However, while the experienced subjects immediately adjusted the level of GF modulation to the new gravitational field, the inexperienced ones needed approximately five parabolas to incorporate adequately the effects of a gravity change. The new gravitational fields seem to be rapidly integrated by the central nervous system in the internal models that control the grip force.

The study in Chapter 4 examines the grip-load force coupling observed during cyclic vertical arm movements with a hand-held object performed in different environmental contexts. By varying separately, the upper limb accelerations, the object mass and the arm weight in different gravitational conditions (1 g, 1.8 g, 0 g) induced by parabolic flight, it was possible to generate equivalent magnitude of loads at the fingertips while the mechanical constraints on the upper limb and thus the motor commands required to move the arm were modified. The question arises as to how the grip force would be adjusted in this situation. Would the subject exert a higher grip force for equivalent tangential loads at the fingers if the effort required to move the upper limb increased or decreased? The main finding was that the subjects used the same ratio between the two forces whatever the context. The same grip force was used for equivalent load generated either by a change of mass, gravity or acceleration despite the fact that it requires different arm motor commands. It suggests that the internal forward model takes the new dynamics of the upper limb and object into account to predict the arm trajectory and in turn the object acceleration.

The study in Chapter 5 examines the importance of cutaneous feedback to the manipulation of hand-held objects. The objective of the present study was to examine how the internal model would compensate for the loss of cutaneous sensation through local anesthesia of the index and thumb. The results show that in the absence of cutaneous feedback, the object slipped between the fingers in 50% of the trials. The temporal coupling between the grip and load forces was preserved but the subjects were unable to maintain their GF at a level high enough to prevent slip. It suggests that, in addition to their role in the detection of slip, the cutaneous afferents provide a tonic signal needed to maintain a constant safety margin during grasping, and at a more theoretical level, they correct and maintain an internal model of the physical properties of hand-held objects.

Chapter 1: Grip-load-force coupling during object manipulation.

1.1 Introduction

The sensorimotor control of natural hand movements has been studied for about 20 years. In the present account, we focus on the control of grasping and manipulating an object with a precision grip when the object's physical properties are stable and therefore predictable. The chapter 1 provides full review about the coordination between the grip force exerted by the fingers on the object and the load force acting on the fingers. The principal features of the grip-load force coupling are described first during lifting and holding objects and then during active arm movements. The adaptation of the grip-load force coupling to a change of friction and weight was studied. An instrumented object, similar to the one presented in Fig. 1.1 was used. It was equipped with strain gauge transducers to measure the grip force (GF) applied perpendicularly by the fingertips on two parallel brass disks that served as the grasping surfaces. An accelerometer mounted on the top of the object recorded the acceleration along its vertical axis (a). The vertical load force (LF) resulting from the gravitational and the acceleration-dependent inertial force was calculated as the product of the mass and the vertical acceleration of the object as measured by the accelerometer. The object center of mass was located midway between the grip surfaces to prevent rotational torque. In most of the studies the position of the object was recorded with an optical encoder.

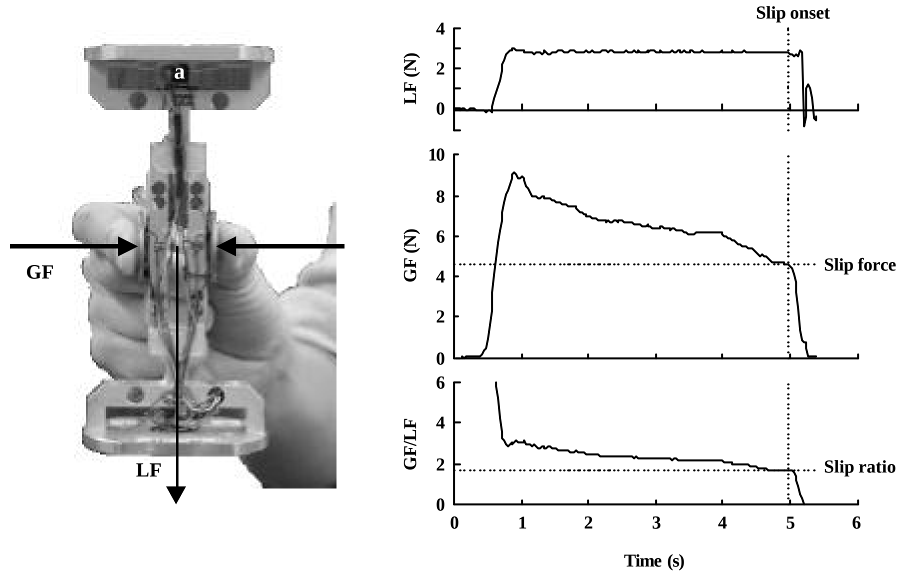

Fig. 1.1: Left: Schema of the instrumented grip object. GF is the normal grip force applied on the object. LF is the tangential load force acting on the object. (a) indicates the accelerometer placed at the top of the object. Right: Grip-load force coordination during lifting and dropping the object. The load force (LF), the grip force (GF) and the force ratio (GF/LF) are shown as a function of time. The horizontal dotted lines represent the slip force and the slip ratio for a coefficient of friction of 0.3. At the vertical dotted line, the GF/LF ratio drops below the slip ratio and the object slips out the fingers. The safety margin is the difference between the force ratio and the slip ratio. (Unpublished data, for illustrative purpose)

1.2 Grip-load force coupling during lifting and holding object.

1.2.1 Safety margin for precision grip

When holding a small object stationary in the air, the grip force (GF) applied normally to its sides is critically balanced in order to prevent either accidental slip caused by insufficient force or to avoid muscle fatigue or crushing the object caused by excessive force. The GF is primarily influenced by the tangential load force (LF) *i.e.* the weight if the object is static, the skin-object friction (CF) and a safety margin factor (SM) related to the individual (Johansson et al 1984). The minimal grip force required to prevent slip is determined by asking the subject to release the grasp slowly until the object is dropped (Fig. 1.1). The GF measured at slip onset is denoted *slip force* and the ratio between the grip and load forces at this time is called *slip ratio*. Half the ratio between the LF and the slip force (Equation 1.1) is used as the approximate coefficient of friction between the skin and the object surface. The factor half is explained by the fact that the LF is distributed on the two fingers.

$$CF = \frac{1}{2}\frac{LF}{SF} \qquad \text{(Eq. 1.1)}$$

The slip ratio depends on the coefficient of friction for the surfaces in contact. For example, the slip ratio for grip surfaces covered with brass is lower than for brass surfaces covered with talc, which is more slippery. The slip ratio corresponds to half the inverse of the static coefficient of friction between the skin and the object surface (Equation 1.2).

$$Slipratio = \frac{SF}{LF} = \frac{1}{2CF} \qquad \text{(Eq. 1.2)}$$

The ratio between the grip and the load forces (GF/LF) provides an index of grasp stability; if the ratio drops below the slip ratio, the object falls (Fig. 1.1). Usually, the GF/LF ratio is maintained slightly above the slip ratio creating a certain safety margin against slip. The safety margin is defined as the fraction of the employed GF/LF ratio that exceeds the slip ratio (Equation 1.3).

$$SM = \frac{GF}{LF} - \frac{1}{2CF} \qquad \text{(Eq. 1.3)}$$

This excess force ratio guards against random fluctuations in the motor system and is scaled in order to economize effort. It constitutes some 10-40% of the actual force ratio depending on subject and context. Nevertheless, to infer the safety margin, we must first assume that the coefficient of static friction is not influenced by the magnitude of the load or grip forces. It appears that for a given texture and for load force magnitudes greater than 1N, this coefficient is fairly constant (Bowden and Tabor 1973; Comaish and Bottoms 1971). It tends to increase for lower forces due to an increased relative contribution of adhesive forces to the friction (Johansson and Westling 1984).

1.2.2 Structure of lifting trial

When an object is gripped, lifted and held in the air, the task can be divided into distinct phases (Fig. 1.2) (Johansson and Westling 1984, 1991). The moment when index finger and thumb first touches the object defines the start of the *preload phase* during which the grip is established (a in Fig. 1.2). The GF is increased while the LF remains close to zero. During the subsequent *loading phase*, the LF rises until it reaches the object weight and the object starts to move (b in Fig. 1.2). Throughout this phase, the GF is increased in parallel with the LF, providing a relatively small and constant safety margin to prevent slips. Then during the *transitional phase*, the object is moved from the table to the intended vertical position (c in Fig. 1.2) and the two forces reach their peak values before stabilizing to a steady level during the *static phase* (d in Fig. 1.2) of the stationary holding period. Finally, the object is replaced on the table (e in Fig. 1.2). After a short delay following the object contact on its supports (f in Fig.1.2), the grip force and the load force declines in parallel until the subject releases the object. This last phase is denoted *unloading phase* (g in Fig. 1.2).

1.2.3 Responses of the tactile afferent units of the skin during a lifting trial

The glabrous skin of the hand contains about 17000 mechanoreceptors distributed in four different categories with distinguished properties (see table 1.1).

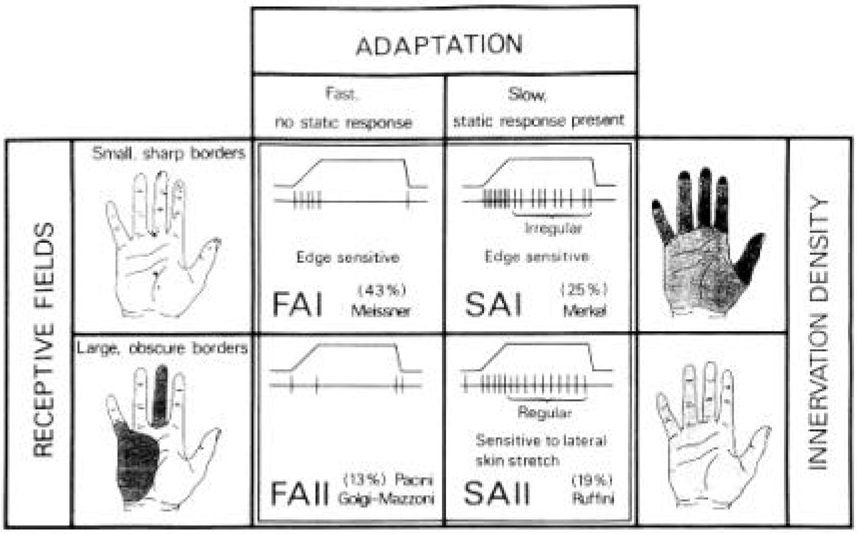

Table 1.1: Types of mechanoreceptive afferent units in the glabrous skin of the human hand (Vallbo and Johansson 1984). The graphs in the middle schematically show the impulse discharge (lower traces) to perpendicular ramp indentations of the skin (upper traces) for each unit types. Two types show fast adaptation (FA) to maintained skin deformation, i.e. they only respond to skin deformation changes. The other two types adapt slowly (SA), i.e. in addition to being dynamically sensitive (particularly the SAI) they exhibit a response related to the strength of maintained skin deformation. The type I units (FAI and SAI) have small and well-defined cutaneous receptive fields. This together with their high densities in the skin of the fingertips makes them suitable to encode detailed spatial information. In contrast, the FAII and SAII units have lower and more uniform densities and are responsive to more remote stimuli, i.e. they have receptive fields that are larger and less well defined. The FA II are responsive to transient mechanical stimulation (50-500 Hz vibrations), whereas the SAII are sensitive to lateral stretching of the skin, i.e. they may encode direction and magnitude of tension profiles in the skin. (From Johansson and Westling 1991)

These sensors provide important information about the physical features of the contacted object but also about the functional outcomes of manipulative actions (Johansson and Westling 1991). For example, the transitions between the different phases of a lifting trial coincide with discrete mechanical events that are encoded in the pattern of signals in the tactile afferent channels (lower part in Fig 1.2). These afferent signals monitor the task progress and trigger the release of the motor commands related to the particular phase. This type of control has been defined by Johansson and its colleagues as “sensory discrete event-driven control”. Fig. 1.2 illustrates burst discharges in tactile afferents associated with different mechanical events of a lifting trial (Fig. 1.2):

FAI responses to contact:

Discharges especially in FAI units indicate the moment of finger contact with the object to confirm that adequate grasp has been made before releasing the motor commands required for further manipulation. This response appears at low GF < 1N. It is caused by the propagating front of skin deformation passing over the receptive fields of the FAI units as and when the GF increases after object contact. Indeed, there is a good correlation between the discharge rates and the speed of the skin deformation front, which is maximum at low GF and minimum at high GF (Johansson and Westling 1991). It is estimated that about 300 FAI afferents are engaged at each digit for GF < 1N. In absence of cutaneous afferent, during digital anesthesia, the preload phase is prolonged and the loading phase takes place later with abnormally high GF.

FAII responses to movement:

Discharges in the vibration sensitive FAII units triggered the end of the loading phase by indicating the lift-off of the object and the end of the unloading phase by indicating the sudden cessation of the movement at touch down of the object on its support. Due to their sensitivity remote to events, the FAII units in the wrist and the palm also show responses when the object starts to move. In this way, the transitional phase take place even if the fingers are anesthetized except if the lift-off is too gentle (Johansson and Westling 1988). In this case, the FAII units fail to respond and the GF increase continues well after the object take-off (Johansson and Westling 1991). The FAII units are considered as event detectors that signal the transitions between successive movement phases. It is estimated that 500 FAII units respond at lift-off (Johansson and Westling 1987).

Tonic SAI and SAII responses:

During the entire manipulation task, there is a tonic input from tactile SAI and SAII units. In accordance with their directional sensitivity to horizontal skin strain, these units register the magnitudes and directions of

LF and its balance with the GF during the manipulative task. It is considered that such tonic input furnish general facilitation of motor commands that account for finger movements.

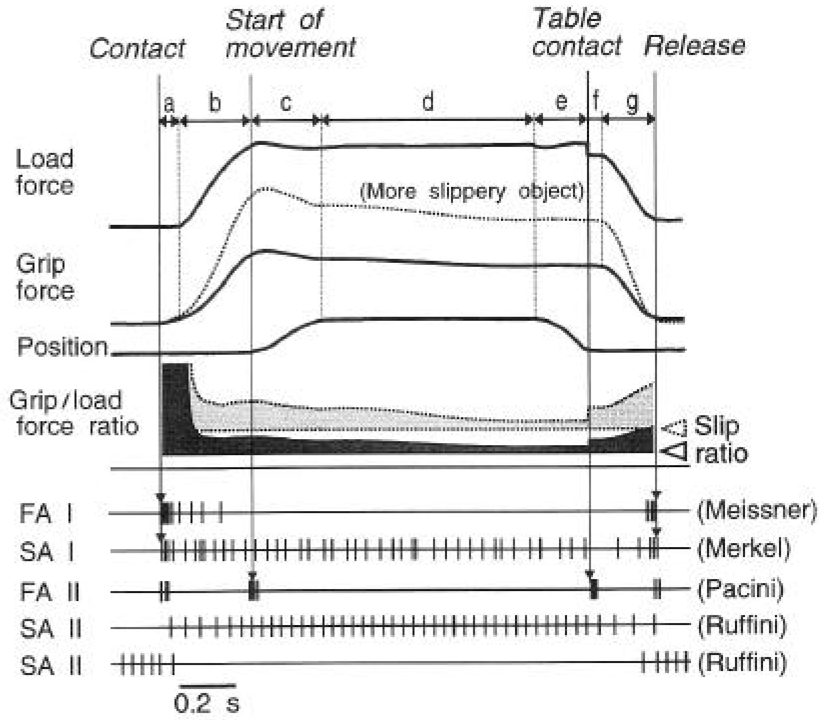

Fig 1.2: General structure of a lifting task. The load force, the grip force, the position, the force ratio and responses of the tactile afferent units of the glabrous skin are shown as a function of time. The dotted curve illustrates the grip force for a more slippery object. The slip ratio is given for the two surfaces. The safety margin is indicated by darker and lighter stippling. (a) the preload phase, (b) the loading phase, (c) the transitional phase, (d) the static phase, (e) replacement of the object, (f) delay before the unloading phase, (g) unloading phase. Vertical arrows indicate the mechanical events at which the FAI and the FAII respond. (Adapted from Johansson and Westling 1991)

1.2.4 Frictional adaptation

Except during the preload phase, the GF and LF increase and decrease in parallel in a nearly linear fashion as though the motor commands were subjected to coordinative constraints, maintaining an approximately constant ratio between the two forces. It has the advantage of reducing the number of degrees of freedom that must be controlled independently (Bernstein 1967). The force ratio represents a flexible parameter that is continuously adapted to the frictional condition between the skin and the object by sensory information (Johansson 1991). Figure 1.3 shows that for equivalent load force (250 g) but different surfaces, e.g. brass (CF=0.8) and brass covered with talc (CF=0.27), the GF is increased as the coefficient of friction (CF) decreases in order to enhance the GF/LF ratio and preserve the safety margin high enough to prevent slip (a-c in Fig. 1.3). It is produced essentially by increasing the GF rate during the loading phase while the LF rate is unaffected (d-e in Fig. 1.3). In this way the slope of the grip-load-force relationship is increased (f in Fig. 1.3). Saels et al (1999) have shown that to transport a slippery object, a higher GF/LF ratio was used by increasing the GF and decreasing the wrist acceleration inducing in turn a reduction of LF.

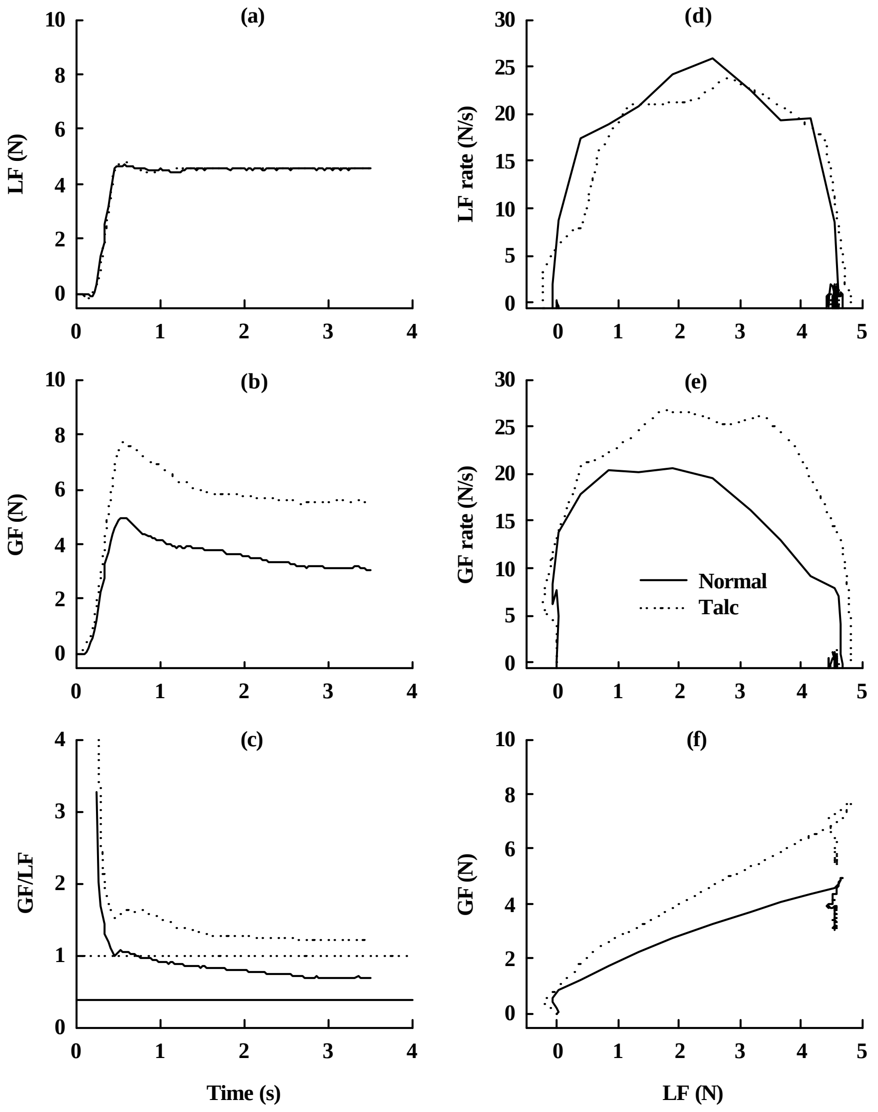

Fig 1.3: Grip-load force coordination during a lifting task with two different skin-object friction: brass (solid line) and brass covered with talc (dotted line). Shown as a function of time are (a) the load force, (b) the grip force, and (c) the force ratio. (d) The load force rate, (e) the grip force rate and (f) the GF are represented as a function of the LF. (Unpublished data, for illustrative purpose)

Motor control of prehension

Before any grip force adjustment, a first approximation of the frictional condition is made on the basis of a “frictional memory” or an internal model that captures the frictional properties of the object related to the precedent lift (Johansson 1991; Flanagan and Johansson 2002). This frictional memory provides an internal representation of the physical features of the object that allows the CNS to set program parameters before the object is touched. This type of control has been defined by Johansson and its colleagues as “anticipatory parameter control”. Initial adjustments to friction occur 100-200 ms after contact, early in the preload phase and are induced by burst discharges of the FAI, FAII and SAI units that convey frictional information (Fig. 1.4 A-B). The new friction information is most likely conveyed by the FAI units since their initial responses are influenced by the surface material; the more slippery the material, the higher the discharge rate (Johansson and Westling 1987). The force ratio adjustment is based on the detection of a mismatch between the actual and the expected sensory event. If the surface is more slippery than expected, the force ratio is increased and it is decreased if the surface is less slippery. If these initial adjustments are insufficient, microslips[1] occur and elicit burst responses in afferent units that re-establish the GF/LF ratio above the slip ratio and update the frictional memory (secondary adjustments) (Johansson and Westling 1987). The latency between the slip and the force ratio increase is on average 74 $\pm$ 9 ms (Fig. 1.4 C-D). This is within the ranges reported for natural tasks, involving automatic initiated responses to external disturbances but still leaves ca. 20-50 ms for CNS transmission and processing (Johansson and Westling 1987). Such latencies, longer than spinal reflexes and shorter than voluntary reaction time seem to be mediated by supraspinal pathways, including the sensorimotor cortex (Johansson et al 1994). Since frictional adaptation is regulated by signals in the tactile afferent as shown by microneurography recordings, it fails during digital anesthesia of the thumb and index finger (Johansson and Westling 1987).

[1] Microslips: small frictional slips localized to only a part of the skin area in contact with the object (Johansson and Westling 1987)

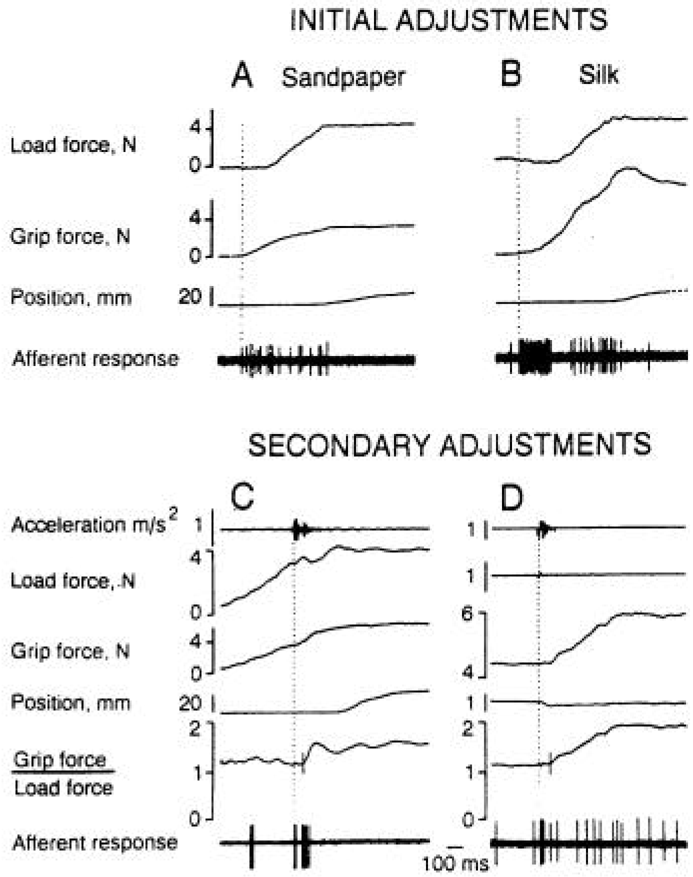

Fig 1.4: A-B Initial FAI responses for two different surfaces (sandpaper and silk). C-D Secondary adjustment following slip during the loading phase (C) and during the static phase (D). The vertical dotted lines indicate the onset of slip signaled by an accelerometer. The short vertical solid lines indicate the upgrading of the force ratio 74 ± 9 ms after the onset of slip (Johansson and Westling 1987).

In the absence of tactile afference, the parallel change of GF with LF is conserved but the GF/LF ratio is no longer adjusted to the frictional condition (Fig. 1.5). The subject uses unnecessarily high GF with rough objects while more slippery objects are often dropped. Interestingly, the stored frictional information acquired with the normal hand during the preceding trial influences the force ratio in the anesthetized side (Johansson and Westling 1984).

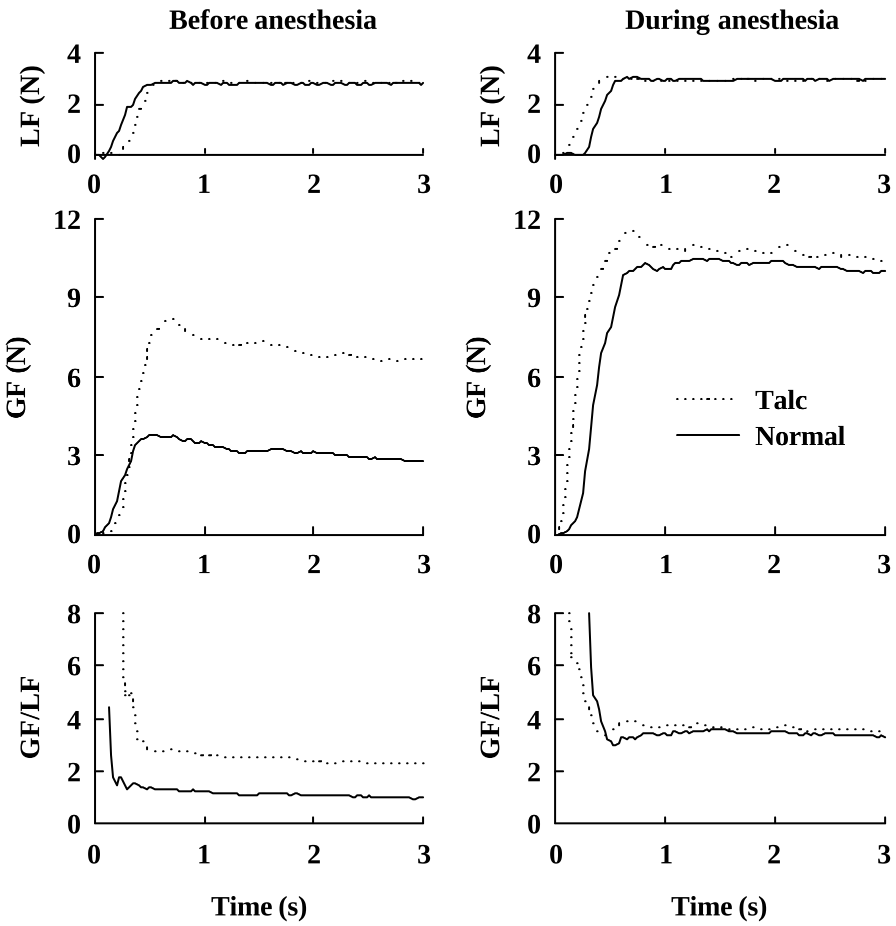

Fig 1.5: Frictional adaptation during a lifting task with intact sensibility (left panels) and with digital anesthesia (right panels). Two different skin-object coefficient of friction are used: brass (solid line) and brass covered with talc (dotted) line. The load force (LF), the grip force (GF) and the force ratio (GF/LF) are shown as a function of time. (Unpublished data, for illustrative purpose)

With different frictional conditions at the thumb and index finger, it has been shown that the GF/LF ratios for each digit are controlled independently (Edin et al. 1992). Both digits still exert the same GF to maintain the object stationary, but the total LF is asymmetrically distributed to reflect the frictional conditions at the separate digits. The LF at the finger touching the smoother surface (e.g. silk) is smaller than at the finger touching the rougher surface (e.g. sandpaper) in order to generate the same safety margins at both digits despite the different frictions (Fig. 1.6:"Initial adjustment"). This unequal distribution of LF generates slight tilt of the object. However in this experiment, as the object had a low center of gravity, this tilting was barely noticeable by visual inspection and was insufficient to induce significant load torque. We will see later in this chapter that torque load can have important contribution in the control of GF especially when the distribution of LF is unequal at the two digits.

Similarly, when a small slip occurs at one digit, the LF is passively redistributed between the fingers, *i.e.* it suddenly decreases at the slipping-digit and increases at the non-slipping digit (Fig. 1.6:"Slip"). This load force redistribution at slip onset increases the GF/LF ratio at the slipping-digit and decreases the force ratio at the non slipping digit. It is followed 80 ms later by a triggered GF adjustment that re-establishes the force ratio at the digit that slipped and restores the force ratio at the other one (Fig. 1.6: "Slip-triggered adjustment"). The anticipatory control of the GF/LF ratio is thus digit specific. These digit specific adjustments are also observed when two subjects grasp the same object (Burstedt et al 1997). It suggests that grasp stability can be assured by anatomically independent neural mechanisms and effector systems that communicate through sensory input related to the mechanical events in the hand-object interface. This also reinforces the theory that the distribution of forces among digits to assure grasp stability is controlled by a “low level” neural mechanism that is digit specific (Edin et al. 1992, Johansson and Cole 1994). Higher level controls are more directly related to the overall goal of the task e.g. the total lifting and normal forces required to lift an object (Johansson and Cole 1994).

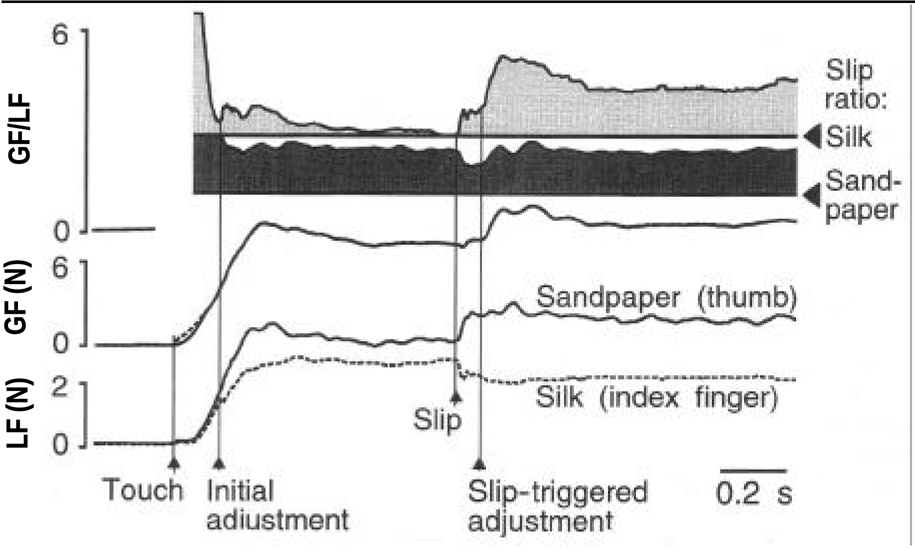

Fig 1.6: Independent control of finger tip forces. The force ratio, the grip force and the load force are shown as a function of time. The thumb is in contact with sandpaper and the index finger with silk (si). At "initial adjustment", the load forces are distributed between the two fingers so that an adequate safety margin is maintained at each digit. The slip at the index finger resulted in a rapid decrease of LF at that digit and a concomitant increase of LF at the non-slipping digit. About 70ms later, GF increased such that the ratio at the digit that had slip increased and the ratio at the nonslipping digit was effectively restored. (Adapted from Edin et al. 1992)

1.2.5 Weight adaptation

Sensory information about the weight is not available before the object is lifted. Therefore, anticipatory control of isometric force during the loading phase is necessary to produce accurate and smooth vertical lifting movement. (Johansson and Westling 1991). As with the frictional properties, there is an internal representation also of the object's weight ("Weight memory") which is acquired through previous manipulation. Through visual or haptic[2] identification, the internal model of the weight of the perceived object can be retrieved allowing the CNS to preprogram adequate parameters before the sensory feedback is available. The initial GF adjustment to the

[2] Haptic perception: Perception through the hand based on tactile and somatosensory information (Flanagan and Johansson 2002)

object's weight reflects predictions based on sensorimotor memory from previous lift with similar object.

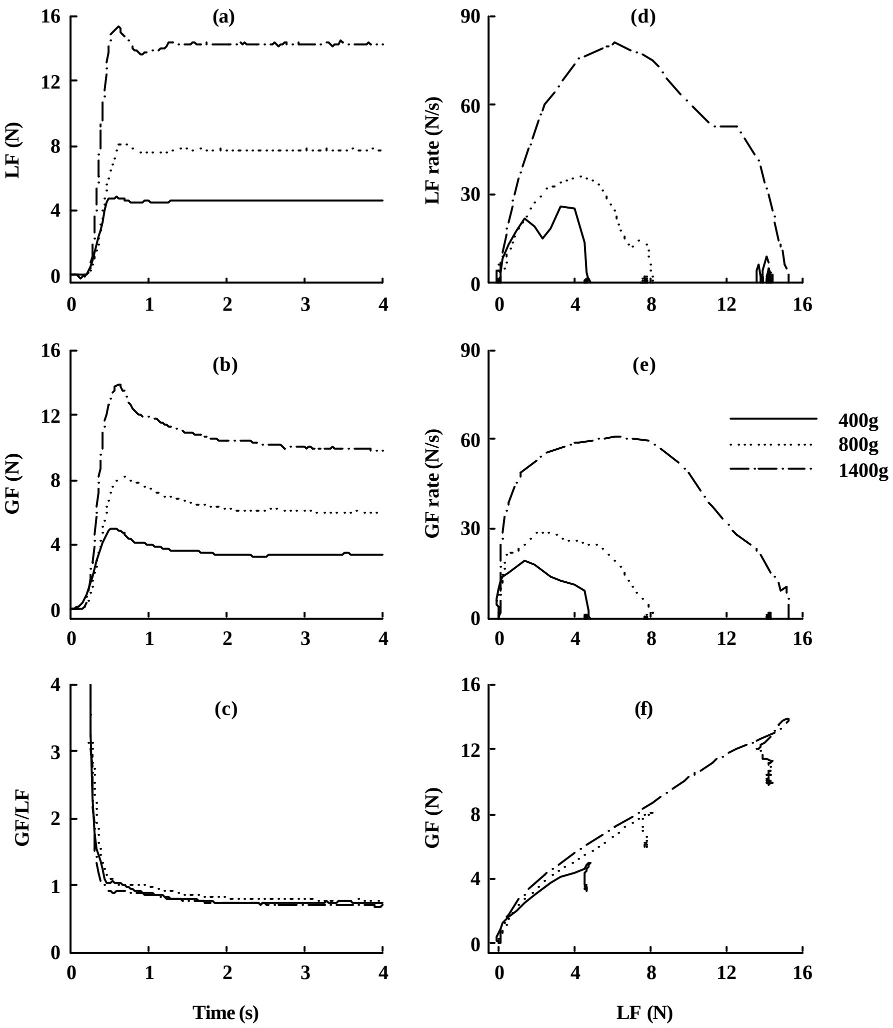

Fig 1.7: Grip-load force coordination during a lifting task with three different weights: 400g (solid line), 800g (dotted line) and 1400g (dashed line). Shown as a function of time are (a) the load force, (b) the grip force and (c) the force ratio. (d) The load force rate, (e) the grip force rate and (f) the GF are represented as a function of LF. (Unpublished data, for illustrative purpose)

Figure 1.7 shows that for different masses, e.g. 400, 800, 1400g, the GF is increased or decreased in order to keep the same force ratio for heavy or light object, respectively (a-c in Fig. 1.7). The rate profiles (first time derivative) of the LF and GF during the loading phase are smooth and single peaked, scaled to the object's weight (d-e in Fig. 1.7). The GF rate is maximum during the middle of the loading phase and it approaches zero when the LF required to lift the object is expected to be reached. The LF rate increases when the object's weight increases so that lighter and heavier objects tend to be lifted in about the same amount of time. Gordon et al (1993) observed however a longer loading phase duration for the heaviest objects. The slope of the grip-load force relationship tends to remain the same whatever the weight (f in Fig. 1.7).

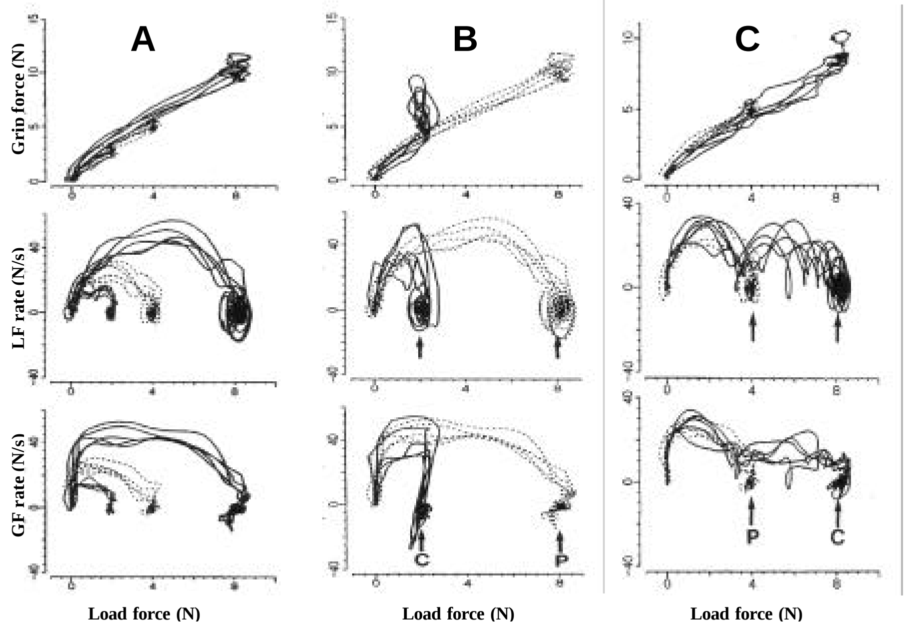

Fig 1.8: Correct program for different weights (A). Erroneous program when the weight is lighter (B) or heavier (C) than expected. The grip force, the load force rates and the grip force rates are in relation to the load force. (A) Five sample trials adequately programmed for 200, 400 and 800g. (B) Five sample trials adequately programmed for 800g (dotted line) and five lifts with 200g programmed for 800g (solid line). (C) Five sample trials adequately programmed for 400g (dotted line) and five lifts with 800g programmed for 400g (solid line). C and P indicate the load force at which the object starts to move in the current and previous trial respectively. (Adapted from Johansson and Westling 1988).

Nevertheless, as we have all experienced, our force prediction is sometimes erroneous. If the weight is lighter than expected, the load and grip force rates are too high when the LF suddenly overcomes the force of gravity (Fig. 1.8B). An abrupt termination of the loading phase is triggered a few milliseconds (ca. 80-110 ms) later by sensory feedback (FAII) about the lift-off. However, the delays in the feedback loop are long enough to cause a pronounced positional overshoot (Johansson and Westling 1991). On the contrary, if the weight is heavier than expected the load and grip force rates are too low to overcome the force of gravity and the lift-off does not occur at the predicted LF. The absence of movement is signaled by a lack of sensory responses at this expected time. This triggers a stepwise increase of the two forces until sensory information about the movement triggers the end of the loading phase (Fig. 1.8C). Multi-peaked profiles of the force rates are observed suggesting a probing strategy rather than anticipatory adjustment. The lift-off of the object is triggered by the vibration-sensitive FAII units located throughout in the hand (Johansson and Westling 1988, Johansson and Cole 1994). A compensatory motor command is thus triggered as soon as there is a mismatch between an expected sensory event and the actual sensory input.

For commonly lifted objects (e.g. a can of soft drink, telephone book…), the forces are adequately adjusted from the first trial before the availability of direct information about the object's weight (Fig.1.8bis) (Gordon et al 1993). For unfamiliar objects, the loading phases are longer and lower LF rates are used during the few first trials. A probing strategy is adopted as though the subject expected a lighter object (see above). Adaptation to new weight occurs essentially after one lifting trial and can be retained for further manipulation with similar object. It is noteworthy that the weight information for novel object is assimilated more easily when its density is similar to the most commonly handled objects than when its density is unusual (Gordon et al 1993).

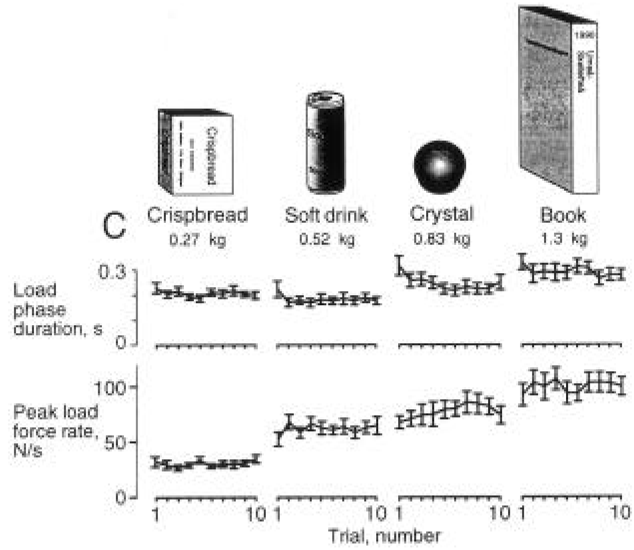

Fig. 1.8bis: Anticipatory parameter control for lifting commonly handled objects of different shapes, weights and densities. The loading phase duration and the peak load force rate are displayed for each of ten consecutive lifts of each object (data averaged across subjects). (Adapted from Gordon et al. 1993)

In conclusion, the memory information about object's weight is rapidly acquired, robust, accurate and can be retrieved through visual identification of the target object. Vision is a very strong source of feedforward information (i.e. available in advance of the onset of movement), which allow the CNS to program the appropriate motor command according to the properties of the object. Interestingly, the information derived from visual cues can lead to the size-weight illusion. There is a relationship between the visual size cues and the weight that predicts that the larger the object, the heavier it is. So, for three objects with identical weight but different sizes, the peaks of GF and LF as well as the rates of both forces during the loading phase increased with object size as though the larger object was heavier (Gordon et al 1991a). The lift-off of the larger box will occur earlier than expected whereas the lift off of the smaller object will not occur when predicted. The difference between the actual sensory feedback obtained by tactile afferent and the expected sensory feedback based on the internal representation of the object leads to the illusion that the smallest object is the heaviest. Compensatory, reflex mediated adjustments in GF will be triggered in either case to scale the GF to the actual weight. After a few trials, the "weight memory" of the objects will be updated and the influence of the visual size cues on the feedforward force control will be reduced. However even after 20 lifts, subjects still reported that the small object was heavier while accurately predicting the fingertip forces. It suggests that there is still a mismatch between erroneous perceptual predictions and the actual sensory feedback. The same illusion is produced when the size information is acquired by haptic exploration of the object (Gordon et al 1991b). Hence, tactile, proprioceptive, haptic, and visual information contributes to the formation of the object internal representation.

1.2.6 Torque adaptation

Usually, when manipulating objects, the grasp points are chosen to pass approximately through the object center of mass (CM) in order to prevent rotational torque. When the grip axis (i.e. line joining the tips of the thumb and the index finger in a precision grip) does not intersect the object CM, the gravitational force (during lift) and inertial force (during transport) acting on the CM produce load torques tangential to the grasp surface. It coincides with the product of the forces and the perpendicular distances of their lines of action between the CM and the grasp axis (Wing and Lederman 1998). The presence of torque tends to rotate the object and requires greater GF in order to avoid rotational slip. The question arises, whether the GF will be adjusted to the torque change by feedback or feedforward mechanisms. Johansson and al (1999) have analyzed the control of grasp stability when rotating an off-axis grasped object by a pronation movement (Fig. 1.9 Upper part). The torque load was maximum when the grip axis was horizontal and minimum when it was vertical. They have shown that when rotating an object whose CM does not lie on the grip axis, the GF is changed in parallel or slightly ahead of the load torque induced by the rotation movement (Fig. 1.9). The torque load and the grip force increased when the object-moment increased whatever the rotation angle (Fig. 1.9). There was a linear relationship between the grip force and the torque load. This coordination was preserved in absence of tactile afferent suggesting feedforward rather than feedback control (Johansson et al 1999). Moreover, as with the slope of the grip-load force relationship in lifting an object with different textures, the slope of the GF-torque relationship increased with smoother objects (Kinoshita et al 1997).

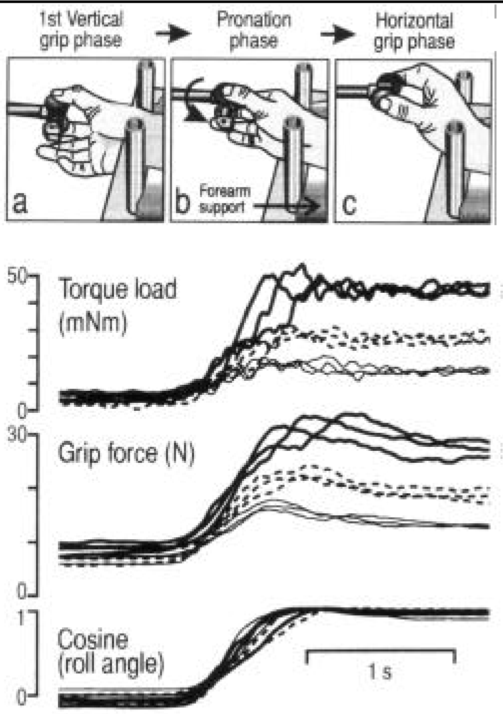

Fig 1.9: Force-torque coordination with three different object moment: 90mNm (thick solid line), 50mNm (dashed line) and 30mNm (thin solid line). (Upper part) Description of the pronation task. (a) For some 2s the object was held with a vertical grip axis. (b) An auditory signal prompted the subject to rotate the object by a pronation movement. (c) The object is held with a horizontal grip axis for 2 s. (Lower part) The torque load, the grip force and the object rotation (roll) angle are shown as a function of time. (Adapted from Johansson et al 1999).

It has also been shown recently that the slip force will not depend simply on the additive effects of tangential force (Ft) and tangential load torque (Tn) acting on the fingertips but it will rather depend on the interaction between both. The minimum GF required to prevent rotational slip with both torques and tangential force increases with a slope that depends on the skin-object friction coefficient (Fig. 1.10). On the basis of data obtained from the human thumbs and index fingers, Kinoshita et al (1997) have defined a simple mathematical function (Equation 1.4) to predict the slip force for different tangential torque and force combinations related to the skin-object coefficient of friction (CF). In their model, a and b were determined as 0.13328 mm-1 and –0.01143 N-1mm-1, respectively.

$$SlipForce = \frac{1}{CF}(Ft + a|Tz| + bFt|Tz|) \qquad \text{(Eq. 1.4)}$$

It appears thus that the consequences of an offset grasp axis about the center of gravity is taken into account in planning movement suggesting that the sensorimotor memory for an object also include a representation of the center of mass.

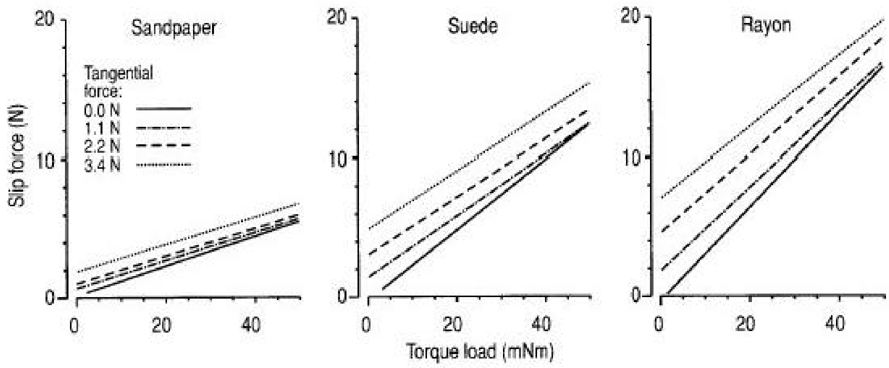

Fig 1.10: Relationship between the slip force and the load torque at different tangential load and for three different surfaces. The slope of the linear relationship between the slip force and the load torque increases as the coefficient of friction decreases (Rayon is the most slippery). (Adapted from Kinoshita et al. 1997)

1.2.7 Development of human precision grip

The parallel coordination between GF and LF in lifting and holding small objects is not innate.

At birth, tactile and proprioceptive reflexes control the infant grasping. The closure of the hand is induced by stimulation of the palm. This innate grasping is probably managed by a genetically defined neural network in the spinal cord or the brain stem (Forssberg et al. 1991). At 4 months of age, the voluntary palmar grasp involving all the fingers appears.

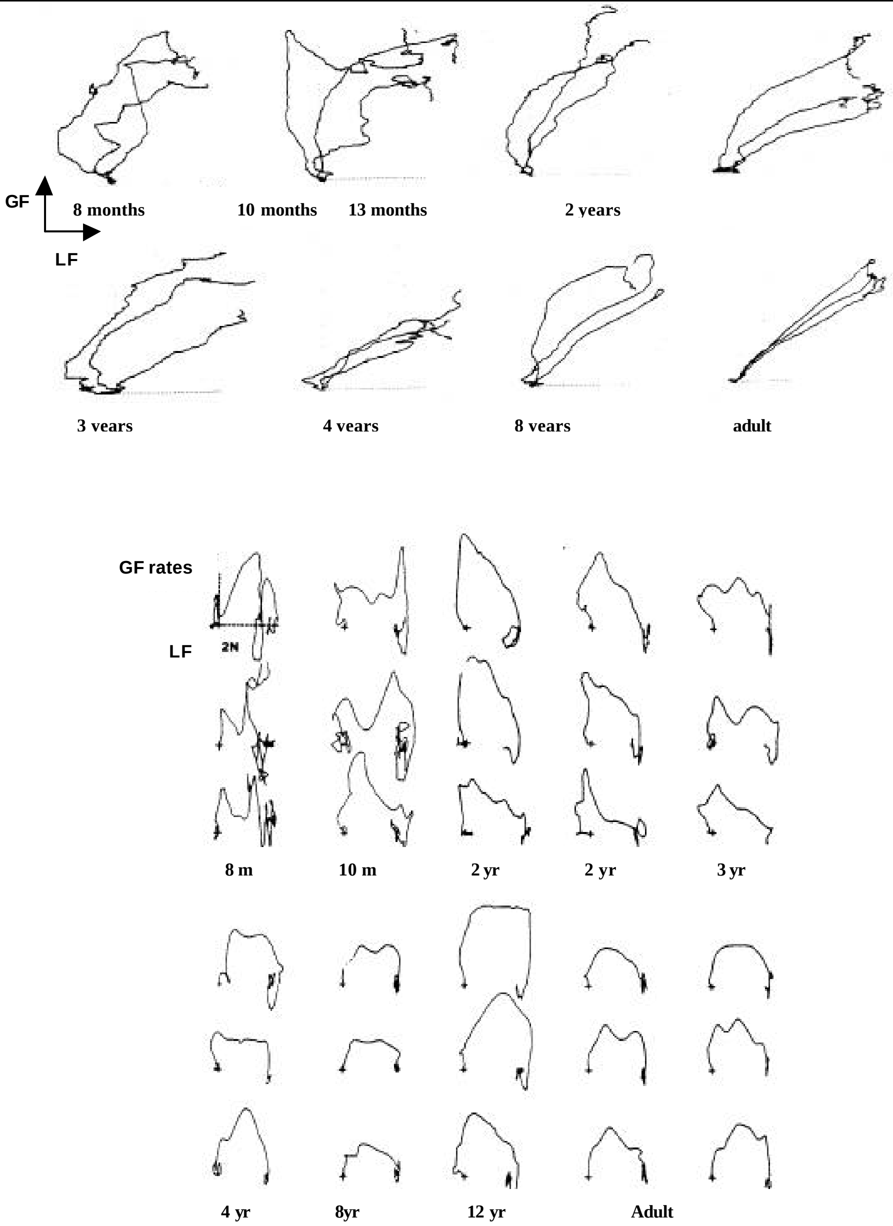

Fig 1.11: Development of the grip-load force coupling. (A) The Grip-load force relationships at different ages are illustrated in 3 trials. (B) The grip force rates are shown as a function of the load force at different ages. Three trials are illustrated for each age group beneath each other. (Adapted from Forssberg et al. 1991)

Then, independent movements of the fingers progressively develop and the precision grip occurs by 10 months. The development of voluntary grasping seems to involve the maturation of the corticospinal tract while the motor cortex seems to play an active role in the formation of the grip-load force synergy. Indeed, the parallel grip-load force coordination observed in the adulthood is not innate (Fig. 1.11).

During the preload phase of a lifting task, small children need several trials to establish a stable grasp reflecting an inefficient utilization of the sensory information at contact. The delay between thumb and index contact is longer than in adults until 18 months of age and the preload phase duration remains about twice as long in children below 3 years of age. This suggests an immature control of hand closure and inefficient triggering of the motor commands by cutaneous afferents. Usually, a reversed coordination is observed, i.e. the object is pressed downward against the table inducing a large GF and a negative LF. During the loading phase, the GF and the LF are not generated in parallel but sequentially (Fig. 1.11A). Indeed, the greatest part of the total GF is generated during the preload phase. Moreover, the GF is increased in steps with multiple force rate peaks until two years of age at which time a bell-shaped profile progressively appears (Fig. 1.11B). The rate profiles are skewed to the left because GF is generated well before the increase of LF. This indicates that children below 2 years old adopt a probing strategy and that they do not program the forces in anticipation of the object weight. As they grow up, the duration of the preload and loading phases are reduced and the GF is progressively increased in parallel with the LF suggesting a change from a feedback control to a weight-related anticipatory parameter control of the forces and a shortening of peripheral reflex latencies. The use of visual information to associate the size with the weight for classes of related objects emerges at 3 years of age (Gordon et al 1992). However they are unable to suppress the influence of the visual size information in situations in which weight and size do not reliably co-vary. Vision plays a strong role on motor coordination in children. Some capacity to adapt the GF to the skin-object friction appears between 1 and 2 years but these young children need repetitive trials to update their force coordination to new frictional conditions while adults need only one lift (Forssberg et al. 1995). Finally the large intertrial variability observed for children may be explained by assuming that the central nervous system tests several spatiotemporal patterns before selecting the best one. Adult levels of performance are typically not achieved before the age of 8-10 years (Forssberg et al. 1991).

1.2.8 Conclusion

In conclusion, relevant motor program parameters are set prior to the release of the muscle commands necessary to adapt the GF to frictional and weight condition. This feedforward command is based on an internal model of the current properties of the object (weight, frictional properties, size and form, moment of inertia and density) gained during previous lifting. Objects are identified by visual or haptic cues and the appropriate motor command parameters are automatically set according to the object properties. These sensorimotor memories are intermittently updated by sensory information. This update takes place, as there is a mismatch between the actual feedback from the tactile afferent of the hand and the somatosensory input predicted by the feedforward mechanism (Johansson et al 1999). This avoids stability problems due to the long delay between the release of the motor command and the feedback from the command. However, sensory information remains important in the development of these anticipatory changes in GF. Tactile afferent are involved in maintaining a constant GF/LF ratio during manipulation and mediate reflex responses to unexpected perturbations that might lead to slip.

1.3 Grip-load force coupling during active movements with a hand-held load.

1.3.1 Definitions

Up to this point, we have described object manipulation in “static” conditions where subjects lift an object 1 or 2 centimeters up and hold it steady a few seconds before replacing on its support. This task does not generate significant object acceleration and it is postulated that the load force remains equal to the object weight (in the absence of load torque). Let us consider now the situation where subjects actively move the object in the air. Periods of acceleration and deceleration will induce significant inertial forces, acting on the object in addition to the force of gravity. Indeed, when an object is moved a force proportional to its acceleration must be applied to overcome its inertia. The resultant LF is thus calculated as the product of the object mass and the vectorial sum of the gravitational and object accelerations (Equation 1.5).

$$LF = m(\vec{g} + \vec{a}) \quad \text{(Eq. 1.5)}$$

For example, in upward point to point movement, the LF function first increases above the object weight to accelerate the object up, then decreases below the weight, to decelerate the object and finally equals the weight when the object is stopped (Fig.1.12).

In order to maintain stability during arm movements with a hand-held load, the question arises as to how GF is modulated with the LF changes induced by the inertial loading. Knowing that 60-90 ms are required for tactile afference to trigger a GF response to load force perturbation and knowing that arm movement velocity can reach 1m/s, it is unlikely that the motor system relies only on reflex mechanism to control GF during voluntary movements (Flanagan and Wing 1993). There are two contrasting possibilities for the controller to adjust GF during LF changes. First, it might calculate a steady level of GF high enough to prevent slippage for any load by predicting the maximum LF expected during movement. Second, the GF might be modulated in parallel with the predicted load force fluctuations depending on the movement direction. The latter would require anticipatory adjustments of grip force for changes in load force arising from arm kinematics.

This issue is examined in the following sections for point to point movements and during cyclic arm movements in the following sections.

1.3.2 Point-to-point movements

In upward and downward movements with a hand-held-load, Flanagan and Wing (1993) have shown that GF is modulated in phase with LF fluctuations from the very first trial. In upward movement, the GF rises with the initial increase of load force as the object is accelerated up. In downward movement, the GF is increased later in the deceleration phase of the movement (Fig. 1.12).

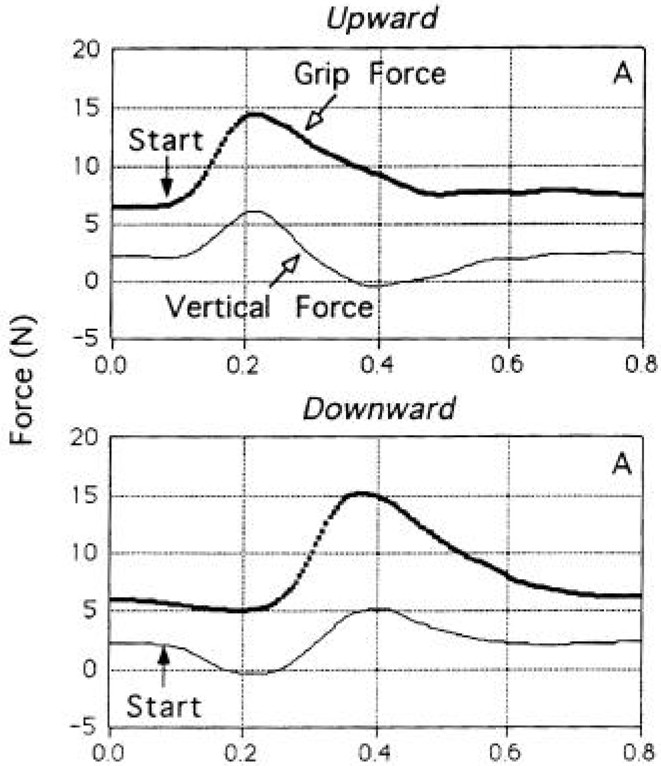

Fig. 1.12: Grip force and vertical records of an upward (top panel) and a downward (bottom panel) point-to-point movement. The trials are aligned on movement onset. (Flanagan and Wing 1993)

The time of the GF peak is strongly correlated with the time of the corresponding LF peak suggesting a strong temporal coupling between the two forces. The grip force is programmed in anticipation of the fluctuations of load induced by voluntary manipulations of familiar object. Thus, not only the object physical properties (e.g. friction, weight) are anticipated but also the consequences of our own actions. This prediction about kinematics of the forthcoming movement, necessary for determining the required GF is probably based on an internal forward model of the motor apparatus and external load. It is also noteworthy that the qualitative pattern of the grip-load force coupling is invariant according to a variety of grips (e.g. inverted or two-handed grips) and independently on the articulators moving the object (e.g. jumping) (Flanagan and Tresilian 1994). It suggests that the underlying anticipatory processes may be relatively high level since they do not depend on any particular skeletomuscular configuration. However the GF modulation does not seem to be directly accessible to conscious control. Indeed, the grip-load force coupling is rarely perceived by the subjects and is difficult to suppress by voluntary control. Even with visual feedback about their force, subjects were unable to keep the GF constant at a level high enough to prevent slippage during the movement (Flanagan and Wing 1993, 1995).

To determine if the GF commands are based on an internal model and not rigidly linked to the commands for arm movements, the GF-LF coordination was examined during movements of an acceleration-dependent inertial load, a velocity-dependent viscous load, and an elastic load that largely depended on position (Flanagan and Wing 1997). In each load condition, GF was modulated in parallel with and thus anticipated the LF that depends on both the dynamics and the kinematics of the object. The properties of the load and the trajectory of the hand were predicted based on an internal model of the external load (object properties) and the motor apparatus (arm). To adjust adequately the GF under the different load conditions, people had to alter the mapping between the motor command driving arm movements and that driving the grip force.

1.3.3 Cyclic vertical arm movements

The robustness of the GF-LF coupling has been highlighted by Flanagan and Wing (1995) during cyclic vertical arm movements with a hand-held load. While in this condition, there may be additional cost involved in modulating GF, the parallel coordination between GF and LF persists throughout cyclic movements. GF is increased and decreased as LF rises and falls according to the arm accelerations. Figure 1.13 shows that when an object is moved up and down, the LF continuously fluctuates around the object weight (a-b in Fig. 1.13). It is maximum at the bottom of the trajectory when the gravitational and the object accelerations act in the same direction. The LF is minimum at the top of the trajectory when the object acceleration is opposite to that of gravity. In order to restrain the object, the GF is automatically modulated in parallel with the LF fluctuations and is always greater than the slip force allowing a adequate safety margin to be achieved (c in Fig. 1.13). It prevents the object from slipping without excessive muscular effort. Flanagan and Wing (1995) showed that the maximum correlation between the two forces signals is high, on averaged 0.85, and occurred at a mean time of –4.8 ms indicating that LF slightly led the GF. The maxima of LF are always precisely synchronized with a single peak of GF so that the force ratio is minimum and highly reproducible at these times (d in Fig. 1.13). In contrast, when the LF is minimal the force ratio is less constant and reaches its maximum because of an incomplete release of GF. Consequently, the safety margin reflected by the difference between the force ratio and the slip ratio is not constant throughout the movement.

The extent of the GF modulation depends on both the frictional condition and the object accelerations.

Friction adaptation

Figure 1.14 (left part), shows that for equivalent LF fluctuations but different surfaces, e.g. brass (CF=0.76) and brass covered with talc (CF=0.24), the mean level of GF and the amplitude of the GF modulation increased for more slippery surfaces so that the minimum of the force ratio is significantly greater than for rougher objects (a-c in Fig. 1.14). In general, both the slope and the intercept of the grip-load force relationship are increased when moving smooth objects (d in Fig. 1.14) (Flanagan and Wing 1995). The right part of this figure also shows that in the absence of cutaneous afferents, the GF is still modulated in phase with the LF fluctuations but that the level of the GF modulation is no longer adjusted to the friction condition (b in Fig. 1.14 right).

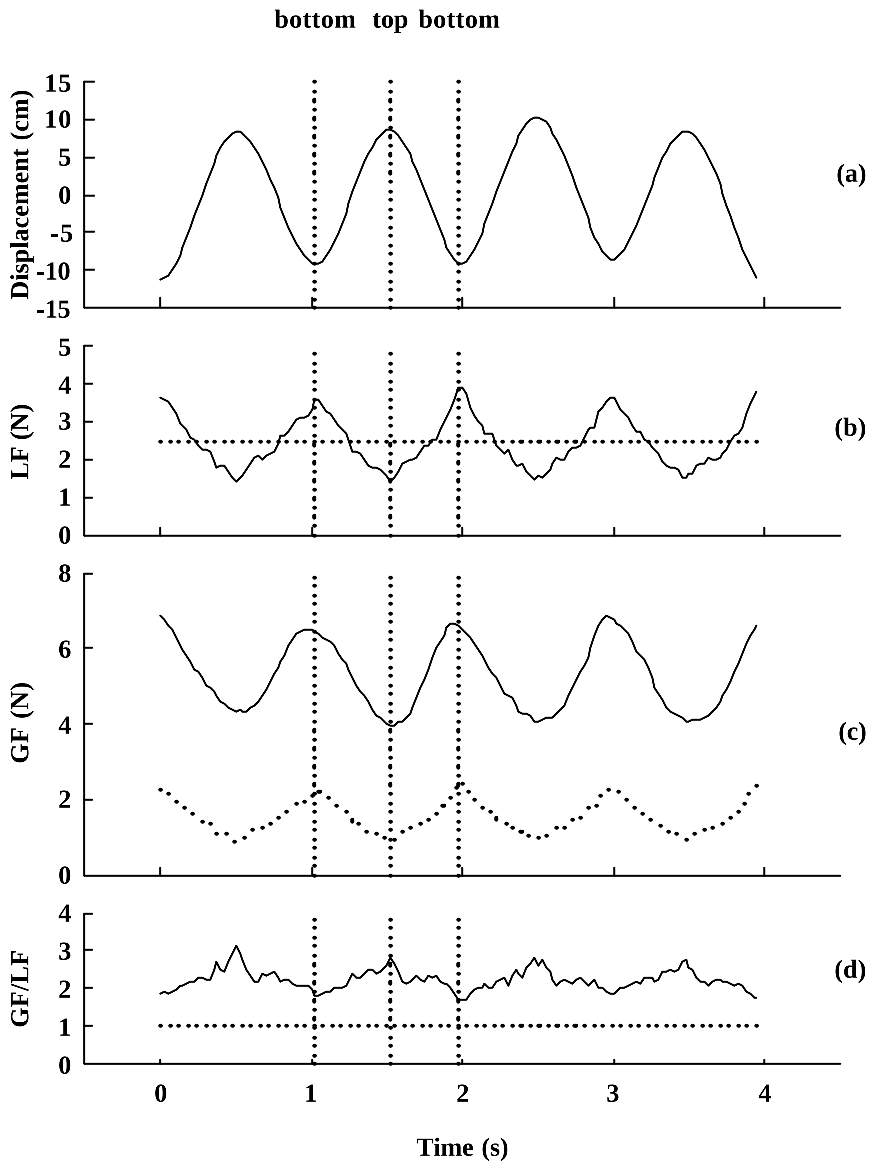

Fig 1.13: Grip-load force coupling during cyclic arm movement with a hand held load. The object displacement (a), the load force (b), the grip force (c) and the force ratio (d) are shown as a function of time. The dotted horizontal line in panel (b) is the object weight (2.5N). The dotted curve in the panel (c) illustrates the slip force. The dotted horizontal line in panel (d) is the slip ratio. The three vertical dotted line indicate the bottom and the top of the trajectory during one cycle of movement. (Unpublished data, for illustrative purpose)

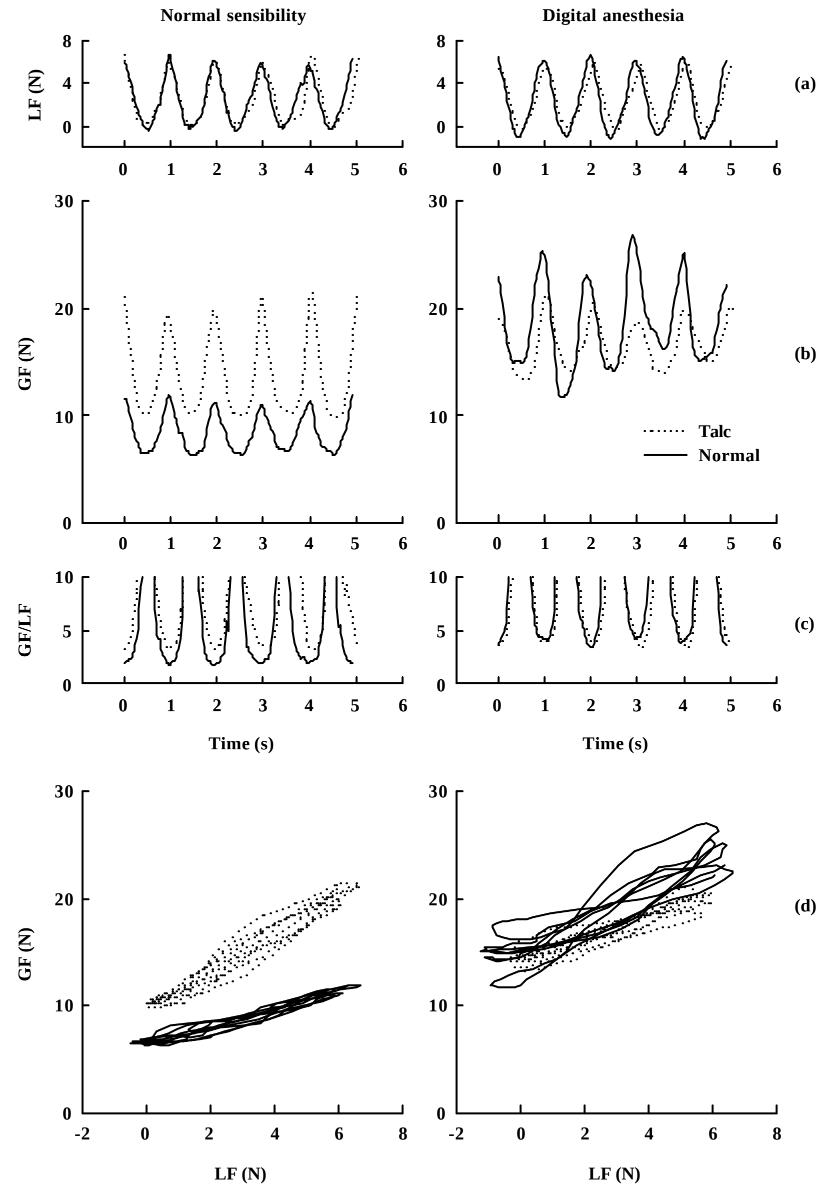

Fig 1.14: Frictional adaptation during cyclic vertical arm movement with a hand-held load with intact sensation (left panels) and with digital anesthesia (right panels). Two object surfaces were used: brass (solid line) and brass with talc (dotted line). Shown as a function of time are the load force (a), the grip force (b) and the force ratio (c). The grip-load force relationship is illustrated in panels (d). (Unpublished data, for illustrative purpose)

Acceleration adaptation

For greater LF fluctuations due to larger arm accelerations, GF is still modulated in parallel with LF even at movement frequencies as high as 3.5 Hz (Blakemore et al 1998). In general, the intercept of the GF-LF relationship increased with the frequency of movement, while the slope tends to slightly decrease for faster movements (Flanagan and Wing 1995). Figure 1.15 shows the grip-load force coupling when oscillating a 200 g load at 1 Hz, on a distance of either 20 cm (Solid trace) or 40 cm (Dotted traces). As the amplitude of the LF fluctuation is doubled, the modulation of GF is increased so that the GF/LF ratio is slightly greater (a-c in Fig. 1.15). The intercept of the grip-load force relationship is increased (d in Fig. 1.15).

Across different conditions, the GF gain and offset can be thus varied independently suggesting the influence of high-level motor commands generating GF on the basis of predicted load and surface slipperiness. However, if the subjects were instructed to increase their GF above the maximum required for the entire task, the slope of the GF-LF relationship decreases but is still positive meaning that the GF modulation persists even if unnecessary to prevent slip. This automatic coupling suggests the influence of some low-level mechanisms not accessible to consciousness (Flanagan and Wing 1995).

Predictive GF modulation can also be obtained by generating cyclic fluctuations of LF with the other hand pushing directly on the object (Fig. 1.16). This suggests that the motor command sent to one hand can be used to produce precise predictive modulation in the other hand (Blakemore et al 1998). By contrast when a cyclic LF function is externally produced by a robot, no predictive GF modulation is seen. The peaks of GF lag ca. 100 ms behind the peaks of LF with a concomitant increase in the GF baseline and in the GF amplitude in order to prevent slip to occur during this delay. Similar lack of anticipation is observed in self-produced movement when the LF is indirectly generated by the left hand via a joystick. Thus self-generation in itself is not sufficient to produce predictive GF modulation, the sensory feedback to the two hands has to obey the physical laws encountered in normal object to allow GF prediction. It suggests that an internal model of the normal physical properties of the objects exists and is used to determine the extent to which the two hands are manipulating these objects (Blakemore et al 1998).

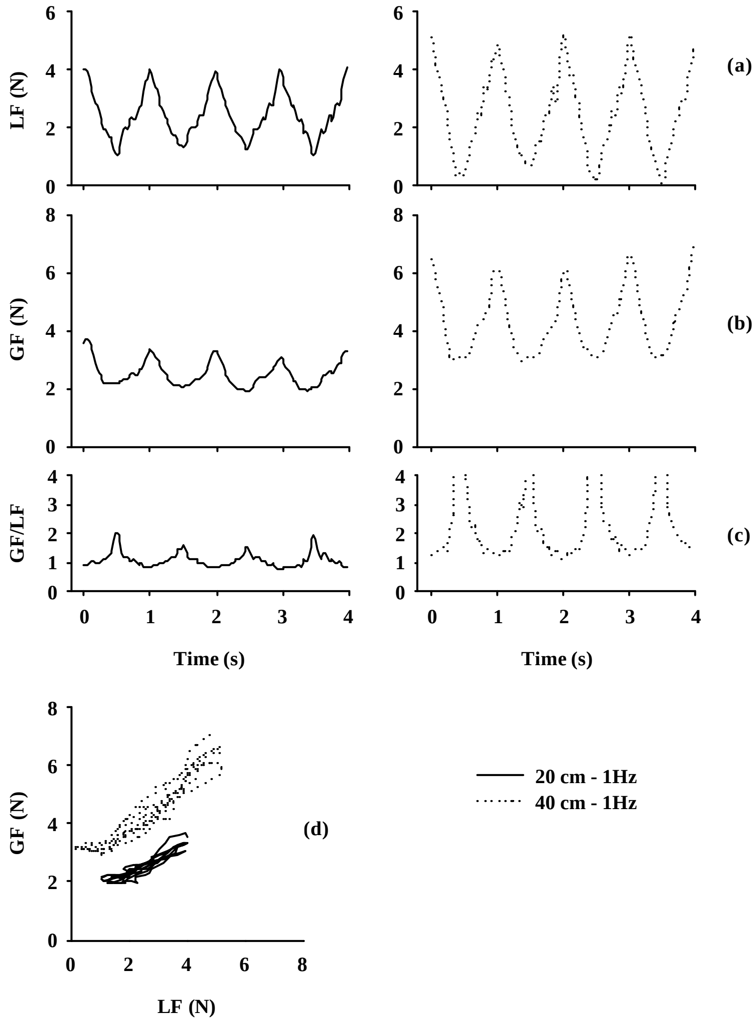

Fig 1.15: Grip-load force coupling during cyclic vertical arm movements with a hand held load at different arm acceleration. A 250g load is moved up and down at a frequency of 1Hz on a distance of either 20cm (solid line) or 40 cm (dotted line). Shown as a function of time are the load force (A), the grip force (B) and the force ratio (C). The grip-load force relationship is illustrated in panel (D). (Unpublished data, for illustrative purpose)

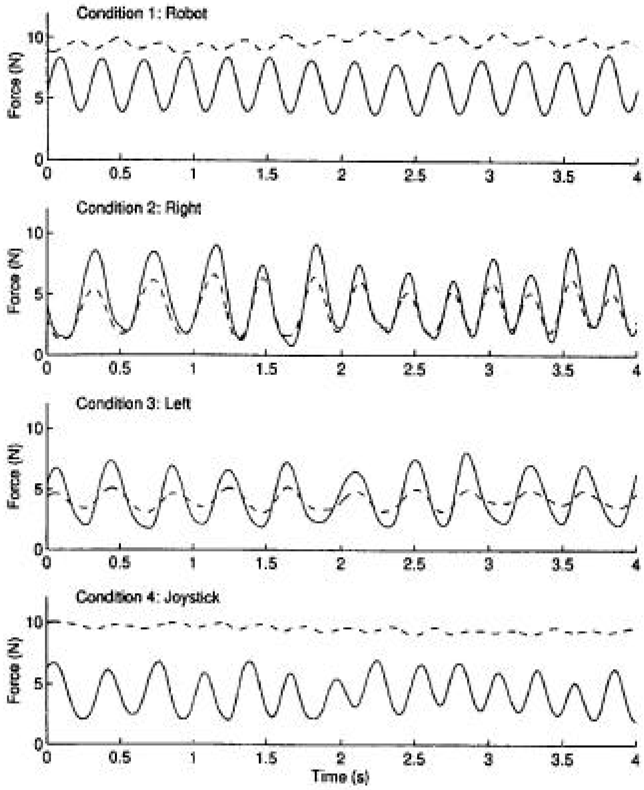

Fig. 1.16: Typical example of grip force (dashed line) and load force (solid line) traces for four conditions taken from a single subject tracking a frequency of 3.5 Hz. In condition 1, the object was attached to a robot that produced the load force waveform. In condition 2, the load force waveform was self-produced by the right hand restraining the object. In condition 3, the load force waveform was self-produced by the left hand while the right hand restrained the object. In condition 4, the load force waveform was produced by a low-friction joystick. (Adapted from Blakemore et al 1998)

Chapter 2: General computational motor control

2.1 Introduction

The experimental data reviewed in the previous chapter gives evidence of the contributions of both feedforward and feedback control to the generation of skilful object manipulation. On the one hand, the extensive functional impairment observed after digital cutaneous anesthesia highlights the importance of sensory feedback as discrete-event, sensori-driven control (Johansson and Westling 1984). The tactile afferent signals the completion of the different manipulative phases, it triggers corrective actions in response to slips and it updates the internal representations of the object underlying the feedforward control (Johansson and Cole 1994). Tactile feedback is also essential when restrain an "active" object (e.g. a dog's leash) that generates unpredictable destabilizing load forces. On the other hand, because of the time delays inherent in feedback control loops, feedforward mechanisms are crucial to successfully performing fast smooth movements. The feedforward component provides some estimate of the appropriate motor command required to allow the skeletal system to make the desired motion. In this way, the motor command can be defined in advance of the onset of movement without the need for sensory feedback. Precise grip-load force coupling would thus result from a trade-off between feedforward and feedback control where the motor command defined prior to the movement is supervised by a powerful feedback loops that adjust and refine it.

In this chapter, we will first describe some important issues, which arise in considering the general computational schema of the human motor control. In the second part, we will apply these concepts to the motor control for the grip-load force coupling during object manipulation based on the different models already proposed in the literature (Kawato 1999, Flanagan and Wing 1996, 1997, Witney et al 2001). This will provide a theoretical framework to introduce the objectives of this thesis.

2.2 Computational motor control

2.2.1 Definitions

In the framework of motor control, the purpose of the human brain is to produce movement. The brain receives as inputs the sensory feedback and produces as outputs the motor commands sent to the muscles in order to realize the desired movement. The aim of motor control is to transform sensory inputs into consequent motor outputs (i.e. sensory-to-motor transformation "*inverse*") or to predict the sensory consequences resulting from a motor command (i.e. motor-to-sensory transformation "*forward*"). The representations of these sensorimotor transformations within the CNS have been defined by the general concept of "internal model". The internal models are neural mechanisms which mimic the behavior of the controlled system (e.g. the arm) (Wolpert et al 2001). There are two sorts of internal models, forward and inverse models. The forward models are internal transformations that mimic the motor-to-sensory transformations predicting the sensory consequences of an action. The inverse models perform a transformation from sensory variables to motor variables in which the desired sensory feedback is transformed into the appropriate motor command. They are therefore well suited to act as controllers. Note that these internal representations are not required to be precise models of the external world. A rough approximation of some external transformations is sufficient to allow the internal model to play a useful role (Jordan and Wolpert 1999). However, as internal models depend on the dynamics of the motor system, which change throughout life and under different contexts, these models must be adaptable.

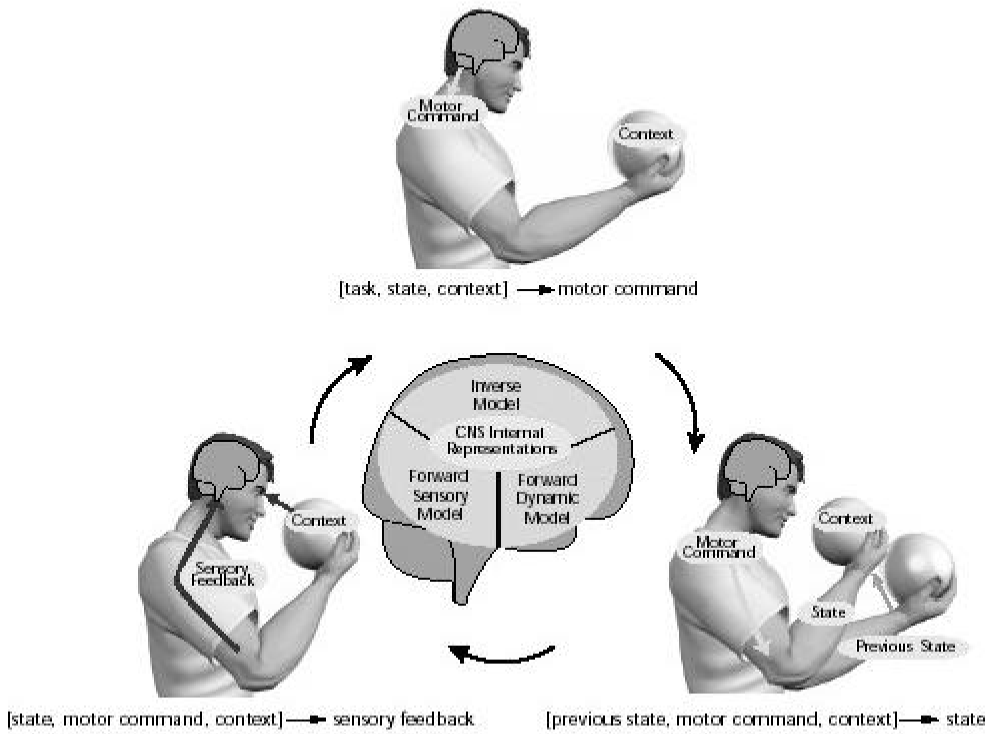

Fig. 2.1: The sensorimotor loop, showing motor command generation (top), state transition (right) and sensory feedback generation (left). Center: internal representation of these stages within the CNS (From Wolpert and Ghahramani 2000).

In this way, the sensorimotor loop can be divided in three stages (Fig. 2.1). (1) The *inverse model* generates the motor command required to realize the desired task according to the current state of the arm and the context. (2) The *forward dynamic model* predicts the new state induced by the motor command given the previous state of the arm and the context. (3) The *forward sensory model* estimates the sensory feedback of this new state.

In the next sections of this chapter, the upper limb will be considered as the system receiving the motor commands emanating from a controller within the CNS and producing sensory information emanating from its sensory receptors. The behavior of the arm in response to the motor command is defined by its state variables which contain all the relevant time-varying information (e.g. joint angles, velocity) needed to predict or control the future states of the system (Wolpert and Ghahramani 2000). For example, knowing the current position and velocity of the arm allows predictions of its future trajectory without the need to know the configurations of all muscles in the upper limb. As the state of the system changes continuously within a movement, the controller has only access to some function of the state through the sensory feedback. Finally, the response of the arm system to the motor command will depend on the environmental conditions defining the context of movement. Contextual information is given by all sensory modalities such as vision, audition, tactile afferent.

A number of different issues in computational motor control will be discussed based on the general schema (Fig. 2.2) described by Wolpert (1997). First, we will describe how *motor planning* specifies the desired outputs of the system given the goal of the task (Box 1 in Fig. 2.2). Second, we will discuss the different control systems that might produce an adequate motor command to realize the desired movement. We will study the *feedback control system* that generates the motor command in real time. Then, we will see how the *internal inverse controller* is needed to calculate a feedforward motor command before feedback is available (Box 2 in Fig. 2.2). Third, we will examine how internal forward models are useful for *motor prediction*, i.e. to predict the sensory consequences of this motor command (Box 3 in Fig.2.2). We will describe the potential roles of forward models in an internal feedback loop, in sensory confirmation and cancellation, and in *state prediction* that provides the controller with the current state of the body (Box 4 in Fig. 2.2). We will also see the benefits of a modular approach in which the brain is assumed to contain multiple modules of inverse and forward models, each of them suitable for one context. Finally, we will show how internal models are updated by *motor learning* (Box 5 in Fig 2.2).

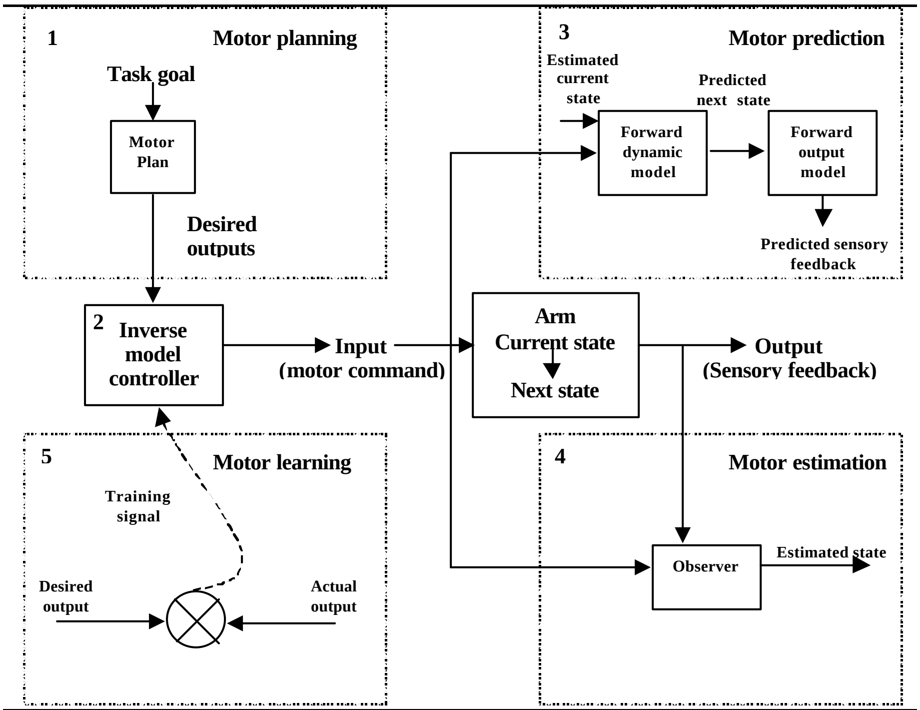

Fig. 2.2: Computational issues of the motor control system. For clarity not all lines are shown. See text for details. (Adapted from Wolpert 1997).

2.2.2 Motor planning

A fundamental property of the motor system is the reduction in the degrees of freedom that occurs during the transition from neural commands through muscle activation to movement kinematics (Bernstein 1967, Wolpert 1997). Indeed, because of kinematics redundancy, almost any task can be achieved in infinitely many ways. The same arm movement goal can be realized by many different hand paths and velocity profiles along this trajectory. Furthermore, the joint configurations to perform this movement are multiple and can be achieved by different patterns of muscle activation. To solve this problem, the motor system uses highly stereotyped movement patterns both between repetitions of the task and between individuals on the same task (Wolpert et al 2001). In this way, several aspects of unconstrained hand movements tend to be invariant i.e. the hand movements tend to be smooth and straight-line with a profile of hand speed unimodal and symmetric (bell-shaped) (Fig. 2.3). Similarly, maintaining the GF/LF ratio constant during manipulative task has the advantage of reducing the number of degrees of freedom that must be controlled independently (Johansson 1991).

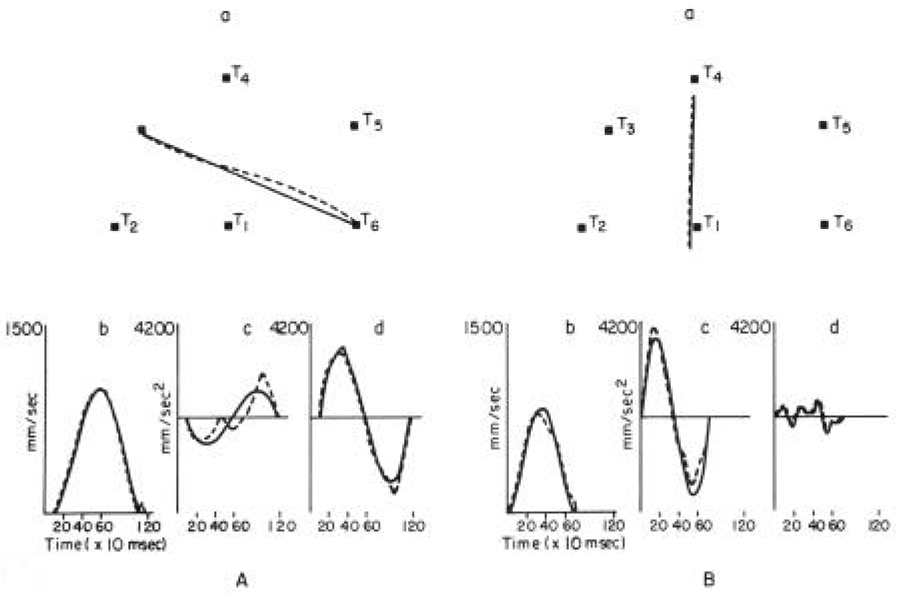

Fig. 2.3: Two unconstrained point to point arm movements (dashed lines) superimposed on the predicted minimum-jerk trajectories model (solid lines). Movement between targets T3-T6 (A) and T4-T1 (B). The hand path (a), the speed (b) and the acceleration along the y-axis (c) and along the x-axis (d) are represented. The predicted trajectory matched the measured one (Adapted from Flash and Hogan 1985).

In this framework, motor planning is defined as the computational process of selecting a single solution of behavior at all levels of the motor hierarchy from the many alternatives that may be consistent with the goal of the task (Jordan and Wolpert 1999). The optimal movement is the movement that minimizes the cost e.g. the total energy expended. An optimization approach proposes that a choice is made between the infinite number of movement functions by comparing them on the basis of a measure of cost (J). The instantaneous cost of the movement quantifies the undesirable aspects of movement (jerkiness, error…) and is used to measure the total cost. The aim of motor planning is to minimize the value of this cost function (Jordan and Wolpert 1999). Different cost functions have been studied to describe the arm movements (i.e. the kinematic and the dynamic costs) but as it is not the main subject of this thesis, we will not further describe them in this work. (See for more details Flash and Hogan 1985, Jordan and Wolpert 1999; Shadmehr and Mussa-Ivaldi 1994).

2.2.3 Control systems.

Once the motor plan is defined, the motor command required to realize the desired movement has to be specified. A current controversy exists over the relative importance of the feedback, feedforward and a trade-off of both (i.e. "Hybrid control system").

Feedback control system

Under feedback control system, the motor command required to realize the task is not defined prior but rather during the movement in “real time”. There is no *a priori* motor plan (Desmurget and Grafton 2000). The current state of the system is continuously compared to reference values. When there is a discrepancy between the two parameters, an error signal is generated and is used to modulate the behavior of the controlled system (Fig. 2.4a) (Desmurget et al 1999). The thermostat is a typical example of a feedback system. It compares the current temperature of the room to a reference value and modulates the response of the radiator. For lifting an object, the controlled system is the hand, the reference value is the weight of the object and the current state is the actual lifting force exerted on the object. As long the object has not lifted off as detected by the tactile mechanoreceptors (FA2), a motor command is generated in real time. The problem of this mode of control is the delay associated with the transport and the treatment of sensory information within the CNS that can generate instability when performing fast movement. Indeed, physiological delay inherent in sensorimotor loops is long (80-100ms) with respect to the duration of some rapid arm movements (300-700ms). Therefore, before the feedback signal starts to influence the ongoing motor command, the position of the arm still changes and the feedback correction is no more appropriate (Desmurget and Grafton 2000). We have shown in the previous chapter that when a “probing strategy” based on sensory feedback was used during the loading phase of a lifting task, multiple peaks were present in the GF and LF rate profiles suggesting that the movement was not smooth. Usually, the GF and LF rate profiles are bell-shaped proving that subjects correctly anticipate the object weight and that the GF was preprogrammed before the movement onset.

Feedforward control system: Inverse model controller

To execute motor control in a pure feedforward manner, i.e. in advance of the onset of movement, it has been proposed that the brain can acquire, through motor learning, an inverse dynamics model of the system to be controlled. This internal inverse model performs a transformation from sensory variables to motor variables allowing the motor control system to transform desired sensory consequences into the motor actions that yield these consequences (Jordan and Wolpert 1999). For example, to make a reaching movement successfully, the motor controller needs to find the appropriate force to displace the upper limb along the desired motion. The inverse model takes into account the inertial and viscous properties of the system (e.g. the dynamics of arm) to estimate the motor command that will achieve the desired sensory response (Desmurget and Grafton 2000). That allows feedforward control when feedback is available too late to guide the movement. So the internal inverse models are the basic module in open-loop control systems computing an appropriate control signal without relying on error-correcting feedback (Fig 2.4b).

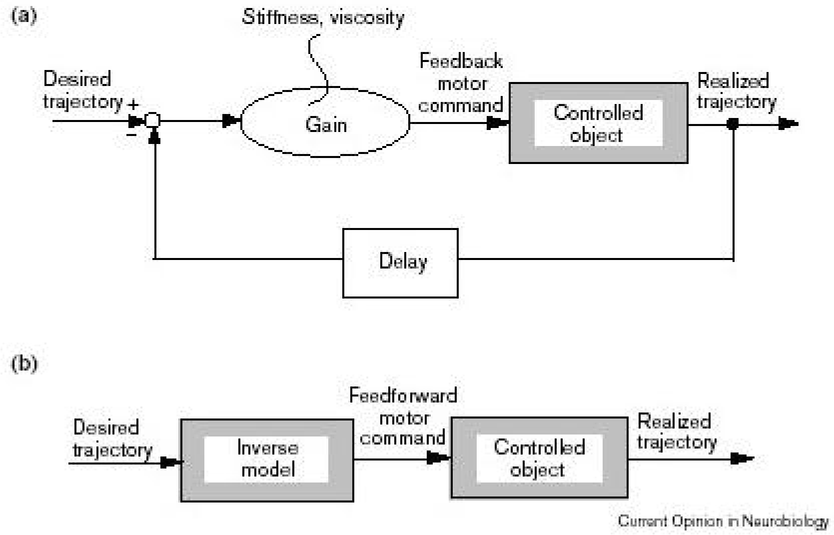

Fig. 2.4: Feedback and feedforward control of a controlled object. (a) The feedback control compares the realized and the desired trajectories in order to compute an error, which will serve to generate the feedback motor command after a certain delay. (b) The feedforward control uses an inverse dynamics model to calculate the motor command necessary to realize the desired movement (Adapted from Kawato 1999).

A good way to observe how the CNS builds an inverse model is to study reaching movement where the hand interacts with a new force field produced by a robot manipulandum changing the dynamics of the arm. In the absence of the force field, the hand path was essentially straight-line to the target. When reaching for a target in the new force environment, the subjects initially show trajectories, which deviate from their normal paths (Fig.2.5A). Through practice, they progressively adapt and the perturbed hand trajectory converges to the trajectory observed during the null field condition (Fig.2.5 B-D) (Shadmehr and Mussa-Ivaldi 1994). One way for the subjects to realize the desired straight-line trajectory in the force field was by developing in internal model of this field. It is suggested that an inverse model of the new force field is learned to approximate the force imposed by the mechanical environment. So, the subjects could add to their motor command a preprogrammed force component equal and opposite to the field. The control system does not need to relearn all the previously acquired motor skills. It only need to superimpose onto the original command, the output of a single inverse model that learns to mimic and cancel the forces produced by the environment. When the null force field was presented after the adaptation period to the new force field, the hand trajectory deviated again from the straight line. It is called an aftereffect of the adaptation. These aftereffects were evidences that the CNS improved performance by creating an internal model that approximate the dynamics of the environment (Shadmehr and Mussa-Ivaldi 1994).

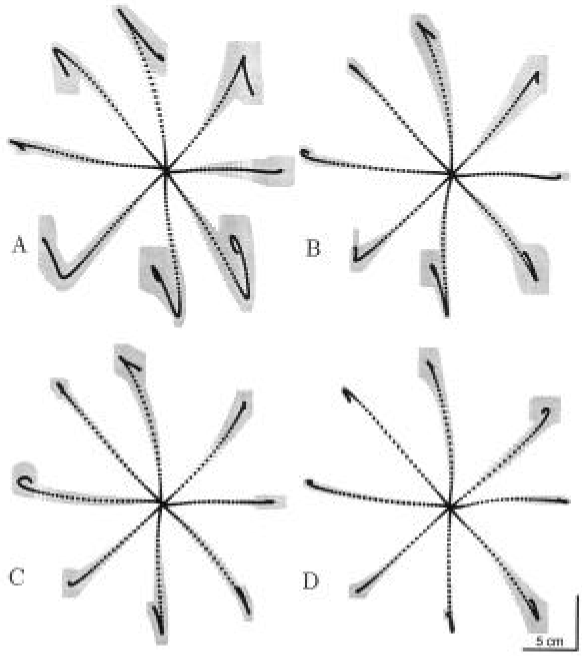

Fig. 2.5: Performance during target reaching performed in a force field produced by a robot manipulandum. Hand trajectories (mean and SD) obtained without visual feedback during the first (A), the second (B), the third (C) and the last sequence (D) of 250 targets reaching in the force field. With practice, the subjects tended to recover the straight-line trajectory normally observed for a reaching movement (D) (Adapted from Shadmehr and Mussa-Ivaldi 1994).

Hybrid control system

Evidences show that movement is not generated exclusively in real time nor purely controlled in a feedforward manner. A dual model of movement control has been proposed which combines both control systems. Fig.2.6 schematizes this model for a reaching arm movement. In order to realize the desired trajectory, the motor command is determined by the inverse model prior to the onset of movement. It ensures rapid transport of the hand to the vicinity of the target. Sensory feedback loop allows corrections at the end of the movement when the arm velocity becomes low, by comparing the hand location with the target position. For example, it has been demonstrated that altering the visual or the proprioceptive feedback affected movement accuracy only when the perturbation occurred at the end of the trajectory. By contrast, viewing the hand or not in the first half of the trajectory did not change the movement accuracy (Beaubaton and Hay 1986; Redon et al 1991).

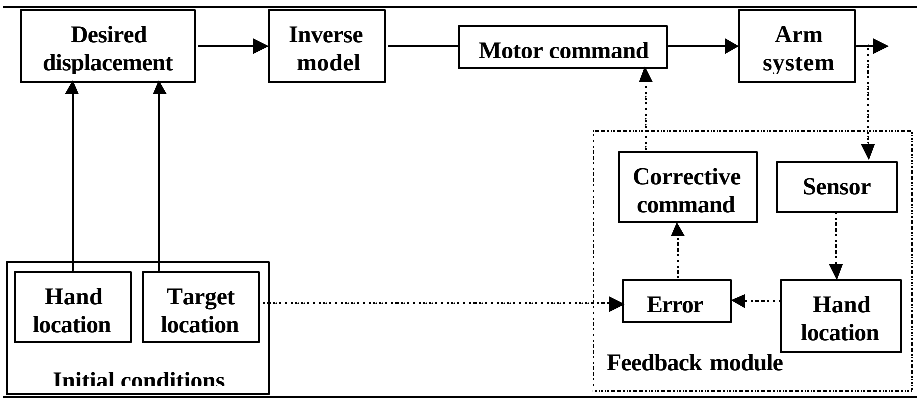

Fig. 2.6: Hybrid model of movement control. From the initial conditions of hand and target locations, the inverse model can calculate the required motor command to realize the desired displacement (black arrows). The sensory feedback module compares the current location of the hand and the target location generating an error, which serve to correct the ongoing reaching movement (dashed arrows). The sensory feedback loop becomes active at the very end of the movement when the velocity is low. (Adapted from Desmurget and Grafton 2000)

2.2.4 Motor prediction: Internal forward model

Predicting the consequences of a motor command despite the complexity of multi-joint motion requires a mechanism that can simulate the dynamic behavior of our body (position, velocity) and environment (Wolpert and Flanagan 2001). This system is called an internal forward model as it is internal to the CNS, it models the behavior of the body and it captures the forward or causal relationship between actions and their consequences. It calculates the next state of the system given the current state and an efference copy of the motor command (Box 3 in Fig. 2.2). A forward model thus predicts the behavior of the motor system (e.g. arm) in response to a command and allows the CNS to estimate the current and future state of the arm without delay and without sensory information (Desmurget and Grafton 2000). Such mechanisms are thought to be useful for solving a number of different problems in motor control.

Forward model for internal feedback.

A problem of using external sensory feedback in motor control is the delay associated with the transport and the treatment of sensory information within the CNS that can generate instability when performing fast movement. One means of maintaining the stability is to intersperse movement with rest, i.e. introduce a refractory period after each movement to allow time for veridical sensory feedback to be obtained. Alternatively, it has been suggested that the brain progressively learns a forward model that estimates the behavior of the motor system in response to a given command (Desmurget and Grafton 2000). This forward model provides an internal feedback of the predicted outcome of an action, which is used before actual feedback is available. For example during a reaching arm movement, the forward model of the dynamics of the arm will predict the end point location of the hand based on an efference copy of the motor command. By continuously comparing the end-point estimate with the target location, an error signal is generated that triggers a correction of the ongoing motor command (Fig. 2.7).

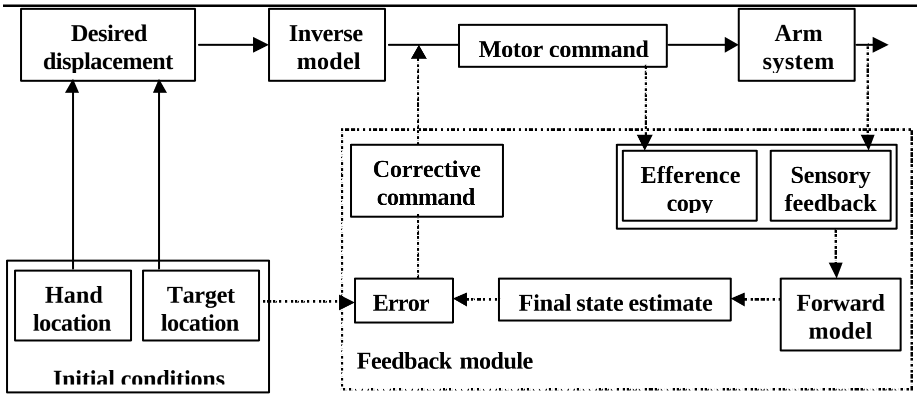

Fig. 2.7: Use of a forward model of the dynamics of the arm as an internal feedback for controlling a hand movement. From the initial conditions of hand and target locations, the inverse model can calculate the required motor command to realize the desired displacement (black arrows). From an efference copy of the motor command and the actual sensory feedback, the forward model can estimate the end point location of the hand. The comparison between the target location and the end-point prediction generates an error, which serve to correct the ongoing reaching movement (dashed arrows) (Adapted from Desmurget and Grafton 2000)

As unpredictable disturbances of the system can occur, the actual sensory feedback cannot be neglected in determining the current state of the system. One difficulty arises as to how the system detects the mismatches between the rapid predictions of the movement outcome issued from the forward dynamic model and the actual feedback that arrives later in time. To synchronize the internal and the actual feedback, a mechanism known as a Smith predictor has been suggested. It is thought that there is a forward output model that estimates the time delay before actual feedback is received (Miall et al. 1993) (Fig. 2.8). By delaying the internal feedback, an error resulting from the comparison between the predicted and actual feedback can be calculated and used to update the current forward dynamic model of the arm.

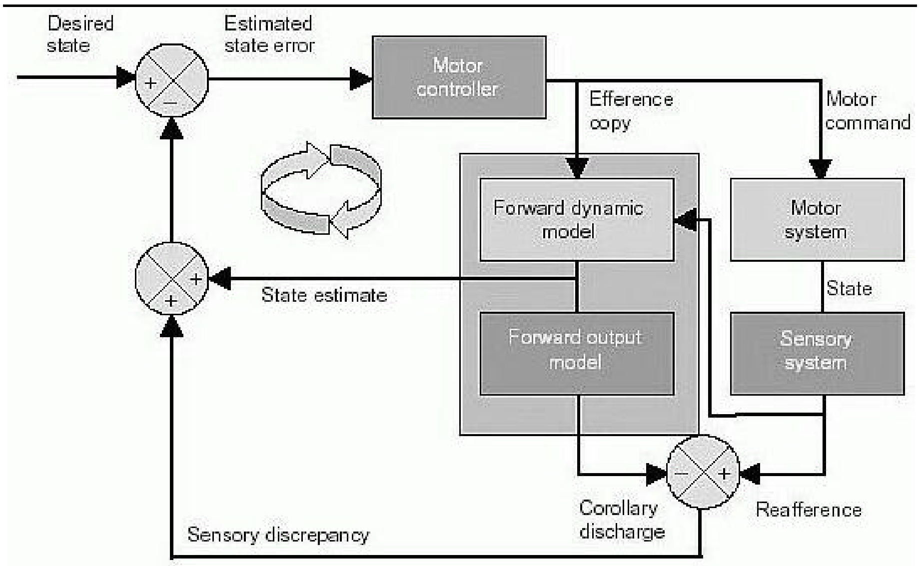

Fig. 2.8: The Smith predictor model. The outer loop indicates a feedforward control loop in which a motor controller evokes motor commands to act on the motor system, causing reafferent sensory inputs. A forward dynamic model generates an internal state estimate indicated by the circular arrow. It is combined with a forward output model (the Smith predictor) which predicts the delay of the actual sensory feedback. The error between the sensory prediction of the forward models and the actual sensory feedback can be used to correct the ongoing movement and update the forward models (Adapted from Wolpert et al 1998).

Forward model for sensory confirmation and cancellation.

The forward model predictions are also important to filter sensory information in order to reduce the effects of unwanted information and highlight the critical information for control (Wolpert and Flanagan 2001). Forward models allow the system to anticipate and cancel sensory effects of movement by using an efference copy of the motor command. So the effects of sensation induced by self-motion (e.g. self-tickle) are cancelled and self-produced motion are distinguished from the sensory feedback caused by contact with the environment (Jordan and Wolpert 1999).

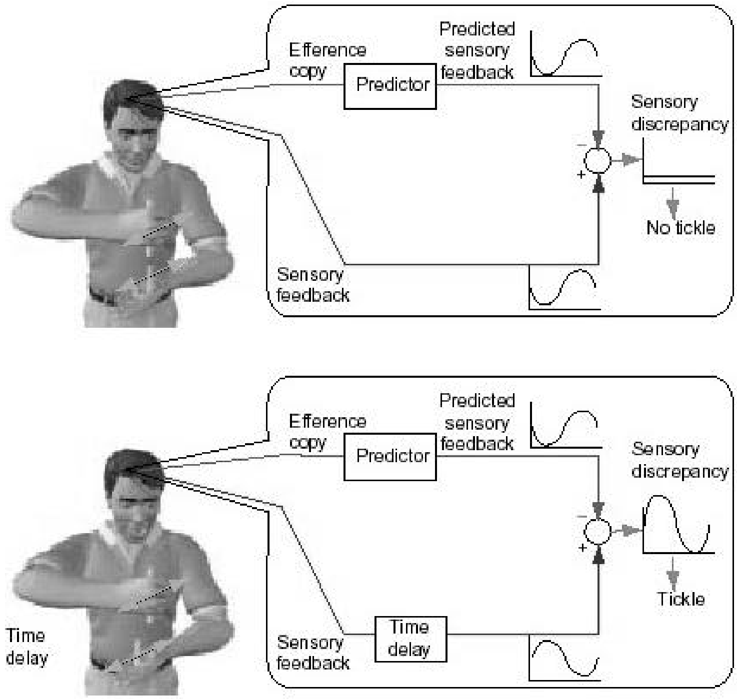

Fig. 2.9: Sensory confirmation and cancellation during self-tickle. (Upper) The motion of the right hand is directly transmitted to the left. From an efference copy, the predictor can estimate the sensory consequences of the motion. There was no discrepancy between the predicted and the actual sensory feedback. No tickle was perceived. (Lower) There is a delay between the motion on the right hand and the effect on the left. The prediction is out of synchronization with the actual feedback leading to a large sensory discrepancy, which is felt as a tickle. (Adapted from Wolpert and Flanagan 2001).

For example, as a subject tickles himself, there is no discrepancy between the sensory feedback predicted from the efference copy of the motor command and the actual sensory feedback so that the tickle sensation is attenuated (Fig.2.9A). By contrast, if a delay is introduced (via a robotic interface) between the motor command and the resulting tickle, it appears a sensory discrepancy between the predicted sensory feedback and the actual one so that the tickle sensation is enhanced (Fig 2.9B).

Forward model for state estimation

To produce accurate motor commands, the controller must know the current state of the body segments, i.e. their positions and velocities. As these variables are not directly available to the controller, a mechanism estimating the state is required. Such a system is known in engineering as an observer that estimates the unknown state of the motor system by monitoring its inputs (motor commands) and outputs (sensory feedback) (Fig. 2.10). It compensates for the delays in the sensorimotor system and reduces the uncertainties inherent in the defects (noise) of both the sensory and motor signals (Wolpert and Flanagan 2001). These online state estimates are stored and then recursively updated as further sensory and motor signals arrive (Wolpert et al 1998). In particular, Wolpert has envisaged an observer of the sensorimotor integration acting like a Kalman filter model. In this view, the forward model plays an essential role to estimate the next state based on an efference copy of the motor command. The person interested could refer to the original paper for more details about the functioning of this model (Wolpert et al 1995).

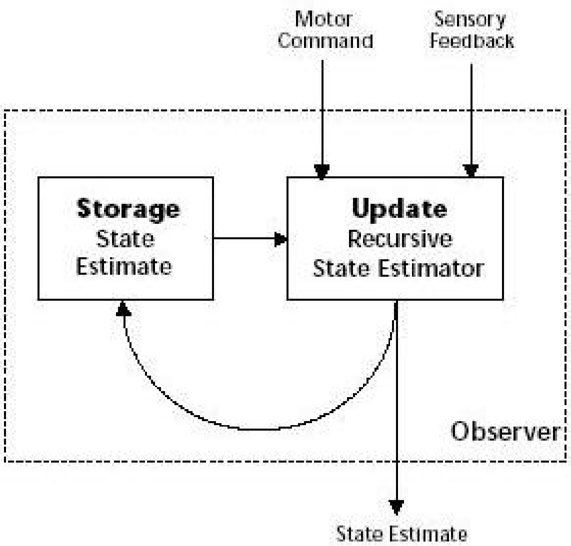

Fig. 2.10: Observer for state estimation. The observer monitors and integrates both the inputs (motor commands) and outputs (sensory feedback) of the system by recursively updating the stored state estimate. (Adapted from Wolpert et al. 1998).

2.2.5 Context estimation: a modular approach

The problem in human motor control is to select the motor command to achieve some desired sensory feedback in a particular context. This motor command will depend on many variables both internal and external to the body. It will depend on the state of the body (e.g. joint angles, velocities), on some constants such as masses, moments of inertia, center of masses of the body segments and on the interaction with the environment (e.g. object physical properties, gravity) which is the context of the movement (Wolpert and Kawato 1998). The existence of a single controller, which uses all the contextual information, is unlikely because it would need to adapt every time the context of movement changed before it could produce adequate motor commands and large errors will be generated. In order to generate accurate and appropriate motor behavior in different environments, the CNS can use a modular approach in which multiple controllers co-exist, each of them suitable for one or a small set of contexts (Wolpert and Flanagan 2001). Basically, the brain would contain multiple pairs (modules) of corresponding forward (predictors) and inverse (controller) models tightly coupled during motor learning and used to select the motor commands dependent on the context.

Faced with an environmental context, the brain prepares many modules. Each of which contains three elements: a forward model, an inverse model and a responsibility predictor. The figure 2.11 illustrates the multiple paired forward and inverse models in the framework of a subject grasping an object. (1) The visual information provides the *responsibility predictors* with the *contextual signal* about the object. The most appropriate module for the identified object (e.g. a racket) is pre-selected by the *responsibility predictor* that predicts the highest responsibility for its own module prior the onset of movement. In this example, the module 1 is selected. (2) The corresponding *inverse model* generates the *motor command* required to realize the *arm desired trajectory*. (3) This *feedforward motor command* is sent to the arm muscles that execute the movement. (4) The *forward model* receives an *efference copy of the motor command* and predicts the sensory consequences of the motor action generated by its paired inverse model. (5) *The arm predicted trajectory* is used by the *grip force controller* to adequately program the grip force applied on the object. (6)

The *actual arm trajectory* is compared with the predicted arm trajectory and a sensory *prediction error* is calculated as a probability, called responsibility signals comprised between 0 and 1. If the error is small, the probability that the forward model captures the current behavior is high and the module continue to be used. If the visual information is erroneous and the object actually grasped is a fork, the pre-selected module prediction is bad while the prediction of the fork module is better. The racket module is turned off and the fork module is turned on.

In the framework of learning a new environment, it is envisaged that the brain runs in parallel multiple modules that are adequate for contexts previously experienced. The final prediction of the next state of the system in a new context is made by modulating the contribution of each forward model prediction to the final prediction. In this way, a *soft max* function gathers all *prediction errors* and computes the responsibility signal. Over time, the forward model will learn to divide up the system dynamics experienced and the responsibilities will reflect the extent to which each forward model captures the current dynamics of the system (Wolpert and Kawato 1998). For each behavior captured by a forward model, an inverse model would be learned. The aim is that each inverse model learns to provide suitable motor commands to realize the desired next state under the context for which its paired forward model provides good prediction (high responsibilities). If one forward model prediction is good its corresponding inverse model receives the major part of the motor error signal and its output contributes significantly to the final motor command. In this way, this model can produce motor commands under a variety of contexts and is able to switch between controllers as the context changes.

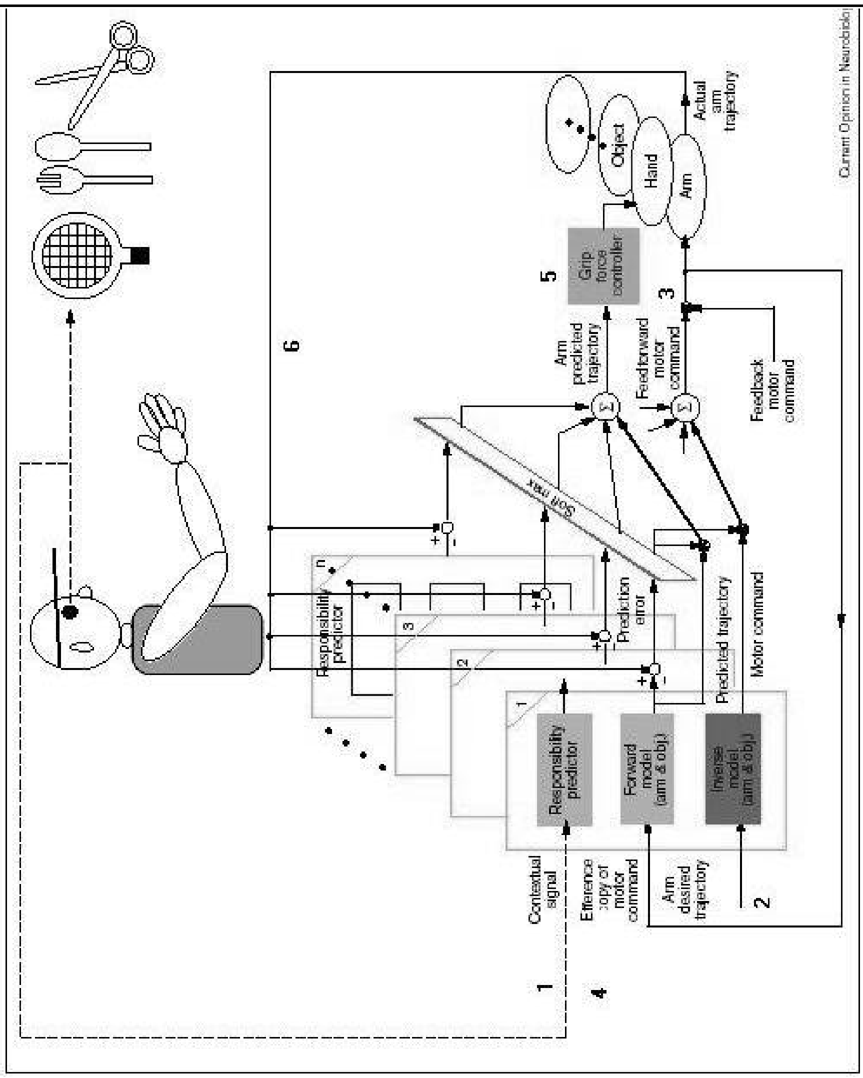

Fig. 2.11: Multiple paired forward and inverse models in the context of the grip-load force coupling for different objects. The brain contains n modules of corresponding responsibility predictor, forward and inverse models each appropriate for one context. By visual information about the racket (contextual signal), a module is selected by the responsibility predictors. The inverse model generates a motor command for the desired movement. The forward model predicts the sensory consequences of this motor command. If the prediction match the actual arm trajectory, the module continues to be used. If the context signal is erroneous and the object is a fork, the error prediction of the racket module is high while the prediction of the fork module is good. The racket module is turned off and the fork module is selected (Adapted from Kawato 1999).

There are three potential benefits in employing such modular approach. First, as we interact with multiple different objects and environments, the world can be better coded by using multiple inverse models, each of them providing the motor command necessary when manipulating a particular tool within a particular environment. Second, these individual modules can participate in motor learning without affecting the motor behaviors already learned by other modules. It reduces interference between what is already learned and what it is to be learned. Third, many contexts are derived from combinations of previously learned situations. By modulating the contribution to the final motor command of the outputs of the inverse modules, an enormous repertoire of behaviors can be generated (Wolpert and Kawato 1998). As few as 32 inverse models would generate as much as 2^{32} behaviors that are sufficient for a new behavior for every second of one's life (Jordan and Wolpert 1999).

2.2.6 Motor learning

Learning involves changes in behavior that arise from the interaction with the environment. To interact with new objects in different environments or to compensate for changes in the musculoskeletal system due to growth or injury, the motor control system has to be able to maintain and to update its internal models of the kinematics and dynamics of different environments. Its goal is to improve performance. The motor learning can be viewed as the acquisition of forward and inverse internal models appropriate for different tasks and contexts. The following sections describe two experiments illustrating the learning of forward and inverse models.

Forward model learning

To assure appropriate and accurate prediction, the forward models need to be updated during the growth and according to the objects and environment we experience. Forward models can be trained and update by comparing the predicted and the actual outcome of a motor command. The learning and decay of predictive grip force in object manipulation have been studied by Witney et al (1999, 2000). A virtual object paradigm was used to simulate either a single object manipulated between the two hands (linked trial) or two independent objects that act independently on each hand (unlinked trials). In linked trials, when the object was held with one hand and pulled on with the other hand, a predictive grip force response was observed in the restraining hand to prevent the object from slipping. In unlinked trial, when one hand pulled on the object, no force was generated on the other hand on so no predictive response should be appeared in this hand. Interestingly, when a series of unlinked trials were presented after a linked trial, the anticipatory grip force response persisted for at least six trials, despite the absence of load force generation (Fig.2.12). This response is purely predictive and occurs as a consequence of an internal model. In the "one-link" series, one linked trial was presented before seven unlinked trials. In the "three-link series, three linked trials were presented before the unlinked series. The anticipatory grip force response was greater in the "three link" series, suggesting that prediction is higher with increased experience of the relation between action of one hand and the consequence of movement of the other hand (Fig.2.12). In contrast to the fast development of prediction, decay occurred slower meaning that the forward model is robust.

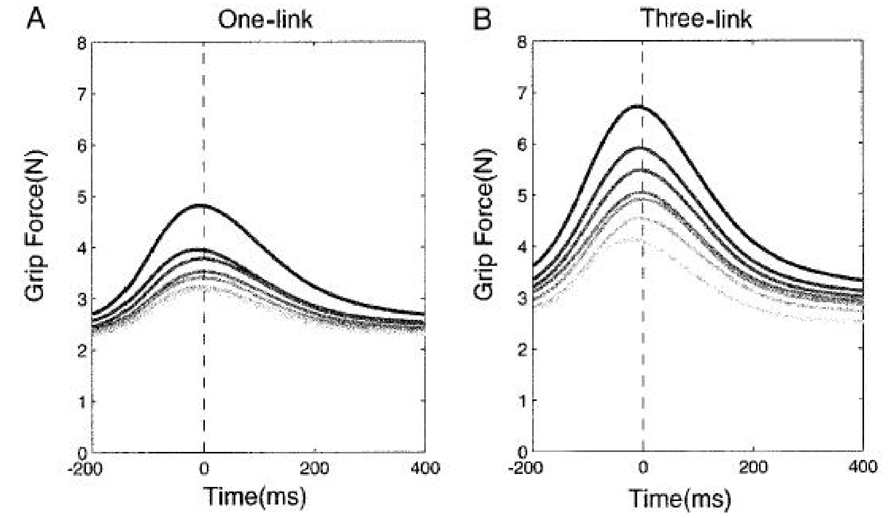

Fig. 2.12: Predictive grip force modulation during object manipulation between 2 hands. In linked trials, a single object was held generating a load force in the restraining hand. In unlinked trials, 2 independent objects were held and no load force was generated in the restraining hand. A) Seven grip force responses obtained during the unlinked trials that followed one linked trial ("One-linked"). B) Seven grip force responses obtained during the unlinked trials that followed three linked trials ("Three-linked"). The different shaded lines are for the 1st (dark gray) to the 7th (light gray) successive unlinked trials since the last linked trial. Despite the absence of a load force to the restraining hand, a predictive grip force response was evident for at least 6 "unlinked" trials (Adapted from Witney et al 2000).

Inverse model learning

As seen in the previous section, humans are able to learn multiple controllers and switch between them according to the context. The issue is whether the CNS uses a small number of global internal models or whether it maintains a large number of internal models for different contexts. In the first case, it must re-learn the properties of tools and environments whenever they are altered. In the second case, the multiple internal models hypothesis proposed by Wolpert and Kawato (1998) assume that each model learns the properties of a particular environment or tool and can be mixed to cope with a single task. The composition hypothesis holds that the CNS can effectively combine internal models of two previously learned sensorimotor transformations when dealing with novel environment in which both transformations are present.

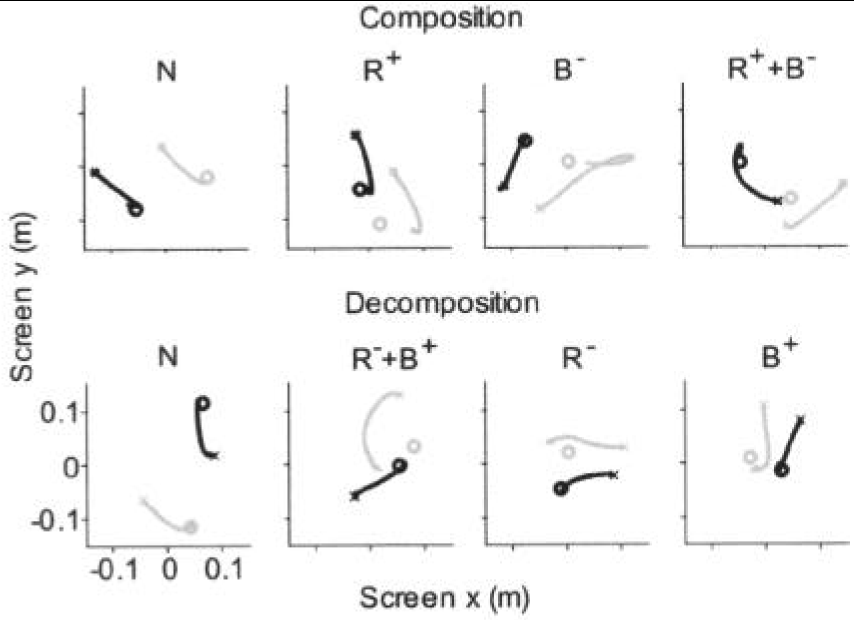

Fig. 2.13: Hand paths during target reaching in normal condition (N), in visuomotor transformation (R): rotation 60° (R+) or –60° (R-), in dynamic transformation (B): (viscous force field) and in combined visuomotor and dynamic condition (R+B). The performance is shown in the early (gray lines) and in the late (black lines) stage of the learning. The initial position of the hand is indicated by a (x) and the final position by a (o). In normal condition, the hand path is straight and precise both in early and late trial sets.
Upper graphs: In the composition experiment, large directional errors are observed in the early stage of learning for the visuomotor (R) and the dynamic condition (B). However the errors in the early stage are generally decreased in the combined condition (R+B) after learning the 2 conditions separately.
Lower graphs: In the decomposition experiment, large errors are observed in the early trials for the combined condition (R+B). However the errors in the early stage are smaller in the two separate conditions (R) and (B) after learning the combined condition. The straight hand paths are recovered after adaptation in each condition. (Adapted from Flanagan et al 1999)

For example, the learning process of reaching movements was examined in a novel environment with either a dynamic transformation (viscous force field (B)), a kinematic transformation (60° visuomotor rotation (R)) or the combined transformation (R+B). Figure 2.13 shows that the performance under a combination of visuomotor and dynamic transformations was facilitated by previously learning the two transformations separately. Target errors were smaller under the combined transformation after exposure to the separate rotational and viscous transformations (Flanagan et al 1999).

The decomposition hypothesis holds that when encountering a complex environment featuring more than one sensorimotor transformation, the CNS can effectively decompose the environment into separate internal models for the separate transformations. In the study of Flanagan et al (1999), the performance under the two separate transformations was however only partly facilitated by previously learning of the combined transformation. The subjects were able to learn and recall the visuomotor transformation but not the dynamic one.

2.2.7 Conclusion

Motor control has to resolve some problems inherent in the human motor system. Because of the considerable time delays in both the transduction and transport of sensory signals to the CNS, sensory information cannot be used to guide rapid arm movements. Skilled performance requires feedforward control supported by internal inverse models. Moreover in order to co-register actual and desired behaviors which are temporally shifted, internal forward models are useful for predicting the sensory signals in advance. Furthermore, there is neural noise in the sensory inputs and motor commands, which limit the ability of the motor system to perform simultaneously rapid and accurate movements. To counteract the effects of this noise, the CNS has to estimate the current state of the system by using both the actual sensory feedback with a forward model prediction. It must also take into account that the musculo-skeletal system is non-linear and non-stationary. It means that the sum of two motor commands is not equal to the sum of the corresponding movements and that the relationship between motor commands and movements (the dynamics) changes every time we interact with a novel object or environment. Such complex behavior is possible through learning multiple simple internal models. Finally, the motor system has to solve a high-dimensional control problem. It receives a multitude of sensory inputs and has to control thousands of motor sub-units.

To solve this problem, it has to build lower dimensional representation of this high dimensional space (Wolpert et al 2001).

2.3 Motor control underlying the grip-load force coupling.

2.3.1 Sensorimotor loop for the grip-load force coupling.

As we have seen in the previous chapter, during arm movements with a hand-held load, the grip force is modulated in parallel with the load fluctuations generated by the arm accelerations (Flanagan and Wing, 1995). Such control requires that the consequences of the arm motor command are anticipated (Fig. 2.14). When the load force is generated by a self-produced arm movement (e.g. left hand strikes the bottle held by the right hand), an efference copy of the motor command can be sent to a predictor that will predict the upcoming load force. According to this prediction, the grip force can be generated in parallel with the load force (Top, in Fig.2.14). By contrast, when the load force is externally applied to the object (e.g. another person strikes the bottle), it cannot be predicted and the grip force is applied in reaction to the load force based on tactile information about the shear force on the skin. The baseline of the grip force is increased as compensation against the possibility of slip before reflex rise in grip force (Bottom, in Fig. 2.14) (Wolpert and Flanagan 2001). The same phenomenon was observed in postural adjustments observed when subjects were asked to maintain stable their forearm against loads either imposed by an experimenter (passive) or voluntary exerted by the subjects (active) (Hugon et al 1982). An anticipatory postural adjustment (APA) occurred prior to self-induced unloading of the forearm (active) whereas reflex postural response followed the passive unloading. Interestingly, APA occurred both in normal and deafferented patients while the reflex response was only present in normal subject (Forget and Lamarre 1995). In self-produced unloading, APA can be generated on the basis of internal timing cues while afferent information is required to produce postural response in reaction of imposed unloading.

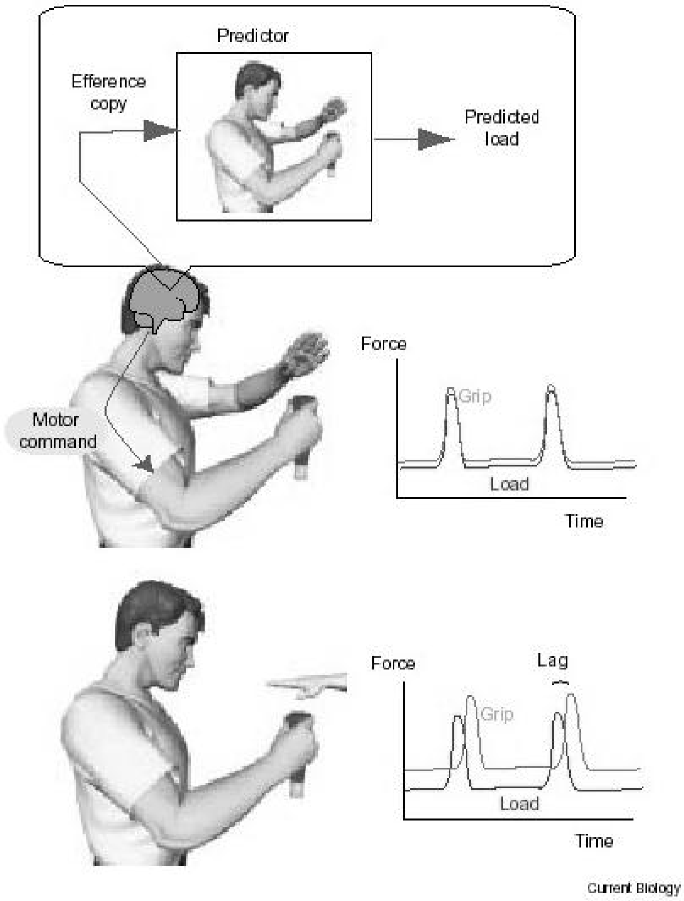

Fig. 2.14: Grip force response according to the load force. (Top) When the load force is self-generated, an efference copy of the motor command can be sent to a predictor that will predict the upcoming load force. The grip force is modulated in parallel with the load force. (Bottom) When the load force is externally applied on the object, it cannot be predicted and the grip force is applied in reaction of the load force. The baseline of the grip force is increased to prevent object slippage during the delay of the response (Adapted from Wolpert and Flanagan 2001).

This grip-load force coordination provides one of the most convincing evidences for the existence of forward models. In the last years, several motor control schemas for the grip-load force coupling have been proposed in the literature with different degrees of complexity (Kawato 1999, Flanagan and Wing 1996, 1997, Witney et al 2001). In this section, we will describe an adaptation of the theories of motor control originally proposed by these authors, applied to our own task (Fig.2.15). This theoretical consideration about the motor control of prehension, based on the concepts defined in the previous sections, was the starting point of our experiments. The principal purpose was to perturb some parts of the motor control schema and observe how it adapts.

The task consisted of moving the arm up and down at a given frequency and amplitude while holding an object without slip. Figure 2.15 shows the sensorimotor loop required to generate the adequate GF according to the LF fluctuations acting on the object during these arm movements. Consider as initial situation that the object was already lifted from the table and held stationary in the air. So the *current state* of the system was defined by the fixed position of the arm and by the grip force adjusted to the weight and texture of the static held object. The *desired trajectory* was a cyclic vertical arm movement with a hand held load. Given the *current state* and knowing the dynamics of the arm and object through previous experience, the *arm controller* can calculate the appropriate motor command to displace the arm and object along the *desired trajectory*, prior to the movement onset. This *feedforward arm motor command* is then sent to the *arm muscles* and executed (Black arrows in Fig 2.15). The motor command execution changes the state of the whole system. Indeed, the arm is accelerated; the arm acceleration is transmitted to the object and the tangential load force acting on the fingers changes. This load force change requires a grip force adjustment in order to restrain the object. In this way, prediction of the future LF by a forward model is used (Dotted arrows in Fig. 2.15). An *efference copy* of the arm motor command is sent to the *arm forward dynamic model* that will predict the state modification of the motor plant in response to this command, i.e. the predicted arm acceleration. Moreover, the *context cue* such as the visual information about the object allows the selection of the appropriate forward dynamic model that will predict the load force generated by the object weight according to its surface friction. The total load force induced both by the arm acceleration and object weight can be therefore estimated. This *predicted LF* is then used by the *GF controller* to calculate the necessary level of GF in advance of the load perturbation. The *feedforward GF motor command* is then sent to the *hand muscles* to be executed. In this way, the GF increases and decrease in parallel with the LF fluctuations. The actual changes in LF and GF at the fingertips are encoded by the cutaneous afferent. It signals mechanical events occurring at the skin such as slip produced by too low GF/LF ratio. That *triggers a GF response* scaled to the LF and frictional condition after a feedback delay of about 80-100ms (Dashed arrows in Fig. 2.15). By comparing the *predicted LF* with the *actual LF* feedback, a sensory *error* signal can be generated to update the dynamics forward models and correct the GF command in the next trial. It is supposed that a mechanism such as a Smith predictor (Miall et al. 1993) would synchronize the predicted and actual feedback that arises later in time.

2.3.2 Robustness of the sensorimotor loop for the grip-load force coupling.

In the next chapters, we will describe, across three studies, how this model for grip-load force coupling will adapt as different aspects of the sensorimotor loop are modified. In a first study entitled “The effects of a change in gravity on the dynamics of prehension”, we have modified the gravitational context by performing the task during parabolic flight. The subjects had to realize the cyclic arm movements with a hand-held load during successive periods of 1*g*, 1.8*g* and 0*g*. In this situation, the weight of the upper limb and the object is changed without modification of their mass and therefore without modification of their inertia. Such a perturbation requires learning of the new dynamics of the system at the control (inverse) and prediction (forward) levels. Different questions arise. (1) Would the controller generate adequate motor command to move the arm according to the desired trajectory? (2) Would the forward dynamic model be correctly updated to predict the load force in order to allow adequate GF adjustment? (3) How would motor control adapt with practice? Comparison was made between the performance of experienced and naive subjects.

In a second study, entitled “ Influence of the environmental contexts on the control of the precision grip", we examined the relationship between the normal force and the overall destabilizing force while moving an object up and down in different environmental contexts. The manipulative task was realized by using different combinations of objects and arm masses with different gravity fields and different arm accelerations. In this way, it was possible to generate equivalent magnitude of loads at the fingertips while the mechanical constraints on the upper limb and thus the motor commands required to move the arm were modified. It was interesting to observe how dynamic constraints such as gravitational force and inertial resistance of the arm and object would be taken into account in the control of precision grip. The question arises, as whether the GF will be the same for equivalent load forces when for example, the arm was twice as heavy in 2*g* than in 1*g*.

Finally in a last study entitled “ Further evidence of the important contribution of cutaneous feedback to the manipulation of hand-held objects”, we suppressed the sensory feedback by anesthetizing the thumb and index finger restraining the object. Without sensory feedback, the error signal about the LF prediction from the forward model could not be generated and triggered GF response could not occur. The GF controller could only rely on the predicted LF. The question arises as whether the feedforward mechanisms would be precise enough to compensate for the absence of sensory feedback. This paradigm would highlight the role of sensory feedback in the updating of the internal representation of the arm and environment.

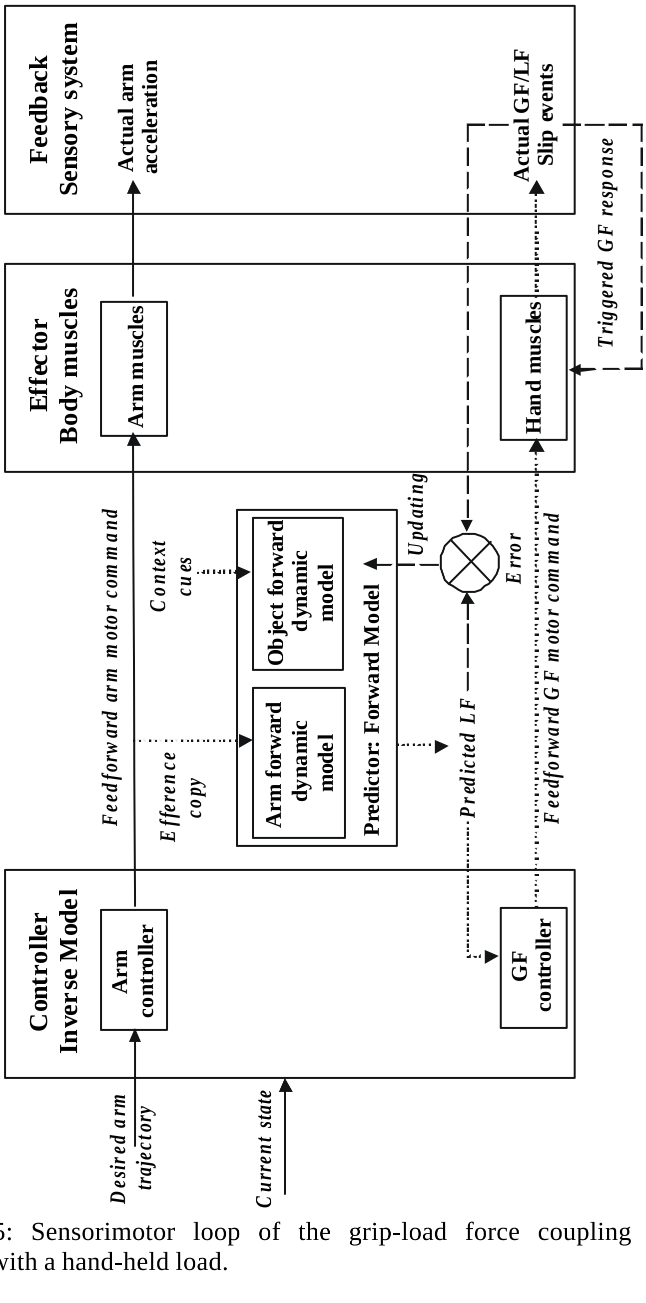

Figure 2.15: Sensorimotor loop of the grip-load force coupling during arm movement with a hand-held load.

Chapter 3: The effects of a change in gravity on the dynamics of prehension.[3]

3.1 Preliminary remarks

The dynamics of the arm change significantly both during development where bones grow and muscle mass increases but also in a shorter time scale when grasping objects. Therefore, the arm controller needs to be robust to variations in the dynamics of the arm to maintain the hand performance stable. It has been shown that subjects adapt quickly to a change of object's texture, shape or weight (Johansson and Westling 1984; Johansson and Westling 1988; Jenmalm and Johansson 1997). In this first experiment, we were interested in studying how subjects adapt to new dynamics of their arm as the hand interacts with a new gravitational environment. We have considered the task where subjects performed vertical arm movements with a hand-held load in 1, 2 and 0G during parabolic flight maneuvers. We measured the grip force applied on the object while the load force varies both because of the arm acceleration and the new gravity field. Adequate GF motor command in anticipation of the LF change would require correct prediction of the LF by the forward dynamic model of the arm and object (see Fig.2.15 in Chapter 2). Thus, the grip force output indirectly reflects the precision of the forward model prediction. The grip force profile when a subject encounters new gravity for the first time would give an idea about the robustness of the forward model. Comparing the grip-load force coupling of experienced and novice subjects in parabolic flight might be a good way for studying how the CNS updates its internal model and learns new arm dynamics. It would also give information as whether the gravity is internally represented or by contrast, considered as an external force that must be counteracted continuously. The results of this experiment are detailed hereafter as a full paper entitled "The effects of a change in gravity on the dynamics of prehension".

---

[3] Published as "The effects of a change in gravity on the dynamics of prehension" Exp. Br. Res. (2003) 148: 533-540

3.2 Abstract

Investigating cyclic vertical arm movements with an instrumented hand-held load in an airplane undergoing parabolic flight profiles allowed us to determine how humans modulate their grip force (GF) when the gravitational and the inertial components of the load force (LF) are varied independently. Eight subjects participated in this study; four had already experienced parabolic flights (ES) and four had not (NES). The subjects were asked to move the load up and down continuously in three different gravitational conditions (1 *g*, 1.8 *g*, and 0 *g*). In 1 *g*, the grip force precisely anticipated the fluctuations in the load force which was maximum at the bottom of the object trajectory and minimum at the top. When gravity changed, the temporal coupling between GF and LF persisted for all subjects from the first parabola. In 0 *g*, the grip force was accurately adjusted to the two load force peaks occurring at the two opposite extremes of the trajectory due to the absence of weight. While the experienced subjects exerted a grip force appropriate to a new combination of weight and inertia since their first trial, the inexperienced subjects dramatically increased their grip when faced with either high or low force levels for the first time. Then they progressively released their grip until a continuous grip-load force relationship with regard to 1 *g* was established after the fifth parabola. We suggest that a central representation of the new gravitational field was rapidly acquired through the incoming vestibular and somatic sensory information.

3.3 Introduction

During tool handling, grasp stability is ensured by a close coordination between the grip force (GF) applied normal to the object’s surface and the load force (LF) acting tangentially on the fingertips. When an object is moved, the grip force is automatically modulated in parallel to fluctuations in the load force resulting from the object weight (*i.e.* the product of the mass and the gravity) and the inertial object accelerations due to the arm movements (Flanagan and Wing 1995). Moreover the grip force is always somewhat greater by a safety margin than the minimal force required to prevent slippage (the 'slip force') at any load according to the skin-object friction (Johansson and Westling 1984). The close temporal coupling between the grip force and load force is independent of the grip and mode of object transport (Flanagan and Tresilian 1994), the movement frequency, or the texture of the gripping surface (Flanagan and Wing 1993a, 1995).

The synchronous GF-LF modulation suggests that the grip force controller within the CNS is provided with the load consequences of the arm movements before the actual feedback from the cutaneous receptors is available (Flanagan and Wing 1993b). It is hypothesized that with acquired experience, the CNS builds and uses internal models that capture the dynamics properties of the arm, objects (texture and weight) and external environments (*e.g.* gravity) in order to predict the upcoming LF (Flanagan and Tresilian 1994, Flanagan and Wing 1997, for review, Flanagan and Johansson 2002). Previous experiments argue in favor of a central representation of the gravity both as an orientation reference (vertical direction) and as mechanical load acting on the center of mass of the limbs (Pozzo *et al.* 1998; Papaxanthis *et al.* 1998). According to this theory, the consequences of the gravitational acceleration both on the load force and on the planned movement (McIntyre *et al.* 1998) must be taken into account in computing an adequate grip force.

Preliminary evidence that grip force control mechanisms are able to cope with hyper- and micro-gravity during parabolic flight has been shown by Hermsdörfer *et al.* (1999). The grip force exerted against an object held stationary throughout a whole parabola was scaled to the weight of the object under normal and high gravity conditions. During weightlessness, although no force was necessary to stabilize the object, the subjects used a low grip force that could be seen as a pure safety margin in the event of a possible perturbation. Moreover, the grip force was also adjusted adequately in anticipation of the load fluctuations during horizontal and vertical arm movements performed during parabolic flights (Hermsdörfer *et al.* 2000). However, the time course of adaptation to a new gravitational environment could not be tested because the two subjects had already experienced weightlessness before beginning the experiments.

In the present study, the grip force exerted on a hand-held object during cyclic vertical arm movements was examined at 1 *g* and at different simulated gravity fields (0 *g* and 1.8 *g*) attained during parabolic flight maneuvers of an airplane. A modification of the object's weight was obtained without modification of its mass, and thus its inertia was constant across the different gravitational conditions. By contrast, on earth, the weight of an object cannot be changed without changing its inertial properties. Therefore, the parabolic flight environment offered us the unique possibility to study the effect of a change in gravity on the GF-LF coupling while maintaining the inertial component of the load unchanged. Eight subjects were asked to perform cyclic vertical arm movements while holding an instrumented load during ten parabolic flight maneuvers. Half of the subjects had never experienced parabolic flights. We hypothesized that the GF-LF coupling would be progressively adapted to a new gravity level in the naive subjects, while it would be appropriately adjusted in the experienced subjects from the first time they executed the task in the aircraft.

3.4 Methods and materials

3.4.1 Subjects and experimental procedure

Eight adult subjects (6 men and 2 women) participated in the study. They were examined in the Belgian Center for Aerospace Medicine in order to qualify for parabolic flights (NASA class III medical examination). No subject reported sensory or motor deficits, all but one were right-handed. Four subjects had no previous experience in microgravity (the non-experienced subjects, NES) while the other four had more than 100 parabolas each to their credit (the experienced subjects, ES). In order to prevent motion sickness, the novice subjects had taken medication (scopolamine). All participants gave their informed consent to participate in the study, and the procedures were approved both by the European Space Agency safety committee and by the local ethics committee.

The grip-load force coupling was measured during cyclic vertical arm movements with a 164 mm high 250 g instrumented hand-held object (Fig. 3.1). It was equipped with strain gauge transducers to measure the grip force (GF) applied perpendicularly by the fingertips on two parallel brass disks, 30 mm in diameter and 30 mm apart, that served as the grasping surfaces. An accelerometer mounted on the top of the object recorded the acceleration along its vertical axis (a_v). The vertical load force (LF) resulting from the gravitational and the acceleration-dependent inertial force was calculated as the product of the mass and the vertical acceleration of the object as measured by the accelerometer. The object center of mass was located midway between the grip surfaces to prevent rotational torque.

The subject was seated in a chair with an attached seat belt. The right shoulder was abducted at about 30 degrees, the elbow was flexed at 90 degrees and the hand was resting on a horizontal surface beside the subject. At a signal from the experimenter, the instrumented object was grasped between the thumb and index finger of the right hand. The subjects were instructed to perform cyclic vertical arm movements at a frequency of approximately 1 Hz, aided by a metronome. The amplitude of the oscillations was maintained by lightly constraining the movement within two parallel rubber bands about 20 cm apart (Fig. 3.1) which served to guide the endpoints of the arm displacement. The upper limb displacement was performed by the subject using unconstrained shoulder and elbow movements. The subjects were required to maintain the vertical orientation of the object (*i.e.* no tilting) by using visual feedback. No specific instructions were provided regarding the grip force.

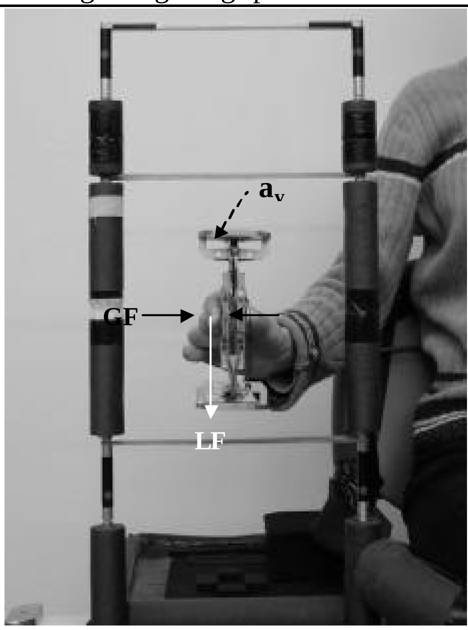

Figure 3.1: Frontal view of the experimental set-up. The subject moved the manipulandum up and down between the two elastic bands 20 cm apart. The grip force (GF, black arrows) was measured by strain gauges, the load force (LF, white arrow) was calculated from the vertical object acceleration measured by an accelerometer (av, indicated by the dashed arrow).

The experiments were first carried out at 1 *g* on the ground before the flight in order to familiarize the subjects with the task. Then the experiments were performed at 0 *g*, 1 *g* and 1.8 *g* during the parabolic flights. Each subject performed the task during ten trials of 30 s duration on earth and during ten parabolas of 120 s in the aircraft.

The flights originated in Bordeaux France using an Airbus A300 “ZEROg” aircraft. The parabolic flight profiles modified the apparent gravitational acceleration in the aircraft. Each profile started from level flight at 1 *g* and consisted of a 20 s 1.8 *g* pull-up phase during which the aircraft climbed from 6000 m to 8500 m, followed by a 20 s microgravity phase (0 *g*) obtained over the top of the trajectory, followed by a 20 s symmetrical 1.8 *g* pull-out phase which brought the aircraft back to steady horizontal flight at the original altitude; there was approximately two minutes between parabolas. These experiments were performed during four flights of thirty parabolas during the 26th and 27th ESA parabolic flight campaigns. Each flight was organized as six groups of five parabolas with a several minute pause between each group. A three-axis accelerometer was fixed on the floor of the aircraft to record the aircraft acceleration along the z-axis (normal to the floor of the airplane), the y-axis (lateral to the long axis of the airplane), and the x-axis (along the fore-aft axis of the airplane). The simulated gravity was recorded along the z-axis.

In the aircraft, the subjects grasped the instrumented object and started the cyclic movement during the 1 *g* phase of the flight, approximately 30 seconds before the start of the pull-up phase. The movement was performed throughout the whole parabola and 30 seconds after the restoration of the 1 *g* condition. Thus the grip force and object acceleration were recorded continuously for 120 seconds while the simulated gravity went successively from 1 *g*, to 1.8 *g*, 0 *g*, 1.8 *g*, and back to 1 *g*. Two subjects were examined per flight. On each flight, the NES performed the experiment on the first fifteen parabolas and the ES was tested during the last fifteen parabolas. In this way, the NES experienced microgravity for the first time when they performed the task during the first parabola. During the fifteen first parabolas, the ES were not specifically involved in a manipulation task. In this study, we only analyzed the first ten trials performed by each subject.

Moreover, the coefficient of static friction between the fingertips and the grip surfaces was measured, for each subject, by five lift-and-drop maneuvers performed at 1 *g* before and after each group of five parabolas. The subject was instructed to lift and hold the instrumented object stationary, then gradually release their grip until the object slipped due to the acceleration of gravity. The measure of friction was calculated as half the LF/GF ratio at onset of the slip, as detected by the accelerometer (Johansson and Westling 1984). The coefficient of friction for each trace was computed as the average of the ten lift-and-drop measurements. By assuming that the coefficient of friction was independent of the load force fluctuations during the cyclic arm movement, a theoretical slip force could be calculated as half the ratio between the load force and the coefficient of friction. When the grip force dropped below the slip force, the object slipped out of the fingers. The safety margin was defined as the difference between the employed GF/LF ratio and the theoretical slip force/load force ratio. Unpublished results have shown that the coefficient of friction tends to be higher for small loads less than 200 g, and consequently the theoretical slip force was presumably overestimated in 0 *g*.

3.4.2 Data processing and analysis

The signals from the strain gauges and accelerometers were digitized on-line at 200 Hz with a 12-bit PC-LPM-16PNP National Instruments© analog-to-digital converter in a personal computer. After analog-to-digital conversion, the signals were further low-pass filtered with a fourth-order, zero phase-lag Butterworth filter having a cut-off frequency of 15 Hz.

The analysis was performed during periods of constant aircraft and object accelerations. In the ground experiments, a few arm movement cycles were necessary to attain the required 1 Hz frequency and 20 cm movement amplitude, so the load force and amplitude were calculated over the last fifteen cycles of the twenty obtained for each trial. The dynamics of the precision grip observed during this period was used as the control data. During the parabolic flight experiments, only six cycles could be selected as representing the steady state of each gravitational condition for all the parabolas, when both the aircraft and the object accelerations were stable.

The analysis of the force measurements was performed cycle by cycle. The cycles were delimited between the load force maxima. For each cycle the following parameters were analyzed: The “movement frequency”

(Hz) defined as the frequency of the peak LF, the "amplitude of LF" (N) defined as the difference between the maximum and the minimum of the load force, the "mean GF" (N) defined as the mean level of the grip force modulation, the "phase shift" (ms) defined as the delay between corresponding peaks of the grip force and the load force (negative phase shift indicating that the grip force peak preceded the load force peak), and the "safety margin" calculated when the load force reached a maximum.

3.4.3 Statistical analysis

A two-way analysis of variance for repeated measures was performed on the dynamic parameters to test for the differences between the ten repeated trials (factor 1) in each gravitational condition and to test for the differences between the gravitational conditions (factor 2). The interaction between both factors was also examined. A Tukey's pairwise multiple comparison procedure was used to determine which treatments were significantly different. These analyses were performed separately in each experimental group (NES and ES). All the statistical analyses were carried out with SigmaStat 2.03 (SPSS Inc.).

3.5 ***Results***

The GF-LF coupling in the different gravitational environments attained during parabolic flight is shown in Figure 3.2. These signals were obtained during the last trial of an inexperienced subject. In this typical parabola, the aircraft's vertical acceleration was 9.55 ± 0.26 m s^{-2} at 1 *g*; 17.07 ± 0.24 m s^{-2} at 1.8 *g* and 0.11 ± 0.17 m s^{-2} at 0 *g* (Fig.4.3.2A). The load force oscillated around the object weight (dotted line) of 2.5, 4.5 and 0 N at 1, 1.8 and 0 *g* respectively (Fig. 3.2B). In the presence of gravity, the load force reached a maximum at the bottom of the trajectory where the gravitational and the object accelerations were acting in the same direction. The minimum load force occurred at the top of the trajectory, where the object acceleration was opposed to that of gravity. At 1 and 1.8 *g*, the load force was always positive because the downward acceleration of the object required by the frequency and amplitude of the movement was always less than the acceleration due to gravity. In microgravity, the object had to be accelerated both upward and downward because gravity no longer accelerated the object downwards, and thus the load force was positive and negative in the lower part and in the upper part of the trajectory respectively. The amplitude of the load force fluctuations was fairly similar across gravitational environments (about 3 N), suggesting that the NES in this trial was able to maintain the constraints of the imposed movement (1Hz and 20cm). In each gravitational phase, the grip force (thick line; Fig. 3.2C) was increased and decreased when the load force rose and fell respectively. At 0 *g*, the grip force was increased again at the top of the trajectory to prevent the object from slipping between the fingers when the object was accelerated downwards. The grip force was always greater than the slip force (thin line) indicating that no slippage occurred. Moreover, it was interesting to note that the mean level of the grip force modulation was great enough to prevent slip for any load suggesting that the modulation was not obligatory. Peaks of load force were always precisely synchronized with a similar peak in the grip force so that the GF/LF ratio was minimum and highly reproducible at these times (Fig. 3.2D). In contrast, when the load force was minimum, the GF/LF ratio was less constant and reached its maximum because the grip was not completely released or was even re-increased.

The adaptation of the GF-LF relationships in each gravitational condition is shown in Figure 3.3 across four representative trials. The left panels display typical traces recorded from an experienced subject (ES), and the right panels are from a non-experienced subject (NES). Both subjects modulated their grip force in phase with the load force fluctuations induced by the object acceleration in each gravitational condition, starting from their first trial. The ES used the same GF-LF relationship from the first to their last trial in the aircraft. A nearly continuous grip-load force relationship was established across the different gravitational conditions (Fig. 3.3, ES). Note that the level of the GF modulation at 0 *g* remained slightly above that observed at 1 *g*. Conversely, when faced with a new gravitational field for the first time, the NES used a dramatically increased grip force at 0 and 1.8 *g* (Fig. 3.3, NES). By decreasing both the level and the variance of grip force throughout the ten trials, the NES subject progressively tends towards a single GF-LF relationship across the gravitational environments. This process started at the second trial and was achieved after the fifth.

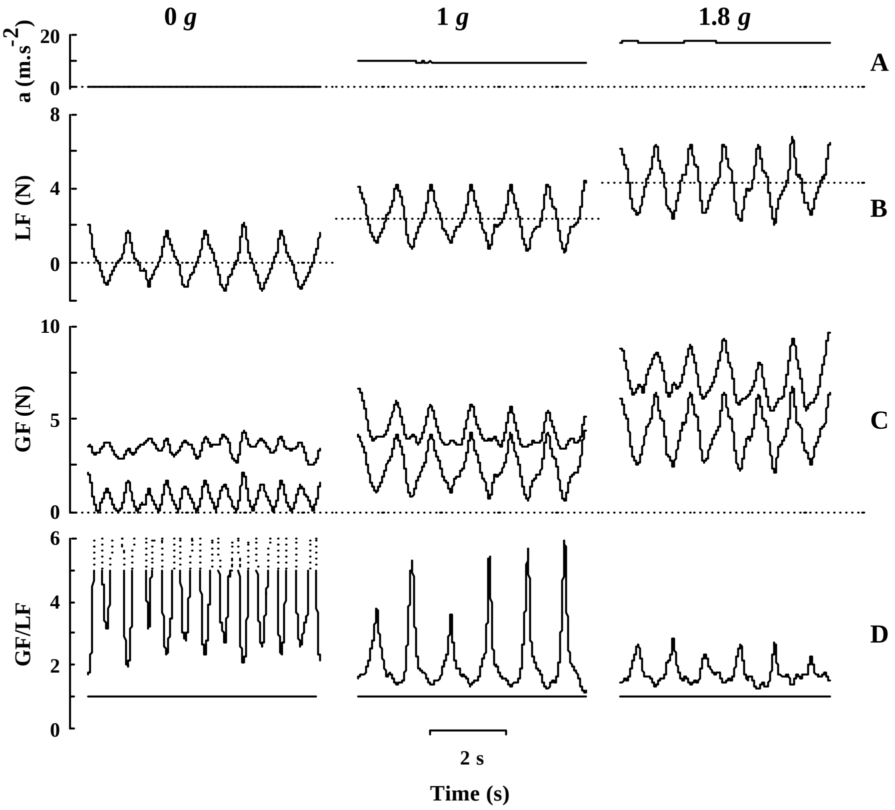

Figure 3.2: Records of 6 contiguous cycles obtained during the stable period in each gravitational phase of the last trial of a NES. The traces presented are the gravity level (A), the load force (B), the grip force (C, thick line), the slip force (C, thin line), the GF/LF ratio (D, thick line), and the slip ratio (D, thin line). The difference between the GF/LF ratio and the slip ratio reflects the safety margin. The friction coefficient was 0.5.

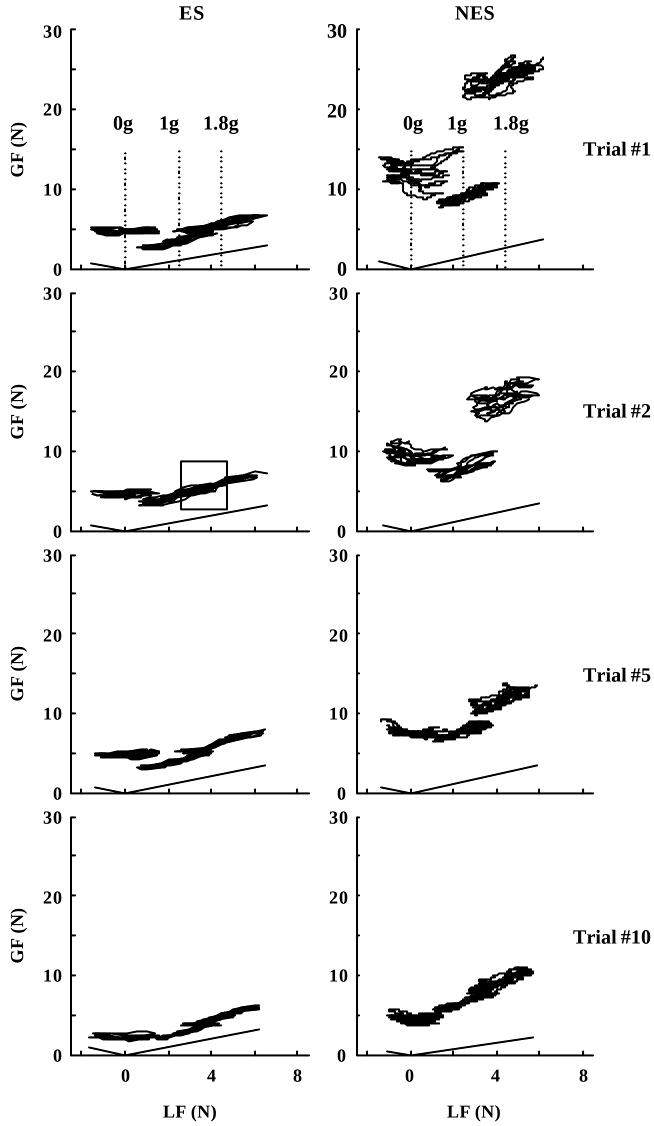

Figure 3.3: The grip force-load force relationship measured during 6 arm cycles under three gravity levels during the first, second, fifth and tenth trials in an experienced subject (ES) (left column) and a non experienced subject (NES) (right column). The dotted lines in the upper panels represent the object weight in each gravitational level. The slip force is presented by a straight line according to the friction coefficient of each trace. The inset in the left column shows the overlap between the load force ranges observed at 1 *g* and at 1.8 *g*. Trial #1 of the NES and the ES corresponded to the first and the fifteenth parabolas of the aircraft, respectively.

Figure 3.3 (inset) also shows that same load force ranges were obtained by varying separately the acceleration of gravity and the acceleration of the object. We observed an overlap in the load force at a low gravitational acceleration (*i.e.* 1 *g*) with a high object acceleration (*i.e.* bottom of the arm trajectory) and in a high gravitational acceleration (*i.e.* 1.8 *g*) with a low object acceleration (*i.e.* top of the arm trajectory). Even though the upper limb was in different simulated gravitational fields, the same coupling between the grip force and load force was observed after the information was integrated, *i.e.* from the first trial for the ES and after the fifth trial for the NES.

Figure 3.4 presents the dynamic parameters of the ES and NES subjects in each gravitational condition for four representative trials. Consider first the differences observed between the ten repeated trials in each gravitational condition within both groups of subjects. All the parameters of the ES subjects were stable from the first trial in each gravitational condition. With NES subjects, some adjustments occurred across the ten trials. The two-way analysis of variance for repeated measures revealed a significant interaction between the effects of repeated trials and the gravitational condition. Indeed, in 1 *g* on earth and in the aircraft, all the parameters were stable from the first parabola. By contrast, during the first trial in 0 and 1.8 *g*, the NES were generating a larger amplitude of load force ($F=1.825$, $P=0.022$), a higher level of grip force ($F=1.877$, $P=0.017$) and a greater safety margin ($F=3.95$, $P=0.002$). In the subsequent trials, these parameters progressively decreased and no further significant evolution was seen after the fifth trial. Note that although the difference was not significant ($F=1.757$, $p>0.05$), the NES movement frequency also tended to decrease across trials in 0 and 1.8 *g* (Fig. 3.4). The phase shift between corresponding peaks of grip force and load force was constant across the ten repeated trials within each gravity level ($F=0.766$, $p>0.05$). On average, grip force peaks occurred before the load force peaks.

Consider now the differences observed between gravitational conditions when all the trials are taken into account. First, the parameters of the grip-load force coordination were not significantly different when the subject performed the task at 1 *g* on earth or in the aircraft. A change of the gravity (1.8 and 0 *g*) induced significant effects on the mean grip force (NES: $F=9.692$, $p=0.004$; ES: $F=11.941$, $p=0.002$) and safety margin (NES: $F=18.78$, $p<0.001$; ES: $F=5.635$, $p=0.02$). The post hoc analysis revealed, that in both groups (ES & NES), the mean grip force was identical in microgravity and in the 1 *g* environment but it was significantly increased in hypergravity (NES: $p=0.006$; ES: $p=0.007$). Consequently, the safety margin was the same in 1 *g* and hypergravity but it was significantly increased in 0 *g* (NES: $p<0.001$; ES: $p=0.03$). This suggests that the subjects adequately increased their GF in hypergravity in order to maintain a safety margin equivalent to that exerted at 1 *g*. By contrast in microgravity, they were unable to decrease their GF below the level exerted in 1 *g* and the safety margin was increased.

Moreover, a change of gravity did not significantly modify the LF amplitude or the frequency of the movement, except for the first trial of the NES as seen above. The phase shift between the two force signals was not significantly different in altered gravity fields compared to 1 *g*.

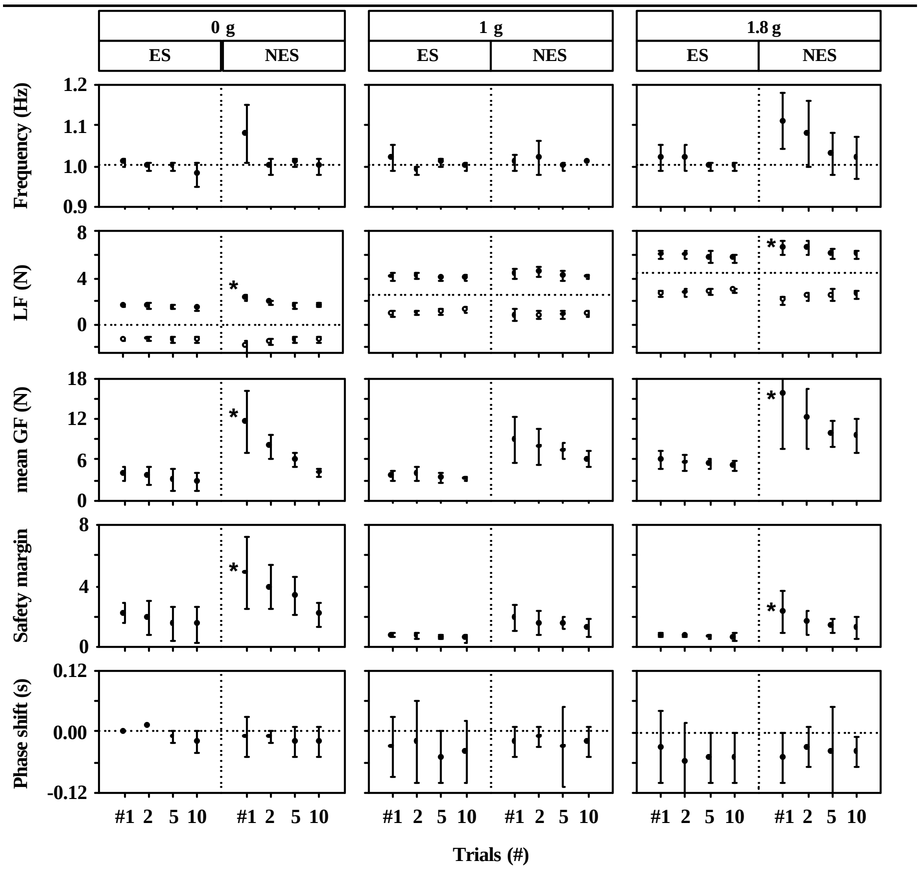

Figure 3.4: The means and standard deviations of the dynamic parameters are plotted for first, second, fifth and tenth trials in 0, 1, 1.8 *g* for the four subjects with previous parabolic flight experience (ES) and the four subjects who experienced microgravity for the first time (NES). The following parameters are shown: the frequency, the minimum (open circles) and the maximum (filled circles) of the load force, the mean level of the grip force, the safety margin when the load is maximum, and the phase shift between the corresponding maxima of GF and LF. A significant effect of repetition between parabolas is marked by an asterisk. Trial #1 of the NES and the ES corresponded to the first and the fifteenth parabolas of the aircraft, respectively

3.6 *Discussion*

The GF-LF co-ordination was studied during cyclic vertical arm movements using a hand-held instrumented load across different gravitational conditions (0, 1, 1.8 g) induced by parabolic flight maneuvers. The transitional phases between gravitational conditions were not analyzed because the large changes in the aircraft accelerations occurring at these times were unpredictable, and would have generated inconsistent grip force reactions. The results showed that the GF was modulated in parallel with the LF fluctuations due to the arm movements regardless of the gravity condition. In new gravity fields, the phase shift between the GF and the LF was equivalent to that observed in 1 g even on the first trials of the NES. By contrast, the level of the grip force modulation was dependent upon the gravity level and its adjustment seemed to require some adaptation for the NES. The experienced subjects (ES) adjusted the level of the grip force modulation to the new gravitational field as soon as they executed the task in the aircraft. The non-experienced subjects (NES) had some difficulty to maintain the imposed movement and applied unnecessarily high safety margins during their first trial at 0 and 1.8 g. In the subsequent trials, they progressively decreased their grip force and no further evolution in the GF-LF coupling was seen after the fifth trial. In both groups of subjects, a continuous GF-LF relationship tended to be established across the different gravitational conditions although the safety margin in microgravity remained slightly above the level observed at 1 and 1.8 g.

In the first part of this discussion, we will consider a possible mechanism involved in the temporal coupling between GF and LF. In altered gravity conditions, the modulation of grip force with the load fluctuations was observed from the first trial. As already observed by Hermsdörfer *et al.* (2000), the tight coupling between the peaks of the two forces was conserved with the same phase shift as on earth (Flanagan and Wing 1995). These results suggest that the anticipatory mechanism predicting the consequences of the arm accelerations on the load force acting on the fingers is a well-tuned process which is available even in altered gravity fields. An accurate prediction of the object acceleration enables the subjects to anticipate the time at which the LF is maximal. As a result the GF is modulated in phase with the LF fluctuations whatever the gravity condition.

While the temporal coupling of the GF-LF relationship was conserved in altered gravitational fields, the mean level of grip force had to be adjusted to the gravitational component of the LF. Evidence for progressive adaptation to a new gravity level was observed in subjects with no previous experience in parabolic flights. They dramatically increased the safety margin in the first trial both in microgravity and in hypergravity. Different interpretations of this observation can be considered. Firstly, the alterations of the limb proprioception due to the modification of the muscle spindle gain in altered gravity condition could result in altered judgement of object weight and mass (Lackner and DiZio 2000). However, the problem of mass discrimination previously observed by Ross *et al.* (1984, 1986) could be ruled out because, in our protocol, the mass could be estimated during the lift of the object in the 1 *g* period preceding the beginning of the parabola. Moreover, the information about the LF is mainly provided by the mechanoreceptors of the skin (Johansson and Westling 1991) that have not been previously reported to be affected by a change of gravity. Secondly, all novice subjects took scopolamine for motion-sickness. Scopolamine may reduce sweating, which can decrease skin friction and subsequently would require a greater grip force to prevent an object from slipping. However, the mean level of NES grip force used at 1 *g* in the aircraft (with scopolamine) or on earth (without scopolamine) was equivalent, suggesting that the medication did not perturb the grip-load modulation. Thirdly and most likely, the parabolic flight experience was exciting, distracting and frightening to most novices. Therefore the stress induced by the unusual and unexpected force circumstance likely contributed to the increased grip force level in order to provide a larger safety margin for the NES. Johansson *et al.* (1992) and Blakemore *et al.* (1998) have observed a similar counter strategy when manipulating an "active" object which produced unpredictable load force. The baseline of the grip force was increased to prevent slip that might occur following a sudden increase of load.

A direct indicator of increasing subject confidence in the new gravitational surroundings was the progressive decrease of the safety margin. For the NES, a maximum of five parabolas was necessary to incorporate the effects of gravity changes into the CNS program that controlled grip forces. While no significant change in the parameters of the grip-load force coupling was observed during the subsequent trials, a decreasing trend persisted out to the tenth trial. It suggests that after a few repetitions, the NES have acquired a better internal representation of the new gravitational field through the incoming vestibular and somatic sensory information. This supports the results of Papaxanthis *et al.* (1998) which showed evidence that gravity is centrally represented in an anticipatory fashion as a driving force during vertical arm movement planning. This also confirms the hypothesis that adaptation of the human motor system to new force environments generating changes in the dynamics of the arm occurs rapidly over a limited number of trials (Lackner and DiZio 1994).

Evidence of such internal representation of the gravity can be seen in the results obtained for the experienced subjects. Subjects with previous participation in parabolic flights (long-term experience) and passively submitted to fifteen parabolas before the experiment (short term experience), adequately adapted the mean grip force to the new gravity fields when performing the task for the first time in these environments. This supports the hypothesis of Flanagan *et al.* (1999) that the brain maintains internal models of the kinematics and dynamics of different environments and has some ability to combine and decompose them as called for by the situation. Nevertheless, as the ES were only tested after fifteen parabolas, it is unknown whether they would also exhibit an adaptation during the first parabola of the aircraft. The present results do not allow us to differentiate the effects of long or short term parabolic flight experience on the dynamics of prehension. Yet, it is obvious that the ES subjects took advantage of their experience to manipulate the objects with an adapted safety margin from their first trial.

The fast adaptation to different gravity and the ability to maintain the gravity representation in internal CNS models probably explain why Hermsdörfer *et al.* (2000) did not observe learning in a similar experiment. In their study, only two subjects were examined, the first one had a previous parabolic flight experience four years earlier, and the second one was a novice. Both subjects participated in the two flights and the novice subject was tested on the second flight. During the five first parabolas, the subject had to maintain an object stationary across the different gravity phases. The cyclic vertical arm movements with a hand-held load were only performed during the three subsequent parabolas. Consequently, neither of the two subjects were really naï ve with respect to micro- and hyper-gravity before starting the oscillatory task which was similar to our experiment. Actually, simple passive exposure to parabolic flight maneuvers leads to rapid perceptual adaptation in term of magnitudes of apparent force experienced (Lackner and Graybiel 1982).

We have also observed that once the subjects were familiar with new gravity conditions, they tended to establish a single GF-LF relationship across the gravitational environments. Ideally, the subjects should increase and decrease their GF at 1.8 *g* and 0 *g* respectively in order to keep the same safety margin than in the 1 *g* condition. Our results showed that even with the ES after ten parabolas, the GF in microgravity remained the same as in 1 *g*, inducing a greater safety margin. We cannot rule out that further adaptation would occur on longer period of microgravity or may be that the subjects did not want to reduce their GF below the level experienced on earth.

Previous studies have shown that a change in gravity perturbed the arm movement kinematics in target pointing, manual tracking (for review Bock 1998) and arm movement control (Fisk *et al.* 1993). In our study, despite an imposed amplitude (20cm) and frequency (1Hz) of movement, we have observed an increase in the load force amplitude when subjects were faced with a new gravity environment for the first time. Since the frequency was not perturbed, this suggests that the peak-to-peak object acceleration was modified by a change of the arm trajectory. Further study will be performed to investigate this hypothesis using a 3D movement tracking system.

Chapter 4: Influence of the environmental context on the control of the precision grip.

4.1 Preliminary remarks

In our previous observations obtained in parabolic flight (Augurelle et al 2003), we observed that experienced subjects were able to exert the same grip force for equivalent load forces obtained either at 1 g with a fast object acceleration or at 2 g with a slow object acceleration even though the dynamics of the upper limb was changed. In the present study, we would like to confirm and strengthen this observation by better controlling the level of load forces. The manipulative task was realized by using different combinations of objects and arm masses with different gravity fields and different arm accelerations. In this way, it was possible to generate equivalent magnitude of loads at the fingertips while the mechanical constraints on the upper limb and thus the motor commands required to move the arm were modified. We measured the grip force applied on the object for these equivalent levels of load while the arm dynamics was different. In order to program adequate GF motor command in anticipation of the LF, the forward dynamic model of the arm must extract the acceleration of the system (arm + object) by differentiating correctly the context of mass and gravity. It was interesting to observe how dynamic constraints such as gravitational force and inertial resistance of the arm and object would be taken into account in the control of precision grip. This experiment was performed by subjects with great experience in parabolic flight who were trained with the manipulative task on earth. We would like to study if they would be able to integrate the new gravity parameters in the motor control of precision grip the first time they realize the task in parabolic flight.

For this experiment, new force sensors were used allowing the computation of the overall destabilizing load (L) that takes into account both the tangential force and rotational torque. Moreover we used a cylindrical manipulandum for its compactness and its symmetry getting more stability for the object. On average, L was approximately 20 % greater than the tangential load suggesting that some rotational torques were induced when moving a freestanding object up and down. From this observation, we can suppose that the load force measured with a one-dimensional accelerometer in our previous experiment was slightly underestimated. Nevertheless, it would not change our conclusions significantly, as this underestimation should not perturb the load force profile.

The results of this experiment are detailed hereafter as a full paper entitled " Influence of the environmental context on the control of the precision grip".

4.2 Abstract

In this experiment, we examined the grip-load force coupling observed during cyclic vertical arm movements with a hand-held object performed in different environmental contexts. Five subjects highly experienced in parabolic flight participated in this study. They had to continuously move a cylindrical object up and down in the different gravity fields (1 g, 2 g and 0 g) induced by parabolic flights. The imposed movement frequency was 1 Hz, the object mass was either 200 or 400 g, the amplitude of movement was constrained to either 20 or 40 cm and an additional mass of 200 g could be wound around the forearm. Each subject performed the task during 15 consecutive parabolas. The coordination between the grip force normal to the surface and the destabilizing tangential load force was examined in nine loading conditions. The main finding was that the subjects used the same ratio between the two forces whatever the context. The same grip force was used for equivalent load generated either by a change of mass, gravity or acceleration despite the fact that it requires different arm motor commands. This suggests that the internal forward model takes the new dynamics of the upper limb and object into account to predict the arm trajectory and in turn the object's acceleration.

4.3 Introduction

To lift an object aloft, the grip force applied normal to the object's sides (hereafter referred to as the 'normal force') must be sufficient to counteract both the gravitational and the inertial components of the tangential load force acting on the fingertips (Johansson and Westling 1984). A tight temporal coupling between the normal force and the tangential load force has been documented in a large variety of tasks engaging different sorts of objects, grips, loads or mode of transport (Johansson and Westling 1984, 1988; Jenmalm and Johansson 1997; Flanagan and Tresilian 1994, Flanagan et al 1999). All studies to date seem to confirm that adjustments of the normal force anticipate tangential load changes when the movement is self-produced provided that the physical properties of the object are predictable (Flanagan and Wing 1993, 1995). There is increasing evidence in the literature that the CNS acquires neural mechanisms called "internal models" that can simulate the behavior of our body and of the environment (physical properties of the object and gravity) (Wolpert et al 1995, Flanagan and Johansson 2002, McIntyre et al. 2001). The principle is that during object manipulation, these internal models would predict future accelerations of the arm by using a copy of the motor command that produces the intended arm movement (Flanagan and Wing 1997, Kawato 1999). From this prediction, and from visual or haptic information about the object's weight, the total tangential load can be estimated and an appropriate normal force can be programmed in a feedforward manner. Thus the loads experienced at the hand could be derived from the arm motor commands. However the relation between arm movement motor commands and the load experienced at the hand depends on the type of load being moved. Flanagan and Wing (1997) showed that grip force was modulated in phase with, and thus anticipated, the tangential load when moving not only inertial but also viscous and elastic loads. These results suggest that the commands for grip force are not simplistically linked to the commands for arm movement but instead are based on an internal model of the motor apparatus and external load. In a previous study in parabolic flight, we measured how subjects adjusted the normal force to changes in gravity that modified the relation between the arm movement and the load force (Augurelle et al, 2003). We observed that after adaptation (five trials for novice subjects) the normal force increased adequately in 2 *g* in order to maintain the same safety margin as on the ground even though the arm was two times heavier. By contrast, the normal force in microgravity (0 *g*) remained the same as that produced in 1 *g* , leading to a greater safety margin in the 0 *g* condition.

In the current experiment we took this study a step further by modifying all components of the load acting on the arm. The weight of the arm was altered either by placing an external mass (200 g) around the wrist or by moving the arm in the different gravity fields (0 *g* or 2 *g*) induced by parabolic flight. In the former case, both the gravitational torque at the joints and the inertia of the arm were modified whereas in the latter case, inertial torques remained unchanged. Similarly, we asked subjects to manipulate objects of two different masses (200 g and 400 g) in the three different gravitational conditions. Under these conditions, different arm motor commands would be required to accomplish the same movement. We posed the question as to whether the arm acceleration and in turn the tangential load would be adequately predicted in order to program an appropriate grip force. Would the subject exert a higher grip force for equivalent tangential loads at the fingers if the effort required to move the upper limb increased or decreased?

4.4 Methods and materials

4.4.1 Subjects

Five right-handed subjects (30-48 years old) participated in the study. They were examined in a Center for Aerospace Medicine in order to qualify for parabolic flights (medical examination type "JAR class II"). No subject reported sensory or motor deficits. They were all accustomed to parabolic flights – all had previously flown between 300 and 2000 parabolas. All participants gave their informed consent to participate in the study, and the procedures were approved by the European Space Agency Safety Committee and by the local ethics committee.

4.4.2 Parabolic flight

The flights originated in Bordeaux (France) using the Airbus A300 “ZEROg” aircraft. A single parabolic flight profile generates a sequence of episodes of hyper- (1.8 *g*), micro- (0 *g*), and hyper- (1.8 *g*) gravity of about 20 s duration each (see also Augurelle et al 2003). For the sake of simplicity , 2 *g* will be used in the manuscript to characterize the 1.8 *g* condition. Thirty parabolas were performed in each of the three flights, organized as six groups of five parabolas with 2-minute periods of 1 *g* level flight between each parabola plus an additional 5 to 8 minutes between each group. A three-dimensional accelerometer was fixed on the floor of the aircraft to record its acceleration along the Z-axis (normal to the floor of the airplane), the Y-axis (along to the lateral axis of the airplane), and the X-axis (along the fore-aft axis of the airplane). On average, for all parabolic maneuvers (n=90), at 1 *g*, the aircraft accelerations were 9.77 ± 0.28 m/s^2 along the Z-axis, 0.07 ± 0.04 m/s^2 along the Y-axis, and -0.30 ± 0.10 m/s^2 along the X-axis. At 2 *g*, the accelerations were 17.31 ± 0.93 m/s^2 along the Z-axis, 0.07 ± 0.05 m/s^2 along the Y-axis and -0.70 ± 0.19 m/s^2 along the X-axis. At 0 *g*, the accelerations were 0.13 ± 0.2 m/s^2 along the Z-axis, 0.01 ± 0.05 m/s^2 along the Y-axis and -0.09 ± 0.02 m/s^2 along the X-axis.

4.4.3 Apparatus

Grip versus load-force coupling was examined while holding a cylindrical object (80 mm diameter, 30 mm width, 200/400 g mass) during cyclic vertical arm movements. The instrumented object was equipped with two circular grip surfaces (brass disks, 40 mm diameter) placed on two parallel lightweight force-torque sensors (Mini40 F/T transducer, ATI industrial automation). Each sensor measured three force (F_x, F_y, F_z) and three torque (T_x, T_y, T_z) components around the corresponding axes passing through the center of the corresponding grip surface (Fig. 4.1a).

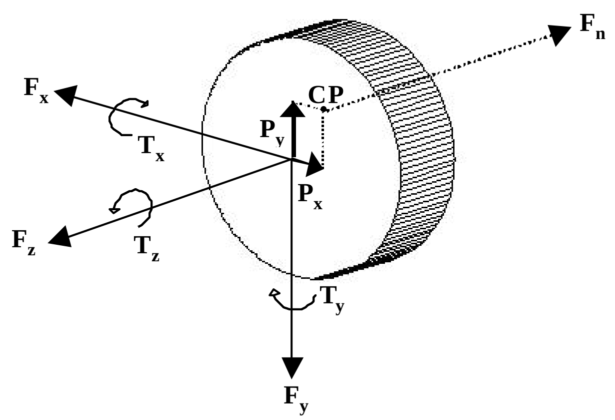

Figure 4.1a: Reference frames for forces (F_x, F_y, F_z) and torques (T_x, T_y, T_z) measured by the force-torque sensor placed under each grip surface. F_n is the normal force applied on the grip surface. CP is the center of pressure of the finger on the grip surface. P_x, P_y are the coordinates of the center of pressure.

Sensing ranges for F_x, F_y and F_z were ±40, ±40 and ±120 N with 0.02, 0.02 and 0.06 N resolution, respectively. The torque sensing range was ±2 Nm for all axes with 0.001 Nm resolution.

4.4.4 Experimental procedure

The same procedure as in our previous experiment was used (see Augurelle et al 2003). At a signal from the experimenter, the instrumented object was grasped between the thumb on one side and the index and middle fingers on the other side at about the center of the grasp surfaces. The fingers were aligned along the X-axis in order to place the Y-axis in the downward direction. The subjects were instructed to perform cyclic vertical arm movements at a frequency of 1 Hz, aided by a metronome. The amplitude of the oscillations was maintained by lightly constraining the movement within two parallel rubber bands spaced either 20 cm or 40 cm apart, which indicated the endpoints of the movement (Fig. 4.1b). Subjects performed the upper limb displacement with unconstrained shoulder and elbow movements. They were instructed to maintain the Y-axis of the object in a vertical orientation without tilting in any direction.

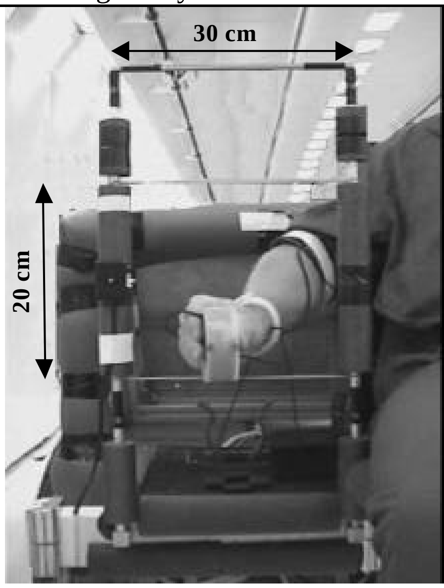

Figure 4.1b: Schematic drawing of the apparatus held between the thumb on one side and the index and middle fingers on the other side. The arm displacement is limited by to rubber bands 30 cm long spaced 20cm apart.

The experiment was first carried out at 1 *g* on the ground before the flight in order to train the subjects on the task. Then the experiment was performed at 0 *g*, 1 *g* and 2 *g* during the parabolic flights. Each subject performed the task over 15 complete parabolas in the aircraft. In the five first trials (P1-P5), the task was performed with a 400 g mass displaced by a distance of 20 cm at a frequency of 1 Hz ("400g20cm"). In the second series of five trials (P6-P10), the mass was reduced by half and the amplitude of movement was doubled ("200g40cm"). As the frequency of movement was kept the same (1 Hz), the acceleration was also twice as great resulting in an equivalent inertial load but an increased gravitational load. In the last five trials (P11-P15), the 40 cm movement was performed with the 200 g mass but a ballast brace of 200 g was placed around the wrist of the subject ("additional mass"). In this case the inertial and gravitational components of the load were the same but the inertial and gravitational components of the arm were increased. Table 1 shows that among the nine load conditions, four levels of equivalent tangential force acting on the fingertips could be reproduced while the upper limb was moving in different gravitational fields.

Table 1: The four levels of equivalent tangential load

Condition	Level	Gravity	m object	Dist	Freq	m arm	GL (N)	IL (N)	Total L (N)
	Ref	**1G**	**200g**	**20 cm**	**1Hz**	**-**	**mG**	**ma**	**m(G + a)**
1	1	2G	400g	20cm	1Hz	-	2m2G	2ma	2m(2G + a)
2	2	2G	200g	40cm	1Hz	-	m2G	m2a	2m(G+a)
3		2G	200g	40cm	1Hz	+	m2G	m2a	
4		1G	400g	20cm	1Hz	-	2mG	2ma	
5	3	1G	200g	40cm	1Hz	-	mG	m2a	m(G+2a)
6		1G	200g	40cm	1Hz	+	mG	m2a	
7	4	0G	400g	20cm	1Hz	-	0	2ma	2ma
8		0G	200g	40cm	1Hz	-	0	m2a	
9		0G	200g	40cm	1Hz	+	0	m2a	

G: Gravity
m object : mass of the object m arm: absence (-) or presence (+) of the 200g mass on the arm
Dist: object displacement
Freq: movement frequency
GL: gravitational load
IL: inertial load
L: load
a: object acceleration
Ref: reference values of gravity mass and distance

The subjects grasped the instrumented object and performed the cyclic movement during a 1 *g* phase of the flight, starting approximately 30 seconds before the start of the 2 *g* phase. The movement was performed throughout the entire parabola (2g, 0g, 2g) and continued 30 seconds after the return to the 1 *g* condition.

4.4.5 Data processing and analysis

The signals from the force-torque transducers, the 3D accelerometers and from the metronome were digitized on-line at 200 Hz with a 12-bit 6071E analog-to-digital converter in a PXI chassis (National Instruments©, Austin, TX). After analog-to-digital conversion, the signals were further low-pass filtered with a fourth-order, zero phase-lag Butterworth filter having a cut-off frequency of 15 Hz.

The grip force (F_n) applied normal to the grasp surface was calculated as $-F_z$. The total grip force was calculated as the average of the normal forces applied by the thumb and the fingers on each transducer.

The magnitude of the tangential force (F_t) was computed according to Kinoshita et al (1997) as: $F_t = \sqrt{F_x^2 + F_y^2}$ (Fig. 1C). The direction of the tangential force vector was calculated as follows: $\alpha = \frac{180}{\pi} \tan^{-1}\left(\frac{F_y}{F_x}\right)$. This force vector should be equal and opposite to the product of the object mass times the vectorial sum of the gravitational and object accelerations. The angle α was chosen between 0 and 360° in such a way that when α equaled 0°, $\vec{F_t}$ was directed along the X-axis. The total tangential force acting on the object was calculated as the sum of the tangential force measured at each finger by the two force-torque transducers.

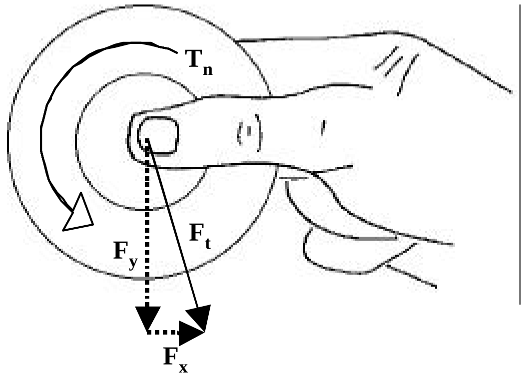

Figure 4.1c: Side view of the object. The plain arrow represents the tangential force (F_t). The dotted arrows are the horizontal (F_x) and the vertical (F_y) components of the tangential load. The curved arrow represents the rotational torque (T_n) acting on the fingers.

The tangential torque magnitude (T_n) that tended to rotate the objects within the fingertips was computed as the difference between the measured tangential torque (T_z) and the off-axis torque, if any. This off-axis torque appeared when the finger centers-of-pressure (P_x, P_y) were not located on the center of the grip surfaces (Kinoshita et al 1997): $T_n = T_z - (F_y * P_x - F_x * P_y)$ where $P_x = -T_y / F_z$ and $P_y = T_x / F_z$. The total tangential torque was calculated as the average of the torques measured on each transducer.

The mathematical model developed by Kinoshita et al (1997) was used to estimate the overall destabilizing load (L) acting on the object taking into account the tangential torque (T_n) and the tangential force (F_t): $L = F_t + a|T_n| + bF_t|T_n|$ where a = 0.1333 mm^{-1} and b = -0.0114 $N^{-1}mm^{-1}$.

The analysis of the force measurements was performed cycle by cycle. A cycle was defined between two successive peaks of load (L). Six consecutive cycles of movement were analyzed in each gravitational phase of all the parabolas (n = 15 parabolas × 5 subjects × 6 cycles) during the steady state of the aircraft accelerations (1 *g*, 2 *g* and 0 *g*). The maximum, the minimum and the average values within a cycle of movement were calculated for L, F_n and F_n / L . A cross-correlation between F_n and L series was calculated for each trial to determine the phase lag at which the maximal correlation (r) between the two series was obtained. A negative phase lag would indicate that the correlation was maximal when the grip force change preceded the load change.

4.4.6 Statistical analysis

A one-way analysis of variance for repeated measures was performed on averaged data to compare the four levels of load. Within each level of load, a two-way analysis of variance for repeated measures was performed on the parameters to test for the differences between the load conditions (factor 1) and to test for the differences between the five trials (factor 2). A Tukey's pairwise multiple comparison procedure was used to determine which treatments were significantly different. All the statistical analyses were carried out with SigmaStat 2.03 (SPSS inc.).

4.5 Results

Figure 4.2 illustrates six typical cycles of movement obtained in each phase of a parabola (1 *g*, 2 *g* and 0 *g*) while oscillating a 400 g mass on a distance of 20 cm at a frequency of 1 Hz. The vertical aircraft acceleration was constant in each gravitational phase (Fig. 4.2A).

4.5.1 Description of the task in 1 g

When moving an object up and down at 1 *g* (Fig.2, left column), the tangential force (F_t) (Fig.4.2B) was primarily due to its vertical component (F_y) because the horizontal component of the tangential force (F_x) was close to zero throughout the cycles. F_t typically fluctuated around the object weight, proportionally to the arm vertical accelerations. It reached a maximum at the bottom of the trajectory when the gravity and the vertical component of the object acceleration acted in the same direction. It was minimum when the object's vertical acceleration was opposite to that of the gravity. The direction of the tangential force vector (α) was on average for all trials, 250 ± 29° and 252 ± 14° at the upper and the lower ends of the arm trajectory, respectively. In 1 *g*, the estimated overall destabilizing load (L) (Fig.4.2C) was 16 ± 10 % greater than F_t indicating that the tangential torques (T_n) (Fig.4.2D) were very small during this task. The normal force (F_n) (Fig.4.2E) oscillated continuously in parallel with the load fluctuation

(L) so that the force ratio (F_n/L) was quite constant across the cycles (Fig.4.2F).

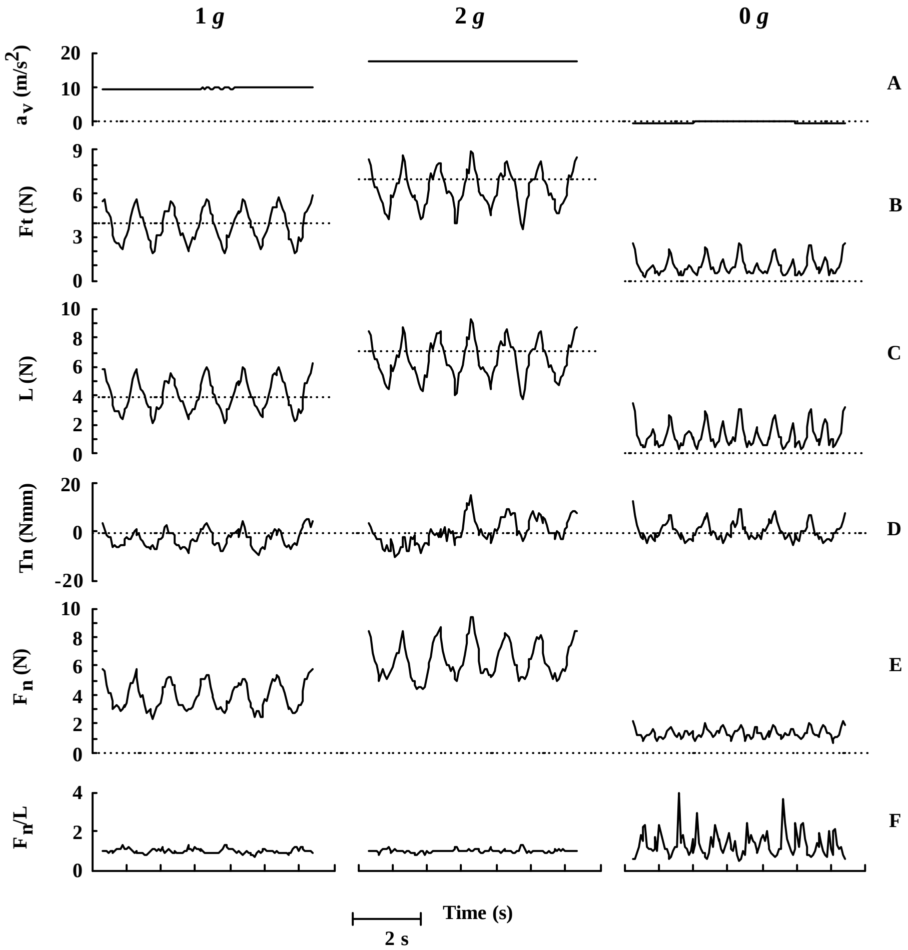

Figure 4.2: Single records of six typical cycles of movement in the stable period of each gravitational phase while oscillating a 400 g load on a distance of 20 cm with a frequency of 1 Hz. The following traces are displayed as a function of time: A) the vertical aircraft acceleration (a_v), B) the tangential load force (F_t), C) the overall destabilizing load (L), D) the rotational torque (T_n), E) the normal force (F_n) and F) the force ratio (F_n/L).

4.5.2 Description of the task in 2 g

In hypergravity (2 *g*) (Fig.2, middle column), F_t (Fig.4.2B) was principally due to its vertical component F_y because F_x remained close to zero. The mean magnitude of F_t increased because the object weight was nearly doubled. Note however that the fluctuations of the tangential force (F_t) were centered on a value less than the object's weight. This indicates that the object's acceleration was greater at the top than at the bottom of the arm trajectory. The tangential force vector was directed in the downwards direction ($\alpha = 263 \pm 19°$ and $\alpha = 251 \pm 13°$ at the upper and lower end of the arm trajectory, where $\alpha = 270°$ is straight down). Moreover, F_t was close to L (Fig.4.2C) because the contribution of T_n to the total load was small (12 ± 10 %) (Fig.4.2D). The normal force (F_n) (Fig.4.2E) varied in parallel with the load fluctuation (L) giving a constant force ratio (F_n/L) across cycles, the same as in 1 *g* (Fig.4.2F).

4.5.3 Description of the task in 0 g

In microgravity (0 *g*) (Fig.2, right column), the object had to be accelerated both upward and downward because the gravity no longer accelerated the object downward. In this way, the tangential force reached a maximum both in the upper and lower parts of the arm trajectory (Fig. 4.2B). Note however that F_t was greater at the bottom than at the top of the arm trajectory indicating that the object acceleration was greater to push the object upward than push it down. The tangential force (F_t) was directed downwards ($\alpha = 242 \pm 23°$) and upwards ($\alpha = 139 \pm 36°$) at the lower and upper ends of the arm trajectory, respectively. The estimated overall destabilizing load (L) (Fig.4.2C) was 27 ± 11 % greater than F_t indicating a significant contribution of the tangential torques in 0 *g* (Fig.4.2D). Subjects increased the normal force (F_n) (Fig.4.2E) in anticipation of the peaks of load both at the top and at the bottom of the trajectory so that the force ratio reached minimum values at these times, comparable with what occurred in the 1 and 2 g gravity fields (Fig.4.2F).

4.5.4 Comparison between the levels of force

Four statistically different levels ($p<0.001$) of overall destabilizing mean load (mean L) were defined among the nine different conditions, corresponding to the four levels predicted on theoretical grounds (Table 1). Within each of these levels the mean L were not significantly different ($p>0.05$) (Fig.4.3A).

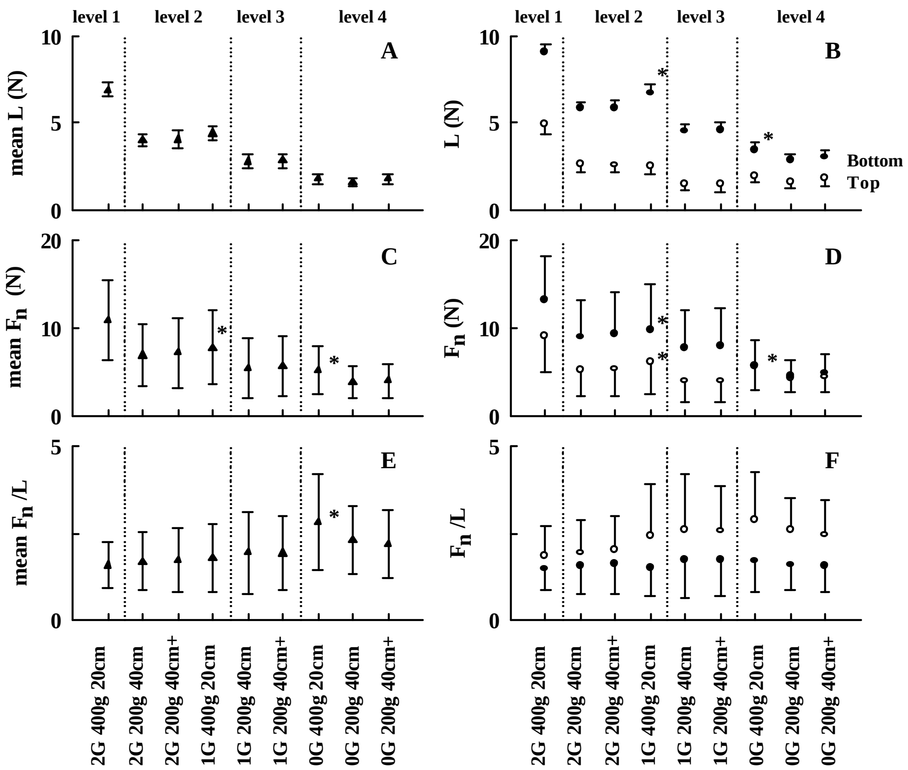

Figure 4.3: The means and standard deviations of the dynamic parameters are plotted for each load conditions for all subjects and trials. The left graphs represent the mean magnitude (triangle) of (A) the overall destabilizing load, (C) the normal grip force and (E) the force ratio. The right graphs represent the minimum (open circles) and the maximum (filled circles) of (B) the overall destabilizing load, (D) the normal force and (F) the force ratio. Vertical dotted lines delimit the four levels of load. Asterisks signal a significant difference between load conditions within each level.

Level 1 (mean L = 6.93 ± 0.38 N) was generated when moving 400 g at 2 *g* on a distance of 20 cm (Fig.4.3A). Level 2 (mean L = 4.17 ± 0.35 N) was generated either by moving 400 g at 1 *g* on a distance of 20 cm or by moving 200 g at 2 *g* on a distance of 40 cm with or without an additional mass on the wrist (Fig.4.3A). Note however that with the 400 g mass, the load reached a higher maximum (Fig.4.3B) than in the other two conditions ($p<0.001$). Level 3 (mean L = 2.83 ± 0.27 N) was obtained with 200 g moved at 1 *g* with or without the additional mass on the wrist (Fig.4.3A). Finally, level 4 (Fig.4.3A) occurred at 0 *g* with either 400 g, 200 g or the additional mass (mean L = 1.74 ± 0.23 N). Once again, the load reached a higher maximum with the 400 g mass than with 200 g ($p=0.003$) (Fig.4.3B). In the 0 *g* environment, it is also interesting to observe that the load was significantly higher at the bottom of the trajectory. This means that the arm acceleration was not symmetric in absence of gravity, i.e. the subjects accelerated the object faster at the bottom of the arm trajectory.

The normal force (F_n) was measured at each level of load (L) to test whether the same normal force was used for equivalent levels of load (Fig. 3C-D) and to test whether the same force ratio (F_n/L) was maintained when the level of load changed (Fig. 3E-F). First, we compared the normal forces for the three load conditions within level 2 (Fig. 3C-D). Mean F_n increased slightly ($p=0.003$) when moving a 400 g mass at 1 *g* to compensate for the higher peak of load. F_n was increased both at the top ($p=0.006$) and at the bottom of the trajectory ($p=0.04$) (Fig.4.3D). In this way, the same force ratio (F_n/L) was maintained in the three conditions ($p>0.05$) (Fig.4.3E-F). For level 3, F_n as well as F_n/L were the same when moving a 200 g mass at 1 *g* with or without the additional mass on the wrist, (Fig.4.3C-E).

Considering level 4, mean F_n was significantly higher ($p<0.009$) when moving the 400 g mass (Fig.4.3C-E) than when moving the 200 g mass with or without the additional wrist ballast. Since there is no significant difference between the mean L, one can observe a significant increase ($p=0.023$) in F_n/L when moving the 400 g mass. In this particular condition, F_n was increased both at the top ($p=0.016$) and at the bottom ($p=0.018$) of the trajectory (Fig. 3D). It is also interesting to observe that the same F_n were used both at the top and at the bottom of the arm trajectory although the magnitude of load (L) was lower at the top (Fig.4.3B-D).

When comparing the four levels of load in Fig.4.3F, the most interesting finding was that the subjects used the same F_n/L ratio for the nine conditions when the load reached a maximum *i.e.* at the bottom of the arm trajectory. This ratio is low and highly reproducible for each subject (1.63 ± 0.81). The F_n/L ratio when the load reached a minimum was higher and more inconstant because the subjects did not release their grip as much as they might have while still maintaining an adequate safety margin.

Considering the effect of repeating five trials consecutively within each level of load, there were no significant differences ($p>0.05$) between the trials at 1 and 2 g. By contrast, the force ratio was significantly higher during the two first trials in each load condition performed in microgravity (level 4) ($p<0.001$).

4.5.5 Correlation

A cross-correlation between the normal force and the overall load was carried out for each of the fifteen trials performed in each level of gravity. The maximum correlation was 0.89 ± 0.05 both at 1 *g* and 2 *g* and 0.66 ± 0.12 at 0 *g*. The maximum correlation occurred at time lags of 2 ± 15 ms, –6 ± 18 ms, 7 ± 20 ms at 1, 2 and 0 *g*, respectively.

4.6 Discussion

In this experiment we examined the relationship between the normal grip force (F_n) and the overall destabilizing force (L) while moving an object up and down in different environmental contexts. On the one hand, we modified each component of the load independently, i.e. the object's mass, gravity and the arm's acceleration. On the other hand, the weight of the arm was changed either with an additional mass or within different gravity fields. In this way, it was possible to generate equivalent magnitudes of loads at the fingertips while the mechanical constraints on the upper limb and thus the motor commands required to move the arm were modified. Similarly, certain trials required similar motor commands to move the arm, but different grip forces to maintain the object safely in the grasp.

In each load condition, the normal grip force was modulated in phase with the load fluctuations, confirming the previous results obtained in similar paradigms performed on earth and in parabolic flight (Flanagan and Wing 1995, 1997; Flanagan et al 1999; Hermsdörfer et al 2000; Augurelle et al 2003). In microgravity, the normal force thus increased again at the top of the arm trajectory to prevent slip as the object was pushed downwards. The main finding was that the magnitude of the normal force was adequately adjusted for each maximum of load in order to maintain the same ratio between the normal force and the overall destabilizing load (F_n/L) in the nine loading conditions. The subjects were able to maintain this optimal ratio in different contexts of mass, gravity and upper limb acceleration. For equivalent loads at the fingertips at 1 or 2 *g*, the subjects used the same grip force despite the fact that it required more force to displace the arm in hypergravity. Furthermore, we have shown that the normal force was modulated with and thus anticipated the combined effects of tangential force and rotational torque, in agreement with previous works (Kinoshita et al 1997; Goodwin et al 1998; Flanagan et al 1999). These results show that grip force is not related to the muscle commands to the upper limb in a simplistic manner.

These results further extend the general framework in which the grip-load force coordination is observed. Not only does the grip-load force coupling reflect a general control strategy for any particular grip or mode of transport (Flanagan and Tresilian 1994) but we have also shown that this strategy is used in different environmental contexts. The similar force ratio observed in the nine loading conditions indicates that dynamic constraints such as gravitational force and inertial resistance of the arm and object were well taken into account in the control of precision grip. The precise temporal coupling between the normal force and the overall destabilizing load also shows that the load was correctly predicted and that the normal force was calculated in a feedforward manner based on this prediction. This suggests that the forward model predicting the load can be adjusted to account for various physical contexts. In other words, subjects were able to identify the environmental context and select the appropriate motor program.

In a modular approach to the problems of motor control, it has been proposed that the brain contains multiple controllers (inverse models) associated with their corresponding predictor (forward models), with each of them suitable for one or small set of contexts (Blakemore et al, 1998; Wolpert and Kawato 1998). Based on several contextual cues such as experience from previous manipulations of the object and based on visual and tactile information about the object's physical properties, subjects can pre-select an appropriate module for, say, displacing a 400 g object on a distance of 20 cm in hypergravity. The selected controller will issue the motor command and the corresponding forward model will predict its sensory consequences. If the prediction is good the module will continue to be used. When the context estimate is wrong, the prediction will be poor and another module will be selected (Kawato 1999; Wolpert and Kawato 1998). This model fits well with our results. In this experiment, the five subjects were familiar with parabolic flights and were trained to perform the manipulative task on earth. In flight, the nine loading conditions were thus different combinations of known environments and previously manipulated objects. The modular model of motor control also assumes that separate internal models learned for different contexts can be mixed to cope with a given task (Wolpert and Kawato 1998; Flanagan et al 1999). It is likely that having learned the task in 1 *g* before the flight, and being already familiar with the different gravity fields, the subjects could execute the task after just a few trials.

In our previous study, we showed that inexperienced subjects needed approximately five trials to adjust their force adequately to the new gravity (Augurelle et al. 2003). In the present experiment, subjects adequately adjusted the force ratio starting from their first trial, except in microgravity where two first trials were needed to adjust to each loading condition. Similarly, both the time lag and the correlation between the two forces were poorer and more variable in 0 g than in the presence of gravity. The mean F_n/L ratio was greater in microgravity than in the other conditions essentially because the subjects exerted the same grip force to push the object downward as to lift it aloft although the load was in fact lower at the top of the trajectory. These deviations from the theoretically ideal performance could reflect an incomplete adaptation of the motor plan to microgravity. Papaxanthis et al (1998) demonstrated that the CNS takes into account static force such as gravity during the planning process of movement. They observed that arm movements on Earth were straighter downwards than upwards and that this difference did not disappear when gravity was removed. A gradual adaptation of the motor plan to the condition of microgravity was observed through a global straightening of hand paths in both directions (Papaxanthis et al 1998). We can expect that with more trials, our subjects would succeed in producing symmetric patterns of load and grip force in microgravity.

Although the coupling between normal force and the overall destabilizing load was preserved in hyper- and microgravity, the kinematics of the arm movements seems to be influenced by the gravitational level. The results reported here showed that the load fluctuations were not symmetric around the object weight, as it would be the case if the arm accelerations were equal and opposite at the top and at the bottom of the trajectory. At 2 g, the load was shifted down with respect to the object's weight indicating that acceleration was greater at the top than at the bottom of the arm movement as if the object were being pushed by the greater gravitational acceleration. At 0 g, the load was shifted up with respect to the weight indicating that acceleration was greater at the bottom than at the top of the arm movement because the arm was no more pushed by the gravitational acceleration. Such perturbations in the arm movement kinematics in a new gravitational environment have been previously observed in target pointing, manual tracking (for review Bock 1998) and arm movement control (Fisk et al. 1993). This alteration in the kinematics had negligible consequences on the dynamics of prehension, suggesting two independent control modes for these different processes. The prediction of the load force based on the arm motor command is precise enough to program the normal grip force in a feedforward manner. We conclude that the internal models used to control precision grip are sophisticated enough to take into account the differing effects of gravitational force and inertial load on the muscular effort required to move the arm and the grip force required to hold the object.

Chapter 5: Importance of cutaneous feedback in maintaining a secure grip during manipulation of hand-held objects.[4]

5.1 Preliminary remarks

Our two preceding studies suggested that forward models are necessary to allow anticipatory program of GF based on the prediction of the incoming LF. However, information about the actual LF is only available by tactile feedback after the movement has occurred. Then the comparison between the predictive and the actual LF generates an error that allows updating of the forward model. We can suppose that with usual objects the error would be small and the prediction of the load and friction would be precise. By contrast, for unusual objects or contexts, the error would be larger and the system would more rely on the tactile feedback in order to update its forward models of the object and environment. The question arises as to what would happen as the tactile feedback is suppressed. Would the forward model prediction be precise enough to allow adequate GF response? To answer to this question, we have studied the grip-load force coupling during arm movement with a hand-held load while the thumb and index finger were anesthetized. In this way, the system would only rely on forward prediction of the load and the object friction to scale the GF. No updating of the forward model would be possible during the task. During arm movements, the LF continuously fluctuates requiring a high performance of the predictive system. If the system is not updated by cutaneous afferent during the task, the error between the predicted and the actual LF would increase and the GF would become inadequate. Results obtained by other authors when lifting objects in absence of tactile feedback showed that the safety margin was increased but the temporal coupling between GF and LF was conserved (Johansson and Westling 1984, Johansson et al. 1992, Nowak

[4] Published as " Importance of cutaneous feedback in maintaining a secure grip during manipulation of hand-held objects." J. Neurophysiol. (2003) 89:665-671.

et al 2001, 2002). Moreover, GF adjustment in response to accidental slip or to unpredictable load were delayed, attenuated or abolished (Johansson et al. 1992).

The results of our study are detailed hereafter in a full paper entitled " Importance of cutaneous feedback in maintaining a secure grip during manipulation of hand-held objects".

5.2 Abstract

Previous research has shown that grip and load forces are modulated simultaneously during manipulation of a hand-held object (Johansson and Westling 1984; Flanagan and Wing 1993). This close temporal coupling suggested that both forces are controlled by an internal model within the central nervous system, which predicts the changes in tangential force on the fingers. The objective of the present study was to examine how the internal model would compensate for the loss of cutaneous sensation through local anesthesia of the index and thumb. Ten healthy adult subjects (5 men, 5 women aged 20 to 57 years) were asked to grasp, lift and hold stationary, a 250 g object for 20 seconds. Next, the subjects were asked to perform vertical oscillatory movements over a distance of 20 cm at a rate of 1.0 Hz for 30 seconds. Eleven trials were performed with intact sensation and 11 trials after a local ring-block anesthesia of the index and thumb with bupivacain (5 mg/ml). During static holding, loss of cutaneous sensation produced a significant increase in the safety margin. However, the grip force declined significantly over the 20 s static hold period. During oscillatory arm movements, grip and load forces were continuously modulated together in a predictive manner as suggested by Flanagan and Wing (1993). Again, the grip force declined over the 30-second movement, and 7/10 subjects dropped the object at least once. With intact sensation, the object was never dropped, but with the fingers anesthetized it was dropped on 36% of the trials and a significant slip occurred on a further 12%. The mean correlation between the grip and load forces for all subjects deteriorated from 0.71 with intact sensation to 0.48 after digital anesthesia. However, a cross correlation calculated between the grip and load forces indicated that the phase lag was approximately zero both with and without digital anesthesia. Taken together, the data from the present study suggest that, cutaneous afferents are required

for setting and maintaining the background level of the grip force, in addition to their phasic slip-detection function and their role in adapting the GF/LF ratio to the friction upon initial contact with an object. Finally, at a more theoretical level, they correct and maintain an internal model of the physical properties of hand-held objects.

5.3 Introduction

When moving a hand-held object, the grip force is automatically modulated in parallel with fluctuations in the load force that depend on the weight and the acceleration of the object (Flanagan and Wing, 1995). Accidental slips rarely occur because the grip force exceeds the minimal force required to prevent slip (the 'slip force') by a safety margin determined by the skin-object friction (Johansson and Westling, 1984). The temporal cross-correlation between the two forces is high and the peak occurs at time lags ranging from –10 ms to +15 ms (Flanagan and Wing 1995). Given the delay associated with cutaneously triggered reflexes (Johansson and Westling 1987, 1988; Collins et al 1999), it is unlikely that the CNS could rely on sensory feedback alone to adequately adjust the grip forces when loads vary rapidly. This suggests that the central nervous system (CNS) is able to program the grip forces in anticipation of the tangential forces arising from self-produced movements of objects with predictable physical properties of friction and inertia (Flanagan and Wing 1993). The CNS would acquire patterns of neural activity, called internal models that are able to simulate and anticipate the dynamic behavior of the arm and of hand-held objects from prior experience (Jordan and Wolpert 1999). In this way, the consequences of a future arm trajectory on the load force acting on the object could be predicted and the grip force necessary to prevent slip could be calculated in a feedforward manner (Johansson and Westling 1988). However, this theorizing does not explicitly state that tactile feedback is unnecessary for reliable and secure object manipulation. According to Johansson and Cole (1994), cutaneous stimuli are used intermittently as discrete event, sensory-driven error signals. The mechanoreceptors of the glabrous skin provide rapid and accurate information about discrete mechanical events like the changes in shear force or slip on the skin (Johansson and Westling 1987). These events then trigger compensatory grip force responses maintaining the grip-load force ratio above the critical slip point and revising the internal models that support the anticipatory control.

Even after digital anesthesia, Johansson and Westling (1984) showed that the grip and load forces were controlled in parallel during the different phases of a lifting task. However, the grip-load force ratio was no longer appropriately adjusted to the skin-surface friction and the initiation of lifting (i.e. the loading phase) was delayed. Moreover, the grip force adjustments in response to accidental slips and the grip force responses to unpredictable loads were delayed, attenuated or totally abolished following anesthetic block (Johansson et al. 1992). During point-to-point arm movements with anesthetized fingers, the grip force was significantly increased but was still modulated in parallel with the load force changes due to both arm acceleration and changes in movement direction with respect to gravity (Nowak et al 2001, 2002).

The objective of the present study was to determine the respective contribution of feedforward and feedback processes during the manipulation of mechanically predictable loads. For this purpose, the grip-load force coupling during cyclic arm movements were examined while tactile feedback was suppressed by locally anesthetizing the thumb and index finger.

5.4 Methods

5.4.1 Subjects and experimental procedures

Ten healthy, right-handed subjects (5 men, 5 women aged 20 to 57 years) gave their informed written consent to participate in this study. The experimental procedures were approved by the ethics committee of the Université catholique de Louvain.

The grip-load force coupling was examined during cyclic vertical arm movements with a hand-held 250 g load. The instrumented object (164 mm high) was held with a precision grip applied on two parallel brass disks (Fig.1a). The force sensors registered grip forces up to 100 N with a force resolution of 0.0244 N/Bit. The strain gauges were connected to a single Wheatstone bridge, which allowed the vertical position of the center of pressure generated by each finger to be estimated. When the grip force was applied midway between the 40 mm separating strain gauges A and B, the reaction forces, FR_A and FR_B, recorded by each gauge were identical and equal to GF/2. As the center of pressure was displaced vertically by a distance Z from the center of the grip surface toward the strain gauge A, the reaction force, FR_A, increased in proportion to Z, whereas FR_B decreased by a similar amount (Fig. 1b). The vertical position of the center of pressure, Z, was calculated as:

$$Z = \frac{L(FR_A - FR_B)}{2(FR_A + FR_B)}$$

The spatial resolution of the position center of pressure was grip force dependent and equal to 0.151 mm for a grip force of 10N.

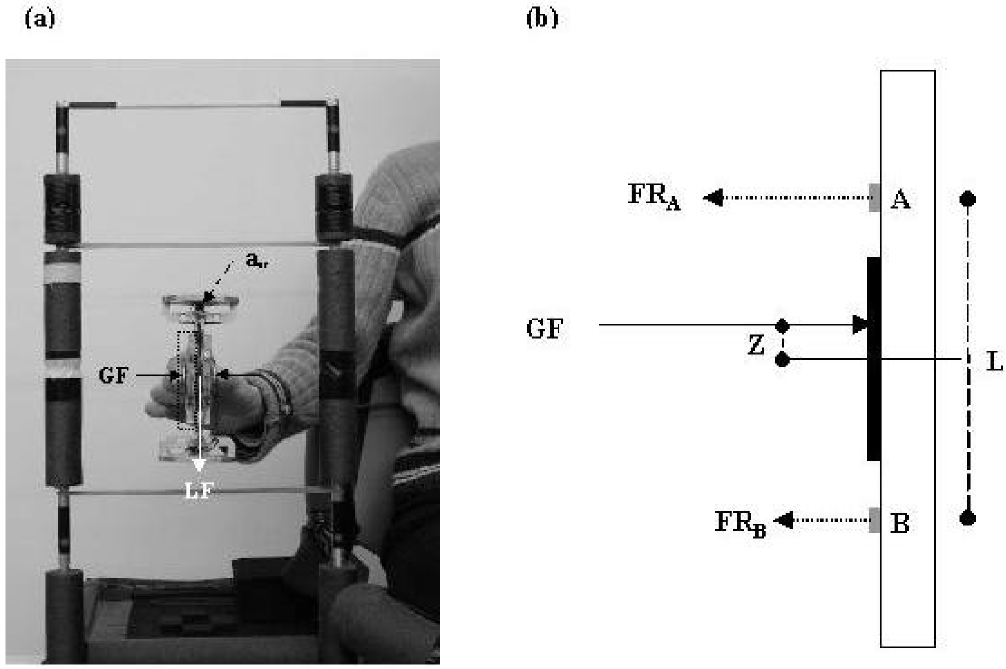

Figure 5.1: (a) Frontal view of the experimental set-up. The instrumented object is hold with precision grip between two parallel rubber bands 20 cm apart. Black arrows represents the normal GF exerted by the fingers on the grasping surface. The white arrow is the vertical LF resulting from the gravitational and object accelerations. The vertical acceleration is measured by an accelerometer av. (b) Schematic drawing of one grasping surface in frontal view (dashed inset in a). Two strain gauges on each side (gray rectangles), separated by 40 mm (L), measure the grip force (GF) applied by the finger (black arrow). Z is the vertical center of finger pressure on the grip surface. FRA and FRB (dotted arrows) are the resultant forces recorded by the strain gauges A and B respectively.

An accelerometer mounted on the top of the object recorded the acceleration along its vertical axis (a_v in Fig.5.1a). The mass-spring accelerometer was oil damped and had a flat frequency response from 0 to 300 Hz (Entran Devices Model EGC-240-5D). The accelerometer amplifier was low-pass filtered with a -3dB cutoff frequency of 16 kHz to eliminate possible high frequency interference from nearby computer equipment. The vertical load force (LF) resulting from the gravitational and the acceleration-dependent inertial force was calculated as the product of the mass and a_v which is the sum of the gravitational and object accelerations.

The subject was seated in a chair with the shoulder slightly abducted and the hand resting on a horizontal surface. At a signal from the experimenter, the subject lifted the object 20 cm high between two parallel elastic bands and held it stationary for 20 seconds (the "static phase") with the elbow flexed at about 90 degrees (see Fig. 1). The subject was then instructed to move the object up and down for 30 seconds with an approximate frequency of 1.0 Hz aided by a metronome (the "dynamic phase). The movement was constrained within the two parallel rubber bands about 20 cm apart (Fig.5.1a). The upper limb displacement was freely performed using both shoulder and elbow movements. Eleven trials were performed before and after digital anesthesia of the thumb and index finger.

The skin-object coefficient of static friction was measured for each subject before and after the eleven trials in a series of five lift-and-drop maneuvers in which the subject lifted and held the instrument stationary, then gradually released the grip until the object slipped due to gravity. The coefficient of friction was calculated as half the LF/GF ratio at slip onset as detected on the unfiltered acceleration signal (Johansson and Westling, 1984). As the coefficients of friction were not significantly different before and after the eleven trials (paired t-test: $p>0.05$), all measurements of friction were averaged and the mean value was used as the estimated coefficient of friction for each subject in each sensory condition. By assuming that the coefficient of friction remained constant regardless of the load force fluctuations during the movement and that the load force was evenly partitioned between the two grasp surfaces, a theoretical slip force could be calculated as half the ratio between the LF and the friction coefficient. The safety margin was defined as the difference between the employed GF/LF ratio and the slip force/LF ratio (slip ratio). The object slipped between the fingers when the GF/LF ratio was inferior to the slip ratio. Cutaneous anesthesia is known to reduce sweating, and consequently reduce the adhesion of the skin to an object surface (Moberg, 1962). To compensate for this effect, talc was applied to the pulp of the index and thumb in order to reduce the difference between the skin-metal coefficient of friction before and after digital anesthesia.

The digital nerves at the base of the index finger and thumb were blocked by injections of about 1 ml bupivacain (5 mg/ml) to achieve a ring-block anesthesia of the entire first two digits. Clinical anesthesia was obtained when all sensations were abolished as indicated by complete insensitivity to skin contact with the Semmes Weinstein monofilaments (Lafayette Instrument Company, Inc.) (Bell-Krotoski 1990). In addition, the maximal voluntary pinch force between the thumb and index finger (MVC) was measured with a B&L pinch gauge according to the procedure described by Mathiowetz et al (1985) before and during digital anesthesia.

5.4.2 Data processing and analysis

The signals from the strain gauges and accelerometer were digitized on-line at 200 Hz with a 12-bit analog-to-digital converter and stored on a laboratory computer. After digitization, the signals were low-pass filtered with a fourth-order, zero phase-lag Butterworth filter with a cut-off frequency of 15 Hz. The static and the dynamic phases were analyzed separately. The static phase started after the object had been lifted and when the vertical acceleration returned to zero (t0). It ended approximately 20 seconds later (t1) when movement was detected by the accelerometer. The dynamic phase was delimited between the first (t2) and the last (t3) peak in vertical load force. The grip force (GF), the load force (LF), the GF/LF ratio as well as the percentage of maximal pinch force (%MVC) were measured at t0, t1, t2 and t3. The vertical displacement of the centers of finger pressure was displayed throughout the task progression and calculated at each of four critical times. A cross-correlation between the GF and the LF series during the dynamic phase was calculated for each trial to determine the phase lag (ms) at which the maximal correlation (r) between the two series was obtained. A negative time lag indicated that the correlation was maximal when the load force change preceded the change in grip force.

5.4.3 Statistical analysis

Paired t tests based on the mean values obtained from each subject were used to (1) test the effects of digital anesthesia on the dynamics of prehension and on the maximal pinch force, and (2) to compare the beginning and the end of the static and dynamic phases with and without digital anesthesia.

Fisher's transformation of r into a Z score was performed to compare the maximal correlation coefficients between the GF and LF series obtained with the cross-correlation procedure before and after the anesthesia.

5.5 Results

5.5.1 Maximal voluntary pinch force

Tip pinch voluntary maximal force (N)				
Subjects		Before anesthesia	During anesthesia	Normative values
DC	F	50.00 (0.00)	41.67 (2.89)	51.26 (11.79)
BC	F	51.67 (2.89)	38.33 (2.89)	
AA	F	68.33 (2.89)	50.00 (0.00)	
DJ	F	70.00 (0.00)	53.33 (2.89)	
MV	F	70.00 (0.00)	38.33 (2.89)	
DF	M	106.67 (5.77)	93.33 (2.89)	77.11 (18.60)
LG	M	106.67 (5.77)	71.67 (7.64)	
SA	M	110.00 (0.00)	70.00 (5.00)	
CF	M	110.00 (0.00)	86.67 (2.89)	
DJM	M	110.00 (10.00)	83.33 (11.55)	

mean (sd)
F = Female
M = Male

Before digital anesthesia, the maximal voluntary pinch force was comparable to the normative values obtained for a similar age and gender-matched population (Mathiowetz et al 1985) (Table 1). Paired t-test based on values obtained before and after digital anesthesia on the same individuals showed a significant reduction of the maximal voluntary pinch force ($t=6.854$; $p<0.001$) that was on average 26.5 ± 9.6 %.

5.5.2 Grip-load force coupling with intact sensation

A typical trial of the grip-load force coupling before digital anesthesia is displayed in Figure 5.2A. During the static phase (t0-t1) the load force was equal to the object weight (250g) and the GF/LF ratio was always maintained above the slip ratio preserving a nearly constant safety margin.

During the dynamic phase (t2-t3), the grip force was modulated in phase with the load force fluctuations generated by the accelerations of the arm during the oscillatory movements. Cross-correlation between the GF and LF series was performed on each trial. The maximal correlation (r) between the two forces was on average 0.75 ± 0.13 for the ten subjects and occurred at a mean time lag of – 7 ± 21 ms. During the cyclic movements, the GF/LF ratio remained well above the slip ratio although it fluctuated during the cyclic movements. The force ratio was minimal and highly reproducible when the load force was at a maximum at the bottom of the trajectory. The force ratios at these times were similar to the ratios observed at the end of the static phase.

Moreover, with digital sensation intact the mean center of pressure of the two fingers was centered on the middle of the grip surface throughout the entire movement sequence. The vertical position of the centers of pressure tended to oscillate slightly (<1.0 mm) during the cyclic movement because of the skin rolling with the tangential forces.

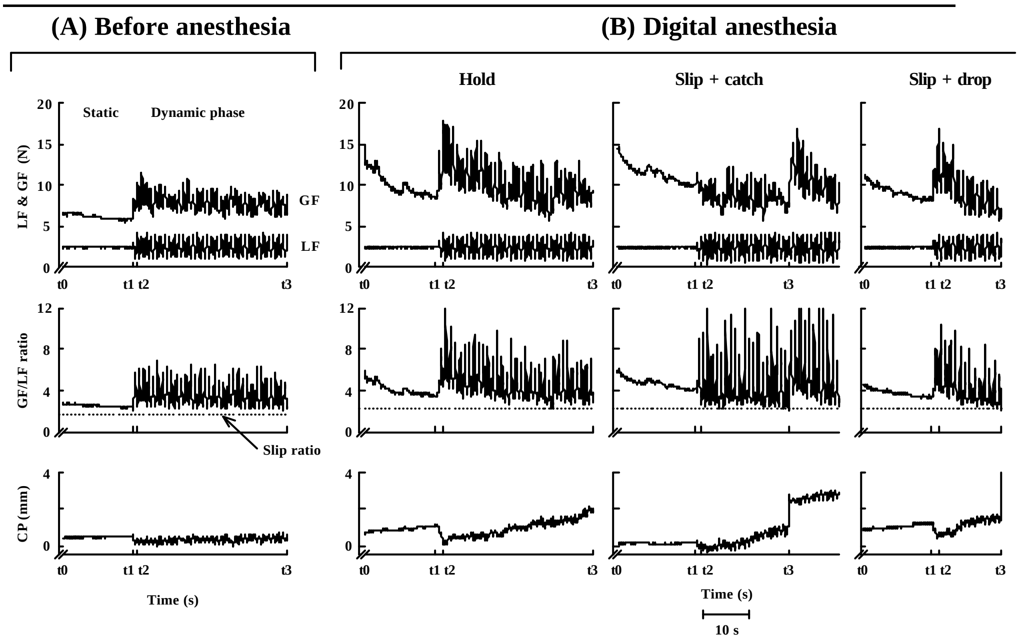

Figure 5.2: Single trials obtained for one subject (A) before and (B) during digital anesthesia. In B are shown the 3 different response patterns ("Hold", "Slip & catch" and "Slip & drop" trials). The upper traces display the oscillating grip force (above) and the load force (below). The static phase is defined between t0 and t1 and the dynamic phase between t2 and t3. The middle panel shows the temporal evolution of GF/LF ratio. The critical slip ratio is shown as a straight horizontal dotted line. The lower panel presents the temporal progression of the vertical position of the fingers on the grip surface. Zero indicates the center of the grasping surface.

The pooled results obtained for the ten subjects with intact sensation are presented in Figure 5.3A and Figure 5.4A during the static and the dynamic phases, respectively. Over the 20 seconds of the static phase, the GF/LF ratio tended to decrease slowly from on average 4.07 ± 1.28 at time zero (t0) to 2.89 ± 0.76 at time one (t1) (t=4.669; p=0.001). At the start of the dynamic phase (t2), the minimum GF/LF ratio occurring at the first load force peak was similar to the force ratio measured at the end of the static phase (t1). Over the 30-second period of cyclic movements, the grip force-load force ratio continued to decrease, but only slightly from 2.77 ± 0.64 at time two (t2) to 2.42 ± 0.62 at time 3 (t3) (t=4.273; p=0.002). The force ratios were always maintained above the critical slip ratio (1.5 ± 0.39) and object slip never occurred. During the entire task, the fingers remained well centered on the grasping surface.

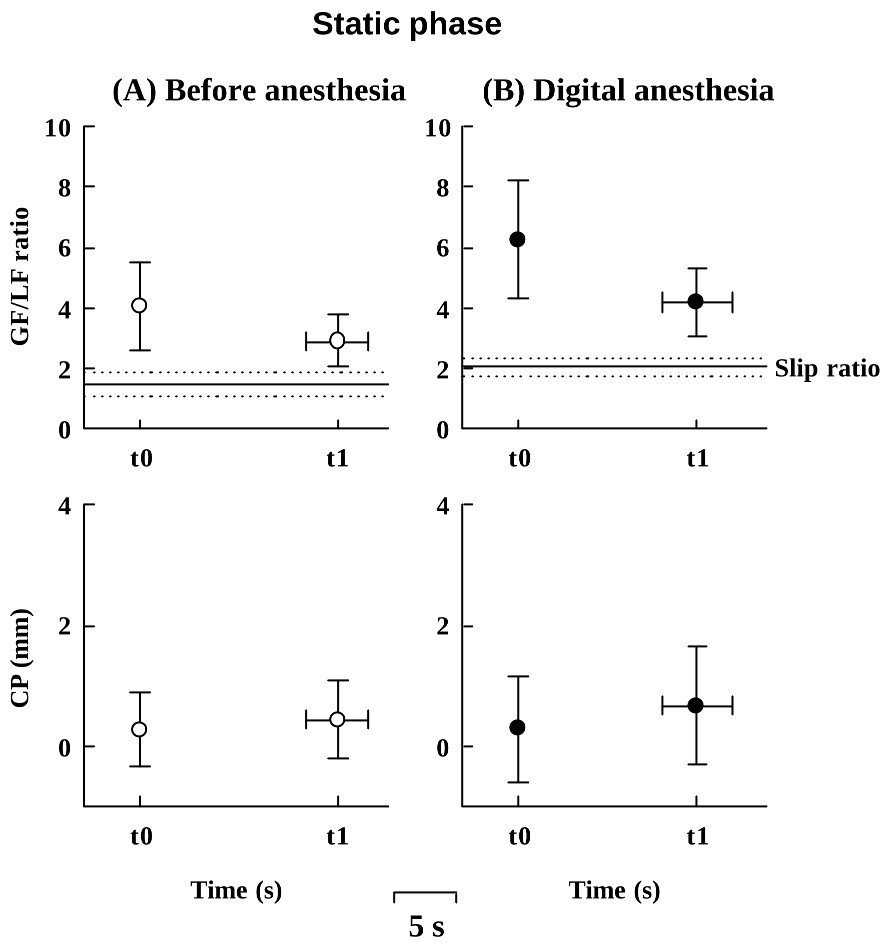

Figure 5.3: Effects of digital anesthesia on the static phase of the prehension task (A) before (open circles) and (B) during digital anesthesia (filled circles). The means and standard deviations are calculated for the 10 subjects in the beginning (t0) and the end of the static phase (t1). The upper panels show the GF/LF ratio where the solid horizontal lines illustrate the mean slip ratio calculated from the coefficient of friction for each condition and the dotted lines represent ± one standard deviations. The lower panels display the finger position with respect to the center of the grasping surface. The horizontal error bars for time indicate the variability (mean ± SD) in the duration of the static phase.

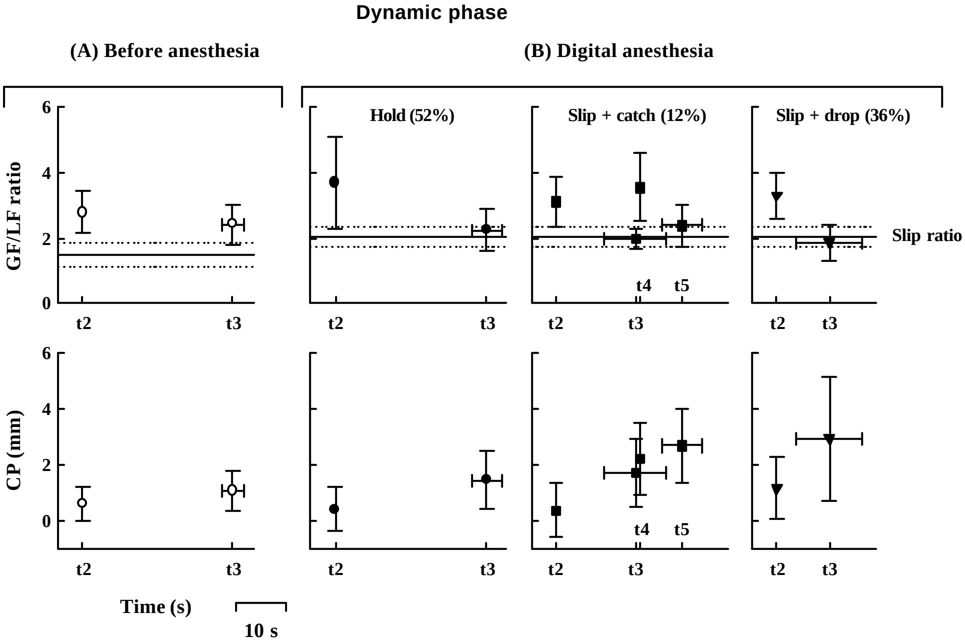

Figure 5.4: The GF/LF ratio during the dynamic phase of the prehension task before (A) and during digital anesthesia (B). The upper panels show the GF/LF ratio before anesthesia shown as open circles and the three types of responses ("Hold", "Slip & catch", "Slip & drop") during anesthesia shown as filled circles, squares, and triangles. The horizontal lines correspond to the mean slip ratio calculated from the coefficient of friction for each condition and the dotted lines represent the standard deviations. The lower panels show the mean and standard deviation of the finger position with respect to the center of the grasping surface before and after digital anesthesia. The horizontal error bars for time indicate variability (mean ± SD) in the duration of the dynamic phase. The means and standard deviations are calculated for the 10 subjects at the beginning (t2) and end of the dynamic phase (t3). In the Slip & catch response, the means and standard deviations are calculated at the beginning of the dynamic phase (t2), then successively when the slip occurred (t3), when the GF/LF ratio was restored (t4) and at the end of the dynamic phase (t5).

5.5.3 Grip-load force coupling with digital anesthesia.

Despite the application of talc to the fingertips, a significant decrease of the skin-brass coefficient of friction was observed after digital anesthesia (t=2.736; p=0.023). Coated with talc, the brass surface had a mean coefficient of friction against the skin of about 0.36 ± 0.11 before and 0.25 ± 0.04 after anesthesia. The critical slip ratio increased in turn from 1.5 ± 0.39

before to 2.08 ± 0.31 following anesthesia.

Static Phase

The effects of digital anesthesia on the grip-load coupling during the static phase is presented in Figure 5.2B between t0 and t1 and in Figure 5.3B. The absence of cutaneous feedback produced a significant increase in the GF/LF ratio both at the start ($t=-5.961$; $p<0.001$) and the end ($t=-4.086$; $p<0.003$) of the static phase generating at both times a safety margin that was, on average, 50% greater than with intact sensation. The mean percentage of maximum pinch force (MVC) used to lift the 250 g object significantly increased from 12.63% ± 5.95 with intact cutaneous sensation to 27.06 ± 12.24% after digital anesthesia. Interestingly, the subjects did not maintain this higher level of grip force. The decrease in grip force during the static phase was on average –2 ± 0.6 %/s following digital anesthesia which was significantly steeper than the –1.5 ± 0.8 %/s decrease observed with cutaneous sensation intact ($t=3.112$; $p=0.012$). Figure 5.3B also shows that the centers of fingertip pressure were correctly located near the middle of the grasping surfaces (<1mm) during the whole static phase.

Dynamic Phase

Although none of the subjects dropped the object prior to digital anesthesia, 7/10 subjects dropped the object at least once with the fingers anesthetized. The slips resulting in dropping the object occurred randomly without evidence of improved performance over the course of the eleven trials. No significant correlation ($r = -0.37$; $p = 0.29$; $n = 10$) was observed between the maximum voluntary pinch force and the occurrence of slip.

During the dynamic phase, three different grip-load force responses ("*hold*"; "*slip and catch*"; "*slip and hold*") were observed following digital anesthesia. Figure 5.2B illustrates examples of each of the three responses observed in a single subject after digital anesthesia. In the "*hold*" situation, the instrumented object was held without significant slip for the required 30-second period of the oscillatory task. In the '*Slip and catch*" situation, a significant slip of the object occurred at a peak of load force at the bottom of the trajectory but the slip was arrested in time. The slip event in the "*Slip & catch*" trial illustrated in Figure 5.2B is shown on an expanded time scale in Figure 5.5. The grip force modulation progressively decreased until the force ratio fell below the critical slip ratio (Fig. 5.5a) and the center of pressure of the two fingers simultaneously moved up on the grip surface. The force ratio was restored a few milliseconds later, quickly enough to catch the falling object at a higher position on the grip surface (Fig. 5.5b). Actually, during this period, the unloading phase of the cyclic movement started and as the load force decreased the grip force became sufficient to restrain the object again. Once the GF/LF ratio was restored, the GF abruptly increased but was still modulated in phase with the LF fluctuations. Indeed, a slight decrease in GF is observed in phase with the subsequent minimum LF (Fig. 5.5c). In the *"Slip and drop"* situation (Fig. 5.2B), the object slipped from the fingers during the dynamic phase because of an irrecoverable drop in the force ratio to a point below the critical slip ratio. The grip force was still modulated in parallel with the load force fluctuations during the dynamic phase, but the mean level of GF could not be maintained constant and was frequently insufficient to prevent slip. The maximum correlation (r) between the grip and load force series declined on average for all subjects from 0.75 ± 0.13 before to 0.48 ± 0.2 after anesthesia (Fisher's transformation of r into z scores: z = +3.29; p = 0.0006). In contrast, the cross correlation analysis showed that the grip force remained well in phase with the LF with a mean time lag of only 2.0 ± 44 ms, which was not significantly different from the 7.0 ± 21ms lag, observed with intact cutaneous sensation (t = -1.099; p = 0.3).

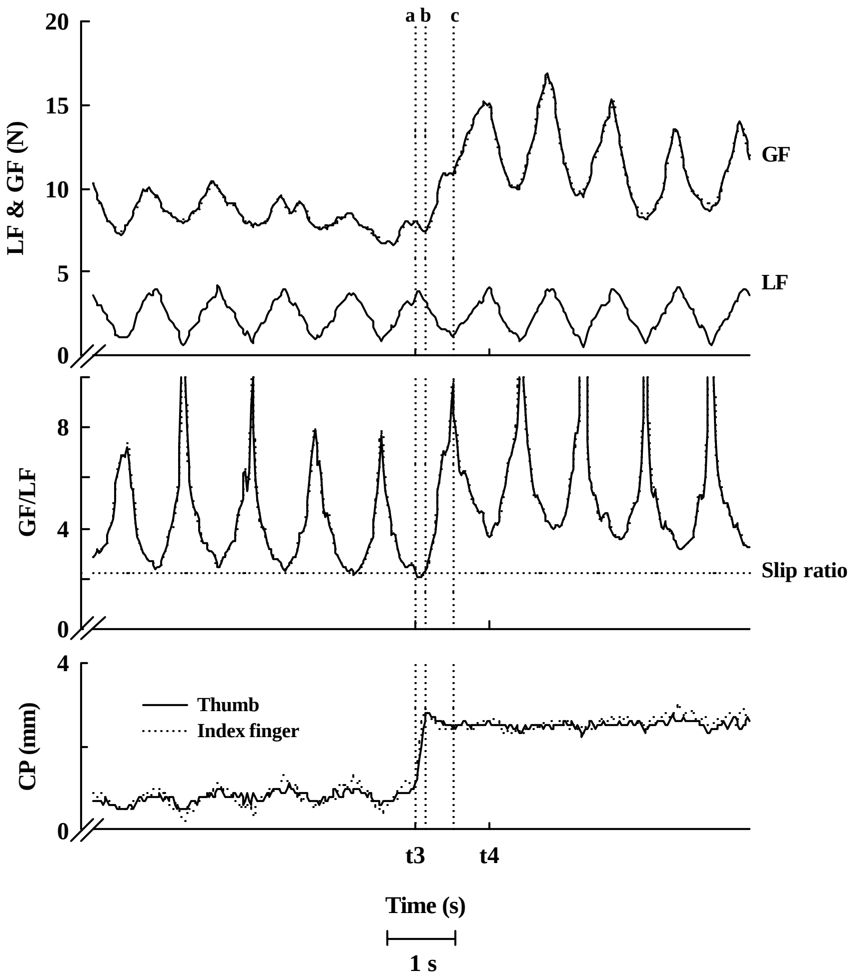

Figure 5.5: Expanded time scale of the slip event in the "Slip & catch" trial described figure 5.2B. The upper traces display the load force (below) and the grip force (above) exerted by the thumb (plain line) and index finger (dotted line). The middle panel shows the temporal evolution of GF/LF ratio which falls below the critical slip ratio (straight horizontal dotted line) as shown by the cursor a. The lower panel presents the temporal progression of the vertical position of the thumb and index fingers on the grip surface. Zero indicates the center of the grasping surface. The cursor b signals the GF reaction in response to the slip. The cursor c is positioned in phase with the minimum of LF.

The results obtained from all trials performed by the ten subjects during the dynamic phase are presented in Figure 5.4B. The GF/LF ratio declined rapidly throughout the dynamic phase without cutaneous feedback whatever type of grip force response occurred. This rapid decline of the GF/LF ratio associated with the increased slip ratio resulted in a significant slip on 48% of the trials. On 36% of all the trials (i.e. the *slip & drop*), the object irretrievably slipped from the grasp after a mean latency of about ten seconds (10.6 ± 6.8s). The centers of finger pressure at the end of the dynamic phase (t3) tracked the slip of the fingers on the grip surface before the object fell (Fig. 5.4B, *slip & drop*). On 12% of all trials (*slip & catch*), the centers of finger pressure started to move up slowly (1.33 ± 0.75mm from t2 to t3), then suddenly slipped on the grasp surfaces for a few milliseconds (0.62 ± 0.49 mm from t3 to t4) before stabilizing at a higher position. Note that the two fingers moved simultaneously and that their vertical displacement was equivalent ($t=-1.358$, $p>0.05$). The GF/LF ratio was restored (t4) on average 160 ± 40ms after the slip (t3) at a level similar to that used at the start of the dynamic phase (t2). The GF/LF ratio decreased continuously until the end of the dynamic phase (t5). Finally, on 52% of the trials (Fig.5.4B, *hold)*, the subjects succeeded in maintaining an adequate grip on the object by exerting a significantly greater grip force at the start of the dynamic phase, compared with the trials where significant slip occurred ($F = 3.53$; $p= 0.035$). Although the object was held during the entire trial, a slow and progressive slip of the centers of pressure was observed throughout the 30 seconds of the oscillatory phase (1.05 ± 0.78mm) suggesting that localized slips occurred more or less continuously in various parts of the contact area.

On average, all the subjects increased their grip force to 24.92 ± 10.87% of their MVC at the start of the dynamic phase after digital anesthesia. The occurrence of slip seemed to depend partly on the GF exerted at the start of the dynamic phase but also on the rate at which the grip force decreased. With intact tactile sensation, the grip force decreased over time at a mean rate of -0.43 ± 0.64%/s, whereas with the fingers anesthetized, the average decrease over time was 1.10 ± 0.52%/s in the "hold", -2.35 ± 1.23%/s in the slip & catch" and -4.90 ± 6.42%/s in the "slip & drop" trials, respectively. A significant correlation of 0.77 ($p<0.01$) existed between the subject's maximal voluntary grip force, and the rate of grip force decrease during anesthesia.

5.6 Discussion

5.6.1 Grip-load force coupling with intact sensation

With normal tactile sensation, the performance of our subjects was similar to that described previously in the literature (Flanagan and Tresilian 1994; Flanagan and Wing 1995). The strong peak correlation found between the load and grip forces and the very brief time lag between the force functions during the oscillatory movements support the observation that the grip force was modulated both in phase and in magnitude with the load force. The GF/LF ratio was adjusted to the skin-surface friction and its minimum during the movement cycles was always maintained slightly above the slip ratio. The force ratio was maximum at each minimum of the load force because subjects did not release their grip as much as would be allowed in order to maintain the safety margin constant.

5.6.2 Grip-load force coupling after digital anesthesia

In a similar study, Nowak et al (2001) observed that the precise anticipatory temporal coupling between grip and load forces was not impaired under anesthesia but that a higher safety margin was used during the entire movement so that the object was never dropped. In their experiment the duration of each trial (6-10 s) was probably too short to allow the appearance of slip and the short breaks (200-300 ms) introduced between each single up-and-down movement enabled the subjects to reinstate the safety margin.

In agreement with the study of Nowak et al (2001), we observed that, the precise temporal coupling between GF and LF was preserved in the absence of cutaneous feedback; the time lags between the two forces being similar to those measured before anesthesia. The fact that the grip force never lagged behind the load force by more than 40 ms suggests the existence of a predictive temporal modulation of grip and load force that is centrally mediated and less influenced by sensory-driven feedback control. There is increasing evidence in the literature, that this predictive mechanism could be derived from internal models of limb mechanics, object~~s~~ properties and task constraints (for review, Flanagan and Johansson 2002). This feedforward control strategy is used in a variety of tasks engaging objects with different weights, shapes or textures (Johansson and Westling 1984, 1988; Jenmalm and Johansson 1997) manipulated with a variety of grips (two or three fingered, unimanual or bimanual, etc.) whatever the mode of transport (Flanagan and Tresilian 1994, Flanagan et al 1999). Moreover, the predictive grip force is also observed when the load conditions are changed (inertial viscous, elastic) (Flanagan and Wing 1997) or when tangential torques are generated (Goodwin et al 1998, Johansson et al 1999).

5.6.3 Cutaneous sensation is essential to adjust the grip force level

Our results show that cutaneous afferents are important for maintaining GF/LF ratio, i.e. for maintenance of both the background grip force and the modulation of the grip force with the cyclic load. Actually, in approximately 50% of the trials performed during digital anesthesia, the object slipped because the GF/LF ratio was not maintained above the slip ratio. There was no correlation between the percentage of slip and the maximum voluntary pinch force across subjects. Moreover, the slips occurred at random in the series, and the grip force applied to the object was significantly below the maximum voluntary pinch forces. It seems thus unlikely that muscle weakness or fatigue could explain the GF decreases, which led to slip. Other investigators also noted a reduction in force generation after blocking cutaneous afferents. Rossini et al (1996) found decreased excitability in the first dorsal interosseous after digital anesthesia and a similar reduction in jaw closing force was reported by Lund and Lamarre (1973) after anesthetizing periodontal pressure receptors. These observations suggest that in certain cases pressure receptors exert positive feedback on the central nervous system.

The most probable explanation of the inability to scale the safety margin adequately with anesthetized fingers would be that the cutaneous feedback is necessary to provide the actual state of the system and update the pre-programmed motor commands. As there are unavoidable disturbances acting on the motor system that are not anticipated by the internal model, the actual sensory information provided by the finger sensors is necessary to ascertain the actual shear or load force and to correct the grip force in order to maintain a secure grasp. This can be related to the “discrete sensory event driven control policy” previously proposed by Johansson and Cole (1994) for control of grasp stability in manipulation. Without cutaneous feedback, the internal models underlying anticipatory control mechanisms are no longer updated. As a result the prediction of the future load force is less accurate and there is an accumulating error in adjusting the balance between the grip and load force for grasp stability. This theoretical concept is in accordance with the observations based on human nerve recordings that suggest that cutaneous signals is necessary for maintaining an adequate safety margin when holding object for a long time (Johansson and Westling, 1987). Under anesthesia the GF correction did not occur and the object slipped between the fingers. In some cases, the force ratio was restored before the object fell. It is possible that on some trials the object slipped and tilted causing it to bind between the fingers (Johansson and Westling 1987, Edin et al. 1992). However, the vertical displacement of the fingers on the grasp surfaces occurred at the same time with the same force under each finger suggesting that the object did not tilt significantly. More likely, the force ratio was re-established because in these few trials the object slipped just at an unloading phase of the cyclic movement and the grip force became sufficient again to overcome the load force. It was also obvious that these slip events were followed by an increase of the grip force. It could be that sensation from more proximal areas (e.g. Pacinian-like units in the palm or proprioceptive cues from skin stretch of the dorsal hand) or visual feedback could have registered the slip in absence of cutaneous afferent (Cole and Abbs 1988; Johansson et al 1992; Häger-Ross and Johansson 1996). However the GF response latencies triggered by non-digital afferents have a longer and more variable latency than with intact sensation (Häger-Ross and Johansson 1996). We observed a response latency of about 160 ms to slips with the fingers anesthetized, which is consistent with this interpretation. This longer latency probably explains why the subjects failed to catch the object when the slip occurred during the loading phase of the cyclic movement in the slip & drop trials. The role of visual feedback was thought to be insignificant because of the rapidity of the cyclic movements and the small amplitude of the finger displacement corresponding to the breadth of a few papillary ridges of the skin. When afferent information from all sources is available, the CNS preferentially uses tactile signals for object manipulation. However when cutaneous feedback is lost, it may switch to alternative sources of afferent information (Collins et al 1999).

In conclusion, the present study re-emphasizes the critical role of cutaneous afferents in object manipulation. In addition to their role in adapting the GF/LF ratio to the friction upon initial contact with an object and their phasic slip-detection function, the cutaneous afferents are required for setting and sustaining the background level of the grip force. Finally, at a more theoretical level, they correct and maintain an internal model of the physical properties of hand-held objects.

Chapter 6: Conclusion

6.1 Summary

The human aptitude for manipulating objects conceals a complex neural control. This complexity becomes apparent when we observe children, the elderly or people with neurological damage (central or peripheral) attempting to perform some manual activities such as buttoning a shirt. A series of elegant studies have shown that the grip force was modulated in parallel with the load force changes during transport of hand-held objects (Chapter 1). The control scheme underlying this grip-load force coupling involves subtle interplay between feedforward and feedback mechanisms. Within the theoretical framework of internal models, anticipatory GF control may be implemented through the combined activation of inverse and forward models of the arm-hand-object system. Based on internal models of the motor system and object properties, the load force can be predicted and the GF motor command can be specified in a feedforward manner (Chapter 2). Moreover, during the course of arm movement, the CNS is informed by sensory feedback about mechanical events such as the lift-off of the object, slippage or excessive grip force. This information is used to correct the motor commands and to update the internal model of the motor apparatus and object (Johansson and Westling 1987; Johansson 1996).

This model of the sensorimotor loop underlying the control of precision grip was used as a starting point for our study. Three experiments were conducted to examine within this model, the relative contributions of sensory-driven and anticipatory control of GF adjustments during cyclic vertical movement with a hand-held load. The main point was to assess whether internal models underlying the grip-load force coupling are robust when the environmental context was changed or when the sensory feedback was suppressed.

The experiments in parabolic flight have provided us the unique opportunity to study the effects of a change in gravity on the dynamics of prehension (Chapter 3). The main perturbation was that the novice subjects applied unnecessarily high safety margins during their first trial at 0 and 1.8

g in order to secure the grasp insofar as the gravitational component of the load force was unpredictable. By contrast, the temporal coupling between GF and LF was maintained regardless of the gravity conditions because the inertial component of the load could be still predicted from the arm motor command (efference copy). Probably the sensory information about new gravity was used to correct and update the internal representation of the gravity within the CNS. In this way, the GF could be adequately adjusted to the gravity level in the subsequent trials.

In a second study in parabolic flight (Chapter 4), we have observed that the subjects were able to exert the same grip force for equivalent load generated either by a change of mass, gravity or acceleration despite the fact that it requires different arm motor commands. Subjects with great experience in parabolic flight can quickly adapt to different environmental contexts by switching between previously learned behaviors. It is hypothesized that the brain contains multiple controllers (inverse models) associated with their corresponding predictor (forward models), with each of them suitable for one or small set of contexts. Each pair (or module) would allow the CNS to generate accurate and appropriate motor behavior under specific sensory contexts (Blakemore et al., 1998). The modular model of motor control also assumed that separate internal models learned for different context can be mixed to cope with a single task (Wolpert and Kawato 1998; Flanagan et al 1999). It is likely that having learned the task in 1 g, and the new gravity during their many previous flights, the subjects could execute the task from their few first trials.

These two experiments brought further evidence that predictive mechanisms largely contribute to GF adjustment. Static forces such gravity are taken into account in the motor plan allowing adequate motor command and precise prediction of the incoming load force change. The GF output would depend on the precision of this prediction that can be evaluated only after the movement onset through sensory information about the actual state of the system.

The third experiment performed in this thesis (Chapter 5) emphasizes the critical role of cutaneous afferents in object manipulation. In addition to their phasic slip-detection function, cutaneous afferents are required for setting the background level of the grip force. In absence of tactile feedback, the temporal coupling between the grip and load forces is maintained but the mean magnitude of GF progressively decreases leading to object slipping. It is hypothesized that accumulating error occurred in the LF prediction leading to inadequate level of GF. Cutaneous afferents are thus required to correct and maintain the internal model of the arm-hand object system.

6.2 Future prospects

The interpretation of the results obtained in this thesis remains at a very theoretical level but it opens up new prospects for fundamental and clinical researches. Studying the grip-load force coupling offers a simple method to evaluate feedback and feedforward control of the hand movement. First, the temporal delay between the grip force and the load force provides a sensitive way to determine the mode of control used to program the GF. The fact that GF slightly leads LF suggests anticipatory GF modulation based on a prediction of the load provided by internal models of the dynamics of the arm and objects. By contrast, the fact that a GF response occurs more than 40 ms after the LF increase suggests reactive GF modulation influenced by sensory feedback control. Second, measuring the safety margin in relation to the load and friction reflects a correct updating of the internal models by sensory feedback provided by the mechanoreceptors of the hand. A high safety margin reflects a low level of prediction and is used when sensory feedback is not available.

From a fundamental point of view, much is left to be done to determine the contribution and the adaptation of the feedforward and the feedback control in different contexts. Experiments in unfamiliar contexts (e.g. microgravity, coriolis force, robot manipulandum) allow to study how the CNS used these two mechanisms to learn new dynamics. As sensory feedback is necessary to provide the CNS with the context cues, altering the sensory feedback in these unfamiliar situations would probably perturb the process of learning. It would be interesting to test different degrees of sensory loss to observe what is the minimal tactile spatial acuity needed to adapt the GF to new contexts. Moreover, in new situation such as microgravity, the visual feedback would certainly play an important role. Actually, the vision provides crucial information about the context and allows to select the appropriate internal model. In order to investigate the eye-hand coordination and the influence of visual feedback on the dynamics of prehension, a 3D eye movement recording system would give important information.

In a clinical point of view, this method might provide further insight into the mechanisms responsible for motor deficits of the hand and a better understanding of the precise neural mechanisms involved in the sensiromotor loop for control of precision grip. In this framework, the measure of the grip-load force coupling might be implemented in a battery of tests including measures of force and dexterity in order to evaluate patients with motor and sensory deficits of the hand. Moreover, neurophysiological studies using imagery (MRI), transcranial magnetic stimulation (TMS)… in combination with the measure of grip-load force coupling in healthy or pathological (e.g. Parkisonian, cerebellar,…) people would bring more information about the cerebral circuits involved in this control. Until now, the functional anatomy of internal model mechanisms is not fully known but two areas with the central nervous system are thought to be critical for updating arm movement: the cerebellum and the posterior parietal cortex (Desmurget and Grafton 2000). Imaging, physiological, and lesion studies have demonstrated that the cerebellum is at least one of the possible sites for internal models controlling arm movements (Kawato 1999; Miall et al 1993; Wolpert and Kawato 1998). In monkeys trained to lift an object, the discharge rate in Purkinje cells and cerebellar neurons in relation with friction and weight occurring prior to and during the grip force application tends to corroborate these observations (Espinoza and Smith 1990; Dugas and Smith 1992). The superior parietal lobe would play a key role in sensorimotor integration by actively maintaining an internal representation of the body state (Wolpert et al 1998).

Studies of the grip-load force coupling in pathological population have already given interesting results. For example, it has been observed that the control of finger movements is altered in congenital hemiplegic patients. There was a clear relationship between the developmental level of the grip-lift synergy and impaired dexterity of these patients (Forssberg et al 1999; Duqué et al 2003). Moreover some correlation was observed between the grip-lift synergy and the lesions in the contralateral cortex, white matter, thalamus and basal ganglia (Forssberg et al 1999). In the same way, patients with degenerative cerebellar lesions exhibited a lack of coordination of GF and LF when performing a lifting task suggesting a failure of the anticipatory process (Müller and Dichgans 1994). By contrast, the parkinsonian subjects can appropriately scale their GF for different weights but they use high GF level (Müller and Abbs 1990). In a more clinical view, this method might also be useful in evaluating the patients with peripheral nerve lesion (e.g. median nerve). Our study with digital anesthesia suggests that the sensory recovery should occur in parallel with a progressive decrease of the safety margin during prehension task.

One limitation of this method is that it only studies the dynamics of restraining object during arm movement. However, there were evidences when measuring the arm acceleration that the kinematics of the arm can be also perturbed especially when the environmental context is changed. Thus, the use of a 3D movement tracking system in further studies would certainly contribute to better understand the relation between the dynamics and the kinematics of arm in manipulative task. New experiments in parabolic flight with such system should reveal perturbations in hand trajectories and their repercussions on the grip-load force coupling. It would be also interesting to study other trajectories such as circular or ellipsoidal arm movements with a hand-held load.

Finally, in the perspective of applied research, this work could have implications in the fields of robotics and prosthetics. The neurophysiological knowledge of the human nervous system and of the sensory-motor coordination processes allows building of anthropomorphic robots. For example the performance of hand prosthesis for amputee patients might be improved by addition of tactile sensors that would allow sensory feedback and corrective GF response to load perturbations.

References

Augurelle, A-S., Penta, M., White, O., and Thonnard, J-L. (2003) The effects of change in gravity on the dynamics of prehension. Exp.Brain.Res. 148: 533-540.

Augurelle, A-S., Smith, A.M., Lejeune, T., and Thonnard, J-L. (2003) Importance of cutaneous feedback in maintaining a secure grip during manipulation of hand-held objects. J. Neurophysiol. 89: 665–671.

Beaubaton, D., Hay, L. (1986) Contribution of visual information to feedforward and feedback processes in rapid pointing movements. Hum. Mov. Sci. 5: 19-34.

Bell-Krotoski J.A. Light touch-deep pressure testing using Semmes-Weinstein monofilaments. In: Hunter J.M., Schneider L.H., Mackin E.J., Callahan A.D. (Eds.). *Rehabilitation of the Hand: Surgery and Therapy*. St Louis: Mosby Co, 1990, 585-93.

Bernstein, N. (1967) The coordination and regulation of movements. Pergamon, London.

Blakemore, S. J., Goodbody, S. J., and Wolpert, D. M. (1998) Predicting the consequences of our own actions: the role of sensorimotor context estimation. J. Neurosci. 18: 7511-7518.

Bock, O. Problems of sensorimotor coordination in weightlessness. (1998) Brain Res.Brain Res.Rev. 28: 155-160.

Bock, O., Howard, I. P., Money, K. E., and Arnold, K. E. (1992) Accuracy of aimed arm movements in changed gravity. Aviat.Space Environ.Med. 63: 994-998.

Bowden, F.P, Tabor, D. (1973) Friction- an introduction to tribology. Anchor Press, Garden City NY.

Burstedt, M. K., Edin, B. B., and Johansson, R. S. (1997) Coordination of fingertip forces during human manipulation can emerge from independent neural networks controlling each engaged digit. Exp.Brain Res. 117: 67-79.

Cole, K. J. and Abbs, J. H. (1988) Grip force adjustments evoked by load force perturbations of a grasped object. J. Neurophysiol. 60: 1513-1522.

Collins, D.F., Knight, B., Prochazka, A. (1999) Contact-Evoked changes in EMG activity during human grasp. J. Neurophysiol. 81: 2215-2225.

Comaish, S., Bottoms, E. (1971) The skin and friction: deviations from Amonton's law, and the effects of hydration and lubrication. Br. J. Dermatol. 84: 37-43.

Desmurget, M. and Grafton, S. (2000) Forward modeling allows feedback control for fast reaching movements. Trends Cogn. Sci. 4: 423-431.

Desmurget, M., Epstein, C.M., Turner, R.S., Prablanc, C., Alexander, G.E., Grafton, S. (1999) Role of the posterior parietal cortex in updating reaching movements to a visual target. Nature neuroscience. 2: 563-567.

Dugas, C., Smith, A-M. (1992) Responses of cerebellar Purkinje cells to slip of hand-held object. J. Neurophysiol. 67: 483-495.

Duqué, J., Thonnard, J-L., Vandermeeren, Y., Sébire, G., Cosnard, G., Olivier, E. (2003) Correlation between impaired dexterity and corticospinal tract dysgenesis in congenital hemiplegia. Brain 126: 732-747.

Edin, B.B., Westling, G., Johansson, R.S. (1992) Independent control of fingertip forces at individual digits during precision lifting in humans. J.Physiol. (Lond.) 450: 547-564.

Espinoza, E., Smith, A.M. (1990) Purkinje cell simple spike activity during grasping and lifting objects of different textures and weights. J. Neurophysiol. 64: 698-714.

Fisk, J., Lackner, J. R., and DiZio, P. (1993) Gravitoinertial force level influences arm movement control. J Neurophysiol. 69: 504-511.

Flanagan J. R., Johansson R. S. Hand Movements. In: VS Ramashandran (Ed), Encyclopedia of the Human Brain. Academic Press: San Diego, 2002, p. 1-16.

Flanagan, J. R. and Tresilian, J. R. (1994) Grip-load force coupling: a general control strategy for transporting objects. J. Exp. Psychol. Hum. Percept. Perform. 20: 944-957.

Flanagan, J. R. and Wing, A. M. (1993) Modulation of grip force with load force during point-to-point arm movements. Exp.Brain Res. 95: 131-143.

Flanagan, J. R. and Wing, A. M. (1995) The stability of precision grip forces during cyclic arm movements with a hand-held load. Exp.Brain Res. 105: 455-464.

Flanagan, J. R. and Wing, A. M. (1997) The role of internal models in motion planning and control: evidence from grip force adjustments during movements of hand-held loads. J.Neurosci. 17: 1519-1528.

Flanagan, J. R., Nakano, E., Imamizu, H., Osu, R., Yoshioka, T., and

Kawato, M. (1999) Composition and decomposition of internal models in motor learning under altered kinematic and dynamic environments. J Neurosci.(Online.) 19: RC34.

Flanagan, J. R., Tresilian, J., and Wing, A. M. (1993) Coupling of grip force and load force during arm movements with grasped objects. Neurosci.Lett. 152: 53-56.

Flanagan, J.R., Burstedt M.K.O., Johansson, R.S. (1999) Control of fingertip forces in multidigit manipulation. J.Neurophysiol. 81:1706-1717.

Flash, T., Hogan, N. (1985) The coordination of arm movements: an experimentally confirmed mathematical model. J. Neurosci. 5: 1688-1703.

Forget, R., Lamarre, Y. (1995) Postural adjustments associated with different unloadings of the forearm: effects of proprioceptive and cutaneous afferent deprivation. Can. J. Physiol. Pharmacol. 73:265-294.

Forssberg, H., Eliasson, A. C., Kinoshita, H., Johansson, R. S., and Westling, G. (1991) Development of human precision grip. I: Basic coordination of force. Exp.Brain Res. 85: 451-457.

Forssberg, H., Eliasson, A. C., Kinoshita, H., Westling, G., and Johansson, R. S. (1995) Development of human precision grip. IV. Tactile adaptation of isometric finger forces to the frictional condition. Exp.Brain Res. 104: 323-330.

Forssberg, H., Eliasson, A. C., Redon-Zouitenn, C., Mercuri, E., Dubowitz, L. (1999) Impaired grip-lift synergy in children with unilateral brain lesions.

Brain 122: 1157-1168.

Goodwin, A.W., Jenmalm, P., Johansson, R.S. (1998) Control of grip force when tilting objects: effect of curvature of grasped surfaces and of applied tangential torque. J. Neurosci. 18:10724–10734.

Gordon, A. M., Cole, K.J., Westling, G., Johansson, R. S. (1993) Memory representations underlying motor commands used during manipulation of common and novel objects. J. Neurophysiol. 69: 1789-1796.

Gordon, A. M., Forssberg, H., Johansson, R. S., and Westling, G. (1991a) Visual size cues in the programming of manipulative forces during precision grip. Exp.Brain Res. 83: 477-482

Gordon, A. M., Forssberg, H., Johansson, R. S., and Westling, G. (1991b) The integration of haptically acquired size information in the programming of precision grip. Exp.Brain Res. 83: 483-488.

Gordon, A. M., Forssberg, H., Johansson, R. S., Eliasson, A. C., and Westling, G. (1992) Development of human precision grip. III. Integration of visual size cues during the programming of isometric forces. Exp.Brain Res. 90: 399-403.

Hager-Ross, C. and Johansson, R. S. (1996) Nondigital afferent input in reactive control of fingertip forces during precision grip. Exp.Brain Res. 110: 131-141.

Hermsdorfer, J., Marquardt, C., Philipp, J., Zierdt, A., Nowak, D., Glasauer, S., and Mai, N. (2000) Moving weightless objects. Grip force control during microgravity. Exp.Brain Res. 132: 52-64.

Hermsdörfer, J., Marquardt, C., Philipp, J., Zierdt, A., Nowak, D., Glasauer, S., and Mai, N. (1999) Grip forces exerted against stationary held objects during gravity changes. Exp.Brain Res. 126: 205-214.

Hugon, M., Massion, J., Wiesendanger, M. (1982) Anticipatory postural changes induced by active unloading and comparison with passive unloading in man. Pflugers Archiv. 393: 292-296.

Jenmalm, P., Johansson, R.S. (1997) Visual and somatosensory information about object shape control manipulative finger tip forces. J.Neurosci. 17: 4486-4499.

Johansson R.S. (1996) Sensory control of dexterous manipulation in humans. Hand and Brain by academic Press, Inc

Johansson R.S., Backlin, J.L., Burstedt, M.K.O., (1999) Control of grasp stability during pronation and supination movements. Exp. Brain Res. 128: 20-30.

Johansson, R. S. and Westling, G. (1984) Roles of glabrous skin receptors and sensorimotor memory in automatic control of precision grip when lifting rougher or more slippery objects. Exp.Brain Res. 56: 550-564.

Johansson, R. S. and Westling, G. (1987) Signals in tactile afferents from the fingers eliciting adaptive motor responses during precision grip. Exp.Brain Res. 66: 141-154.

Johansson, R. S. and Westling, G. (1988) Programmed and triggered actions to rapid load changes during precision grip. Exp. Brain Res. 71: 72-86.

Johansson, R. S. and Westling, G. (1991) Afferent signals during manipulative tasks in man. Afferent signals during manipulative tasks in man. In Somatosensory Mechanisms Edited by Franzen O., Westman J. Macmillan Press, London. 25-48.

Johansson, R. S., Backlin, J. L., and Burstedt, M. K. (1999) Control of grasp stability during pronation and supination movements. Exp. Brain Res. 128: 20-30.

Johansson, R. S., Cole, K.J. (1994) Grasp stability during manipulative actions. Can. J. Physiol. Pharmacol. 72: 511-524.

Johansson, R. S., Hager, C., and Backstrom, L. (1992) Somatosensory control of precision grip during unpredictable pulling loads. III. Impairments during digital anesthesia. Exp.Brain Res. 89: 204-213.

Johansson, R. S., Riso, R., Häger, C., Bäckström, L. (1992) Somatosensory control of precision grip during unpredictable pulling loads. 1. Changes in load force amplitude. Exp.Brain Res. 89: 181-191.

Johansson, R.S. How is grasping modified by somatosensory input ? In : Humphrey and Freund (Ed.). Motor control : Concepts and Issues. 1991 John Wiley and sons Ltd : 331-355.

Jordan, M. I. and Wolpert, D. M. Computational motor control. M. Gazzniga. 1999. The cognitive Neurosciences. Gazzaniga, M. Ref Type: Serial (Book,Monograph)

Kawato, M. (1999) Internal models for motor control and trajectory planning. Curr. Opin. Neurobiol. 9:718-727.

Kinoshita, H., Bäckström, L., Flanagan, J.R., Johansson, R.S., (1997), Tangential torque effects on the control of grip forces when holding objects with a precisiopn grip., J. Neurophysiol. 78: 1619-1630.

Lackner, J. R. and DiZio, P. (1994) Rapid adaptation to Coriolis force perturbations of arm trajectory. J Neurophysiol. 72: 299-313.

Lackner, J. R. and DiZio, P. (2000) Human orientation and movement control in weightless and artificial gravity environments. Exp.Brain Res. 130: 2-26.

Lackner, J.R. and Graybiel, A. (1982) Rapid Perceptual Adaptation to High Gravitoinertial Force Levels: Evidence for Context-specific Adaptation. Aviat. Space Environ. Med. 53:766-9.

Lemon, R.N. (1999) Neural control of dexterity: what has been achieved? Exp.Br. Res. 128: 6-12.

Lipshits, M., McIntyre, J., Zaoui, M., Gurfinkel, V., Berthoz A. (2001) Does gravity play an essential role in the asymmetrical visual perception of vertical and horizontal line length? Acta Astronaut. 49(3-10):123-30.

Lund, J. P. and Lamarre, Y. (1973) The importance of positive feedback from peridontal pressoreceptors during voluntary isometric contraction of jaw closing muscles in man. Jour.Biol.Buccale 1: 245-351.

Mathiowetz, V., Kashman, N., Volland, G., Weber, K., Dowe, M., and Rogers, S. (1985) Grip and pinch strength: normative data for adults. Arch.Phys.Med.Rehabil. 66: 69-74.

McIntyre, J., Berthoz, A., and Lacquaniti, F. (1998) Reference frames and internal models for visuo-manual coordination: what can we learn from microgravity experiments? Brain Res.Brain Res.Rev. 28: 143-154.

Miall, R.C., Weir, D.J., Wolpert, D.M., Stein, J.F. (1993) Is the cerebellum a Smith Predictor ? Journal of motor Behavior. 25 (3) : 203-216.

Müller, F., Abbs, J.H.(1990) Precision grip in parkinsonian patients. In: Advances in neurology (Streifer MB, Korezyn AD, Melamed E, Youdim MBH, eds), 191-195. New York: Raven.

Müller, F., Dichgans, J. (1994) Dyscoordination of pinch and lift forces during grasp in patients with cerebellar lesions. Exp. Br. Res. 101: 485-492.

Moberg, E. (1962) Criticism and study of methods for examining sensibility in the hand. Neurology: 12: 8-19.

Nowak, D. A., Glasauer, S., Meyer, L., Mai, N. and Hermsdorfer, J. (2002) The role of cutaneous feedback for anticipatory grip force adjustments during object movements and externally imposed variation of the direction of gravity. Somatosensory Motor Research 19 (1): 49-60.

Nowak, D. A., Hermsdorfer, J., Glasauer, S., Philipp, J., Meyer, L., and Mai, N. (2001) The effects of digital anaesthesia on predictive grip force adjustments during vertical movements of a grasped object. Eur.J. Neurosci. 14: 756-762.

Papaxanthis, C., Pozzo, T., Popov, K. E., and McIntyre, J. (1998) Hand trajectories of vertical arm movements in one-G and zero-G environments. Evidence for a central representation of gravitational force. Exp.Brain Res. 120: 496-502.

Pozzo, T., Papaxanthis, C., Stapley, P., and Berthoz, A. (1998) The sensorimotor and cognitive integration of gravity. Brain Res.Brain Res.Rev. 28: 92-101.

Redon, C. et al. (1991) Proprioceptive control of goal directed movements in man studied by means of vibratory muscle tendon stimulation. J.Mot.Behav. 23:101-108.

Ross, H. E., Brodie, E. E., and Benson, A. J. (1986) Mass-discrimination in weightlessness and readaptation to earth's gravity. Exp.Brain Res. 64: 358-366.

Ross, H., Brodie, E., and Benson, A. (1984) Mass discrimination during prolonged weightlessness. Science 225: 219-221.

Rossini, P.M., Rossi, S., Tecchio, F., Pasqualetti, P., Finazzi-Agro, A., Sabato, A. (1996) Focal brain stimulation in healthy humans: motor maps changes following partial hand sensory deprivation. Neurosci. Lett. 214(2-3): 191-5.

Saels, P., Thonnard, J. L., Detrembleur, C., and Smith, A. M. Impact of the surface slipperiness of grasped objects on their subsequent acceleration. Neuropsychologia 37: 751-756, 1999.

Shadmehr, R. and Mussa-Ivaldi, F. A. (1994) Adaptive representation of dynamics during learning of a motor task. J Neurosci. 14: 3208-3224.

Wiesendanger, M. (1999) Manual dexterity and the making of tools- an introduction from an evolutionary perspective. Exp.Br. Res. 128: 1-5.

Wing, A. M. and Lederman, S. J. (1998) Anticipating load torques produced by voluntary movements. J.Exp.Psychol.Hum.Percept.Perform. 24: 1571-1581.

Witney, A. G., Goodbody, S. J., and Wolpert, D. M. (2000) Learning and decay of prediction in object manipulation. J. Neurophysiol. 84: 334-343.

Witney, A. G., Goodbody, S. J., and Wolpert, D. M. (1999) Predictive motor learning of temporal delays. J Neurophysiol. 82: 2039-2048.

Witney, A. G., Wing, A.M., Thonnard, J-L., Smith, A.M. (2001) Feedforward and feedback contributions to precision grip. MCC2001. From basic motor control to functional recovery-II, Varna. Ed Gantchev, N.: 163-176

Wolpert, D. M. and Flanagan, J. R. (2001) Motor prediction. Curr.Biol. 11: R729-R732.

Wolpert, D. M. and Ghahramani, Z. (2000) Computational principles of movement neuroscience. Nat.Neurosci. 3 Suppl: 1212-1217.

Wolpert, D. M., Ghahramani, Z., and Flanagan, J. R. (2001) Perspectives and problems in motor learning. Trends Cogn Sci. 5: 487-494.

Wolpert, D. M., Ghahramani, Z., and Jordan, M. I. (1995) An internal model for sensorimotor integration. Science 269: 1880-1882.

Wolpert, D. M., Goodbody, S. J., and Husain, M. (1998) Maintaining internal representations: the role of the human superior parietal lobe. Nat.Neurosci. 1: 529-533.

Wolpert, D.M. (1997) Computational approaches to motor control. Trends in cognitive Sciences. 1: 209-216.

Wolpert, D.M., Kawato, M. (1998) Multiple paired forward and inverse models for motor control. Neural Networks. 11: 1317-1329.

Wolpert, D.M., Miall, C., Kawato, M. (1998) Internal models in the cerebellum. Trends in cognitive Sciences. 2: 338-347.

Glossary

Precision grip: Grip formed with the tips of the thumb and index finger on either side of an object.
MVC: Maximal voluntary contraction
Grip force (GF): Normal force exerted by the fingers restraining an object.
Load force (LF): Destabilizing force acting tangentially to the grip surface due to the weight and the inertia of the object
$\mathbf{F_n}$: Normal force
$\mathbf{F_t}$: Tangential force
$\mathbf{T_n}$: Rotational load torque
L: Overall destabilizing load taking into account both the tangential load and the rotational torque.
$\mathbf{a_v}$: Vertical aircraft acceleration
FAI: Fast adaptive afferent units of type I
FAII: Fast adaptive afferent units of type II
SAI: Slow adaptive afferent units of type I
SAII: Slow adaptive afferent units of type II
CNS: Central nervous system
Internal model: Neural circuits that mimic the behavior of the motor system and environment and capture the mapping between motor outputs and sensory inputs. It represents the sensorimotor transformations within the CNS.
Forward internal model: represents the motor to sensory transformations within the CNS predicting the sensory consequences of an action.
Inverse internal model: represents the sensory to motor transformations within the CNS in which the desired sensory feedback is transformed into the appropriate motor command.
Feedforward command: Command defined by the CNS prior to the onset of movement. It allows anticipatory mechanism
Sensory feedback: Sensory information provided by the sensors to the CNS during the course of movement.